การสังเคราะห์และความว่องไวในการเร่งปฏิกิริยาของนิกเกิล-ซิลิโกอะลูมิโนฟอสเฟต-34 และนิกเกิล-ซิลิโกอะลูมิโนฟอสเฟต-44 ในการเปลี่ยนเมทานอลเป็นโอเลฟิน

นายฐานิสร์ วิริยพรหม

SYNTHESIS AND CATALYTIC ACTIVITY OF NICKEL-SILICOALUMINOPHOSPHATE-34 AND NICKEL-SILICOALUMINOPHOSPHATE-44 IN CONVERSION OF METHANOL TO OLEFINS

Mister Thanit Veriyaprom

A Thesis Submitted in Partial Fulfillment of the Requirements
for the Degree of Master of Science in Petrochemistry and Polymer Science
Program of Petrochemistry and Polymer Science
Faculty of Science
Chulalongkorn University
Acedemic Year 2002
ISBN 974-17-3058-6

Thesis Title	SYNTHESIS AND CATALYTIC ACTIVITY OF NICKEL-SILICOALUMINOPHOSPHATE-34 AND NICKEL-SILICOALUMINOPHOSPHATE-44 IN CONVERSION OF METHANOL TO OLEFINS
By	Mister Thanit Veriyaprom
Field of Study	Petrochemistry and Polymer Science
Thesis Advisor	Aticha Chaisuwan, Ph.D.
Thesis Co-advisor	Suphot Phatanasri, Dr.Eng.

Accepted by the Faculty of Science, Chulalongkorn University in Partial Fulfillment of the Requirements for the Master 's Degree

…………………………………. ………Dean of Faculty of Science

(Associate Professor Wanchai Phothiphichitr, Ph.D.)

THESIS COMMITTEE

………………………………………………… Chairman

(Professor Pattarapan Prasassarakich, Ph.D.)

………………………………………………… Thesis Advisor

(Aticha Chaisuwan, Ph.D.)

………………………………………………. Thesis Co-advisor

(Suphot Phatanasri, Dr.Eng.)

………………………………………………… Member

(Professor Piyasan Praserthdam, Dr.Ing.)

………………………………………………… Member

(Associate Professor Wimonrat Trakarnpruk, Ph.D.)

ได้สังเคราะห์ตัวเร่งปฏิกิริยานิกเกิล-เอสเอพีโอ-34 และนิกเกิล-เอสเอพีโอ-44 ที่มีอัตราส่วนของซิลิกอนต่อนิกเกิลเป็น 40 และ 80 ในการศึกษานี้ใช้เททระเอทิลแอมโมเนียมไฮดรอกไซด์ และไซโคลเฮกซิลเอมีนเป็นสารต้นแบบในการเตรียมนิกเกิล-เอสเอพีโอ-34 และนิกเกิล-เอสเอพีโอ-44 ตามลำดับได้ศึกษาผลของอัตราส่วนของเทมเพลทต่อฟอสฟอรัสเพนทอกไซด์ และอัตราส่วนของซิลิกอนต่อนิกเกิลต่อการเกิดตัวเร่งปฏิกิริยา ได้ตรวจสอบลักษณะเฉพาะของตัวเร่งปฏิกิริยาโดยใช้เทคนิคเอ็กซ์อาร์ดี เอ็กซ์อาร์เอฟไอซีพี-เออี เอสอีเอ็ม แอมโมเนีย-ทีพีดี และการดูดซับไนโตรเจน ได้ทดสอบความว่องไวของตัวเร่งปฏิกิริยาในการเปลี่ยนเมทานอลเป็นโอเลฟิน ตัวแปรชนิดต่างๆ ได้แก่ เวลาที่ใช้ในการเกิดปฏิกิริยา อุณหภูมิ (300-500 องศาเซลเซียส) และอัตราส่วนของซิลิกอนต่อนิกเกิลมีผลต่อค่าการเปลี่ยนเมทานอลและความเลือกจำเพาะต่อผลิตภัณฑ์ จากการใช้สารตั้งต้นที่ประกอบด้วย 22% เมทานอลในไนโตรเจนที่ความเร็วอิสระ 2000 ต่อชั่วโมง พบว่าค่าการเปลี่ยนเมทานอลบนตัวเร่งปฏิกิริยานิกเกิล-เอสเอพีโอ-34 (อัตราส่วนของซิลิกอนต่อนิกเกิลเป็น 40) ที่ 450 องศาเซลเซียส มีค่า 100% พบว่าเกิดโค้กน้อยมากและปริมาณของแก๊สมีเทนต่ำ การลดปริมาณนิกเกิลทำให้ความเลือกจำเพาะต่อโอเลฟินเบาสูงขึ้นและการสะสมของโค้กในตัวเร่งปฏิกิริยาน้อยลง อัตราการเกิดโค้กค่อนข้างต่ำเมื่อเทียบกับตัวเร่งปฏิกิริยาชนิดอื่น

4272267423   : MAJOR   PETROCHEMISTRY AND POLYMER SCIENCE

KEY WORD: NICKEL-SILICOALUMINOPHOSPHATE-34 / METHANOL TO OLEFINS / NICKEL-SILICOALUMINOPHOSPHATE-44

THANIT VERIYAPROM : SYNTHESIS AND CATALYTIC ACTIVITY OF NICKEL-SILICOALUMINOPHOSPHATE-34 AND NICKEL-SILICOALUMINOPHOSPHATE-44 IN CONVERSION OF METHANOL TO OLEFINS THESIS ADVISOR : ATICHA CHAISUWAN, Ph.D., THESIS CO-ADVISOR : SUPHOT PHATANASRI, Dr. Eng., 97 pp. ISBN 974-17-3058-6.

Ni-SAPO-34 and Ni-SAPO-44 catalysts with Si/Ni ratios of 40 and 80 were synthesized. In this study, tetraethylammonium hydroxide and cyclohexylamine were used as template in preparation of Ni-SAPO-34 and Ni-SAPO-44, respectively. Effects of template/P_2O_5 and Si/Ni ratios on formation of the catalysts were studied. The catalysts were characterized using XRD, XRF, ICP-AE, SEM, NH_3-TPD and nitrogen adsorption techniques. The catalysts were tested for their activities in methanol conversion to olefins. Various parameters including time on stream, temperatures (300-500 °C) and Si/Ni ratios affect the methanol conversion and product selectivity. It was found that, using a feed of 22% methanol in nitrogen at a gas hourly space velocity (GHSV) of 2000 h^{-1}, the methanol conversion on Ni-SAPO-34 catalyst (Si/Al = 40) at 450 °C is 100 %. Only little coke formation is observed and the content of methane gas is low. Decrease of nickel content leads to higher selectivity to light olefins, principally ethylene, and less coke deposition in the catalysts. The degree of coke formation is quite low compared to other types of catalyst.

Program…Petrochemistry and Polymer Science……..Student's signature..............................

Field of study…Petrochemistry and Polymer Science..Advisor's signature....................……..

Academic year…….2002…………………………..Co-advisor's signature........................

ACKNOWLEDGEMENT

The author would like to express his gratitude and deepest appreciation to his thesis advisor and co-advisor, Dr. Aticha Chaisuwan and Dr. Suphot Phatanari, for their continuous guidances, supervisions and helpful suggestions througout this study. In additon, he is also grateful to Professor Dr. Pattarapan Prasassarakich, Professor Dr. Piyasan Praserthdam and Associate Professor Dr. Wimonrat Trakarnpruk for serving as chairman and member of the thesis committee, respectively, whose comments have been especially helpful. He deeply appreciates the Department of Chemistry, Faculty of Science, Chulalongkorn University for sustaining the convenience in laboratories and instruments. He appreciates for a special discount in the service cost of analysis, from the Scientific and Technological Research Equipment Center and College of Petroleum and Petrochemistry, both at Chulalongkorn University. He is very grateful to the Graduate School, Chulalongkorn University for his research grant. The author would like to thank Thai Olefins Company for supporting the standard mixtures for GC analysis.

He would also like to express his deepest gratitude to his parents and family member for their great support. Finally, his thanks would be given to all his friends for their friendship and help during his graduate study.

CONTENTS

CONTENTS (CONTINUED)

CONTENTS (CONTINUED)

CONTENTS (CONTINUED)

LIST OF FIGURES

LIST OF FIGURES (CONTINUED)

LIST OF SCHEMES

LIST OF TABLES

LIST OF TABLES (CONTINUED)

LIST OF ABBREVIATIONS

MTG = Methanol to gasoline

MTO = Methanol to olefin

Ni-SAPO-34 = Nickel-silicoaluminopohsphate-34

Ni-SAPO-44 = Nickel-silicoaluminopohsphate-44

GC = Gas chromatograph or gas chromatography

XRD = X-ray diffractometer or X-ray diffraction

XRF = X-ray fluorescence spectrometer

NH_3-TPD = Ammonia-temperature programming desorption

ICP-AES = Inductively coupled plasma-atomic emission spectrometer

SEM = scanning electron microscope

GHSV = Gas hourly space velocity

TOS = Time on stream

PLOT = Porous layer open tube

C_2-C_3 olefins = ethylene and propylene

CHAPTER I

INTRODUCTION

1.1   Background

Light olefins are key components in the petrochemical industry and will likely play a dominant role in any future methanol based chemical economy. Conventionally, they are produced by thermal cracking of naphtha consisting of $C_5 - C_{12}$ alkane. Methanol, which can be produced readily from coal or natural gas via synthesis gas ($CO + H_2$) by existing and proven technologies, can be to be conversed to light olefins an interesting alternative.[1, 2] Mobil's zeolite based process for the conversion of methanol to gasoline provided a new route for the conversion of coal to gasoline. The importance of light olefins as intermediates in the conversion of methanol to gasoline has prompted several studies on methods for selectively producing them from methanol over zeolite catalysts.[3, 4] Catalysts for synthesis of ethylene and propylene from methanol process have structures with small pores, like erionite, zeolite T, and chabazite. Unfortunately, the coke formation is rapid on these catalysts. Some modified forms of ZSM-5 with basic additives to reduce acid strength have been proven to have enhanced selectivity towards lower alkenes and low rates of coke formation, but their activity is reduced greatly. The most straight forward way to change the acid strength and concentration of acid centers is by the isomorphous substitution of elements in the framework of catalysts having different by others atomic electronegativities, concentrations and distributions in the framework.

Aluminophosphate molecular sieves have opened research in this direction.[5] These solids form open crystalline structures with channels and cavities of molecular dimensions. Aluminophosphate frameworks are electroneutral, but they can be modified by the isomorphous substitution of either aluminum and/or phosphorus thus giving negatively charged framework called silicoaluminophosphate when silicon is substituted into the Aluminophosphate framework.[6] The silicoaluminophosphates such as SAPO-34, SAPO-44, and their metal incorporated analogues are similar in structure to a naturally occurring zeolite which is chabazite. They have been found as active catalysts in the conversion of methanol to olefins. M-SAPO-34 and M-SAPO-44 (M = Co, Mn, Cr) showed better activity in methanol conversion than the respective SAPO's.[7-9,10,31]

The highest selectivity to ethylene formation among these catalysts has been found for Co-SAPO-44. The selectivity to ethylene of SAPO-44 and M-SAPO-44 samples are about three-fold of those of SAPO-34 and M-SAPO-34 samples. It was recently reported[11] that Nickel-containing SAPO-34 (Ni-SAPO-34) with the Si/Ni ratio of 40 exhibited the highest selectivity to ethylene with complete conversion of methanol, but it has not been reported about Ni-SAPO-44. Therefore, this project aims to study how to prepare Ni-SAPO-34 and Ni-SAPO-44 with Si/Ni ratios in gel of 40 and 80 and their catalytic activities in the methanol conversion to olefins.

1.2 Objectives

- To synthesize the Ni-SAPO-34 and Ni-SAPO-44 with Si/Ni ratios in gel of 40 and 80.

- To investigate the catalytic conditions of methanol conversion reaction over those catalysts.

1.3   Related work

The discovery of the methanol to gasoline (MTG) reaction happened unintentionally when[3] one group at Mobil was trying to convert methanol to other oxygen-containing compounds over a ZSM-5 catalyst. Instead, they received unwanted hydrocarbons. Somewhat later, another Mobil group, working independently, was trying to alkylate isobutene with methanol over ZSM-5 and the products were found to be a mixture of paraffins and aromatics in the gasoline range. The discovery of MTG was due to a balanced effect in catalysis over many years. The methanol to olefins (MTO) reaction seems to earn benefit from this development, although independent research has been performed since the discovery of MTG. The evolution of the methanol to hydrocarbons technology, from its discovery its realization on demonstration and/or commercial scale, has been accompanied by extensive researches. Zeolite ZEM-5 was well known as a catalyst for converting methanol into hydrocarbons in the gasoline range. The methanol conversion was carried out widely over various kinds of zeolites such as the small pore zeolites, erionite,[12] zeolite T, ZSM-45, ZSM-12, chabazite;[13.] the medium pore zeolites, ZSM-5,[14-16] modified ZSM-5;[17-19.] the large pore zeolites, zeolite Y, zeolite beta,[20] mordenite.[21,22] However, the reaction was also carried out no the silicoaluminophosphate (SAPO) molecular sieves, they are a new generation of crystalline material; for examples, SAPO-5,[23] SAPO-11,[24] SAPO-17,[25,26] SAPO-18,[5] SAPO-34,[27-47] SAPO-41,[6,48] SAPO-44.[49-51] A durable activity for this reaction has not been obtained on any zeolite other ZSM-5 and pantasil metallosilicates. Although, the acid property of zeolites may also affect the catalyst lifetime in methanol conversion because the reaction takes place on the acid sites of those catalysts.

SAPO molecular sieves, with their weaker acidity than H-ZSM-5 are very interesting alternatives to obtain high selectivity to light olefins. The performance of different small pore SAPO catalysts in the MTO process was influenced by their framework structures, such as chabazite-like SAPO-34, erionite-like SAPO-17, levyne-like SAPO-35 and SAPO-18.

SAPO-34 showed the highest selectivity to formation of C_2-C_4 olefins,[4-6,23-26] because of its highest acidity among the SAPO series (SAPO-34 > SAPO-18 > SAPO-17 > SAPO-5) as well as the shape selectivity of its eight-member ring pore aperture. SAPO-5 having larger pore than SAPO-34 facilitated the production of C_4-C_7 olefins with the presence of branched hydrocarbons and a very small amount of aromatics. SAPO-11 (medium pore and acidity is lower than SAPO-34 and SAPO-5) favored the formation of aromatics, C_5 and C_6 hydrocarbons but SAPO-11 showed the highest lifetime for catalytic activity compared with SAPO-34 and SAPO-5[24]. Furthermore, the incorporation of transition metal ions into framework site of SAPO molecular sieves is also interesting for the design of novel catalysts. Transition metal substituted SAPO catalysts, such as M-SAPO-34 (M = Ni, Co, Cr, Fe, Mn, Ga),[7,8,27,30-33] M-SAPO-18 (M = Ni, Mg, Zn),[4,5] M-SAPO-35 (M= Ni, Cr),[4,16] Ni-SAPO-11[4] and Ni-SAPO-17[4] have been investigated for MTO reaction. The methanol conversion on these catalysts, the selectivity to C_2-C_4 olefins and the lifetime were enhanced compared to the non-metal loading material because M-SAPO catalysts exhibited lower acidity and number of acid sites compared to the non-metal loading catalysts.

The catalytic activity and selectivity of SAPO-34 and M-SAPO-34 (M = Fe, Co, Ni) in the conversion of methanol to olefins have been investigated.[11,27,30-32,34,37-38] The catalytic performance in the conversion of methanol to light olefins of all catalyst samples prepared was found to be closely related to the number of strong acid sites that was determined by ammonia-TPD. Zeolite materials possess lots of acid sites and certain acidic strengths related to their high Al contents and tetrahedral Al sites, respectively. In general, aluminophosphates ($AlPO_4$) are prepared in the presence of cationic or neutral amine additives and crystallize with the Al/P ratio in gel of one, resulting in no net charge on the framework. In particular, the incorporation of silicon into framework displayed Brønsted acid sites. Therefore, if the Si is substituted by other transition metal, the number of acid sites should be decreased. All M-SAPO-34 catalysts exhibited lower acidity and number of acid sites compared to the non-metal SAPO-34 catalyst. The methanol conversion at the temperature of $425^{\circ}C$ was above

90% for all the catalysts in the M-SAPO-34 series.[37] The ethylene selectivity was the highest for Ni-SAPO-34 (above 80%), and the order in ethylene selectivity was as follows: SAPO-34 < Co-SAPO-34 < Fe-SAPo-34 < Ni-SAPO-34.[27]

The small pore SAPO molecular sieves exhibit a rather high ethylene selectivity. However, it is for the same reason that it is difficult to apply conventional modification methods, such as ion-exchange and impregnation, to change the properties of the catalyst. Modification in the synthesis of the molecular sieve seems to be critical for improvement of catalytic performance. Remarkable results were observed using Ni-SAPO-34, on which the ethylene selectivity of 88% was found at the temperature of 450°C with 100% methanol conversion. This catalyst was not easy to reproduce because the selectivity is very sensitive to those properties which depend on the preparation procedure. Inui and Kung reported[30,32,39,41,43,52] a reliable procedure for the synthesis of the Ni-SAPO-34 and investigated the factors involved in its preparation. It was pointed out that the order of mixing of the starting materials was important to obtain a homogeneous gel mixture. The sequence of the addition of seed crystallites, milling time, treatment with ultrasonic waves and the application of a rapid crystallization method seem necessary to obtain a satisfactory catalyst. The catalysts have particles 0.8-0.9 µm in size and a sharp size distribution, with low acid density on both the internal and external surface, with 86% selectivity to ethylene at the temperature of 425°C. A linear relation between internal acid density and the selectivity to ethylene was observed, thus one may expect to obtain more selective formation of ethylene by controlling the internal acid density to less than 4 µmol/m^{2}. The amount of Ni incorporated in SAPO-34 was surprisingly very small (Si/Ni $\approx$ 100). So it is interesting to argue what the exact effect of Ni on the catalyst properties and on reaction performance.

Crystalline samples of medium pore SAPO-41 and small pore SAPO-44 have been prepared using diethylamine and cyclohexylamine as templates.[48] Their catalytic performance in the conversion of methanol to hydrocarbons was investigated. SAPO-44 has larger void volume and stronger acidity than SAPO-41. Whereas the products of methanol

conversion on SAPO-41 are dominated by dimethyl ether, the main products on SAPO-44 are ethylene and propylene. Nevertheless, SAPO-44 is less active than SAPO-34 and suffers deactivation in about an hour at 450°C.

SAPO-34 and SAPO-44, small pore molecular sieves with chabazite structure as they are found to be very selective to the formation of olefins in the methanol conversion.[7-9] The acid strength and catalytic activity of SAPO-44 and the isomorphous substituted M-SAPO-44 (M = Co, Mn, Cr, Zn, Mg) molecular sieves in the methanol to hydrocarbons reaction were measured by Hočevar et al.[10,31] In addition, the results were compared to those of $AlPO_4$-5 and $AlPO_4$-14 samples. The acid strength of the samples has been determined qualitatively from the temperatures of dimethyl ether desorption peak and the following sequence were obtained: Mn-SAPO-44 >Co-SAPO-44 ≈ Zn-SAPO-44 > Mg-SAPO-44 > Cr-SAPO-44 > SAPO-44 >>AlPO-5 ~ AlPO-14. Among these catalysts the highest selectivity to ethylene formation was found over Co-SAPO-44. The selectivity to ethylene on SAPO-44 and M-SAPO-44 (M = Co, Mn, Cr) samples were about three times higher than the selectivity to ethylene on SAPO-34 and M-SAPO-34 (M = Co, Mn, Cr) samples.[31]

CHAPTER II

THEORY

2.1 Olefins Processes

Olefins are not found in petroleum or natural gas, but are formed as by-products of the cracking of petroleum fractions. The cracking of petroleum is the most important source of industrial olefins. Cracking may be accomplished with or without a catalyst, but if a catalyst is not used considerably, higher temperatures are required.[1] Olefins are produced from steam cracking of hydrocarbons such as ethane, propane, butane, naphtha and gas oil in tubular reactor coils installed in externally fired heaters (Fig. 2.1). Due to uncertainty of oil prices, depression of product prices, over capacity of olefins facilities, and oversea competition, the olefins industry has struggled to maintain minimum cost and process flexibility. During the past decades, various research and developmental work were pursued to find processes using alternative feedstock and providing cost advantages.

2.1.1 Heavy Oil Cracking Processes

To avoid dependence on oil refineries or gas processors to supply feedstock, processes for the cracking of crude oil directly were developed by various companies. Also, because of the tendency of converting industrial oil fired equipment to coal burning equipment, considerable quantities of residual oil will be released. A technology for cracking residual oil similar to the crude oil cracking process was also developed. Since tubular-furnaces are inadequate to deal with the high severity and coke formation tendencies of heavy feedstock, most processes developed for crude oil cracking are based on nontubular reactor principles (Fig. 2.2).
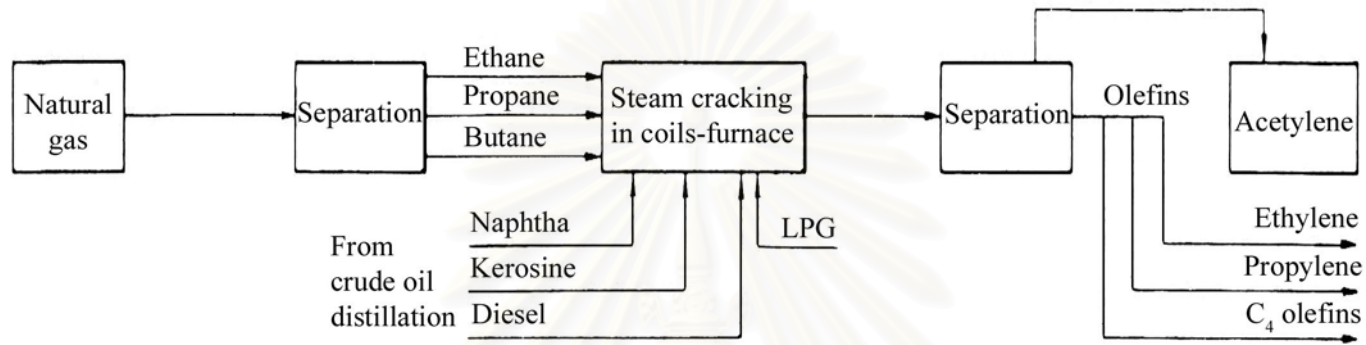
Figure 2.1   Conventional olefin process technology.
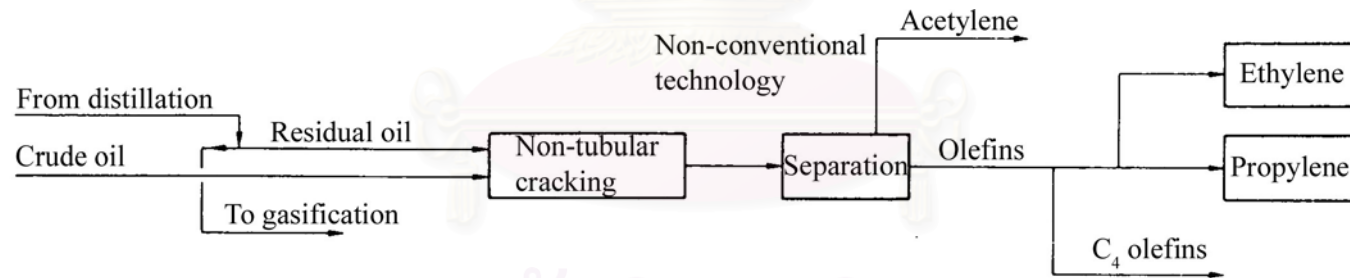
Figure 2.2   Crude/residual oil cracking for olefins.

2.1.2 **Ethanol Dehydration**

A number of catalytic ethanol dehydration unit were built in the 1950s and 1960s in Asia and South America. Some of them are still in operation, but others were shut down when new, large olefins plants based on steam cracking were brought on-stream. Because of uncertainty in the availability of petroleum feedstock, a renewal of interest in ethanol dehydration exists. Ethanol can be produced either from biomass fermentation (Fig. 2.3) or by synthesis from syngas. Both ethanol manufacturing processes and syngas processes have been under rigorous development during the last decade.
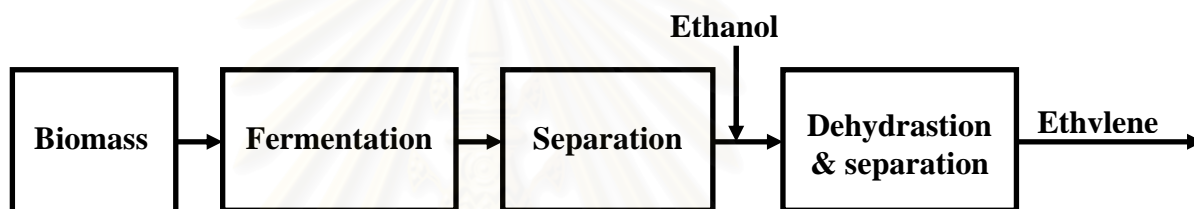
Figure 2.3   Ethylene from biomass through fermentation and ethanol dehydration.

Though the mechanism of ethanol dehydration has not been completely established, for practical purposes the following consecutive reaction sequence may be assumed:

$$2\ C_2H_5OH \rightarrow (C_2H_5)_2O + H_2$$

$$(C_2H_5)_2O \rightarrow 2\ C_2H_4 + H_2O$$
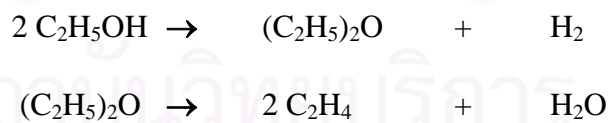
These reactions are endothermic and temperature is the critical operation variable. In the industrial production of ethene, yield is 94 to 99% of the theoretical value depending on the process scheme. Traces of aldehydes, acid, high hydrocarbons, and carbon dioxide, as well as water, have to be removed.

2.1.3 Syngas-Based Processes

Syngas-based processes have been very well documented. The gasification of coal or oil provides an alternative route to produce chemicals (Fig. 2.4). The gasifiers produce CO and H_2 which can be reacted to form a variety of products. Different types of reactions are shown in Table 2.1. The different operating condition and different catalyst product produced are shown in Figure 2.5, various products may be produced by the conversion of syngas. Most of the reactions are based on F-T (Fisher-Tropsch) technology which was developed almost 60 years ago in Germany.
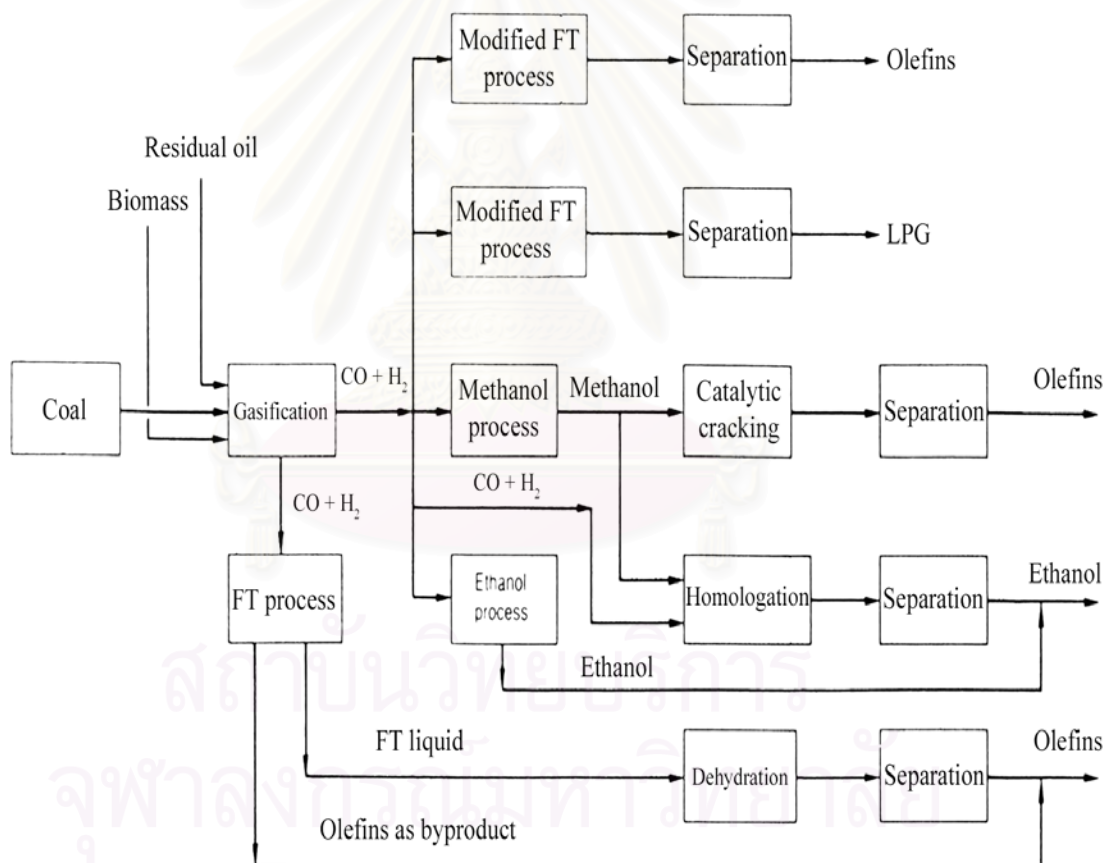
Figure 2.4   Routes to olefins from syngas.

Table 2.1. Possible stoichiometric equations for reactions between

carbon monoxide and hydrogen

Methanation	$3H_2 + CO \rightarrow CH_4 + H_2O$
	$2CO + 2H_2 \rightarrow CH_4 + CO_2$
Alkanes (n > 1)	$(2n + 1)H_2 + nCO \rightarrow C_nH_{2n+2} + nH_2O$
	$(n + 1)H_2 + 2nCO \rightarrow C_nH_{2n+2} + nCO_2$
	$(n + 1)H_2 + (3n + 1)CO \rightarrow C_nH_{2n+2} + (2n + 1)CO_2$
Olefins (n > 1)	$nCO + 2nH_2 \rightarrow C_nH_{2n} + nH_2O$
	$2nCO + nH_2 \rightarrow C_nH_{2n} + nCO_2$
	$3nCO + nH_2 \rightarrow C_nH_{2n} + 2nCO_2$
Methanol	$2H_2 + CO \rightarrow CH_3OH$
Alcohols (n > 1)	$nCO + 2nH_2 \rightarrow C_nH_{2n+1}OH + (n - 1)H_2O$
	$(2n - 1)CO + (n + 1)H_2 \rightarrow C_nH_{2n+1}OH + (n - 1)CO_2$
	$3nCO + (n + 1)H_2O \rightarrow C_nH_{2n+1}OH + 2nCO_2$
Water gas shift	$CO + H_2O \rightarrow CO_2 + H_2$
Boudouard reaction	$2CO \rightarrow C + CO_2$
Coke deposition	$H_2 + CO \rightarrow C + H_2O$
Carbide formation	$xM + C \rightarrow M_xC$
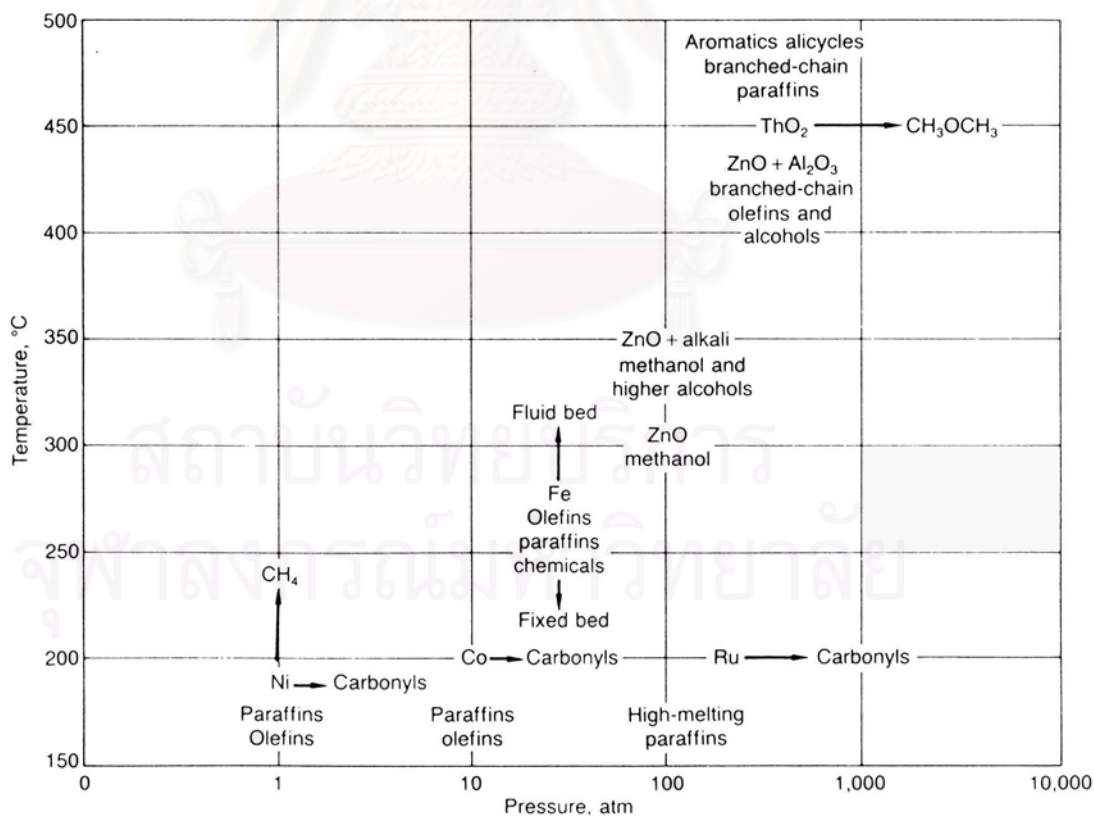
Figure 2.5 Carbon monoxide-hydrogen reaction.

2.1.4 Olefin Disproportionation

The disproportionation (metathesis) reaction provides the basis for petrochemical processes which can interconvert commodity olefins, e.g., propene, to more valuable ethene and butylene. Research in the early 1960s by Banke and Bailey led to the general reaction for such monoolefins:

$$2 \quad R_1-\overset{\overset{\displaystyle H}{|}}{C}=\overset{\overset{\displaystyle H}{|}}{C}-R_2 \longrightarrow R_1-\overset{\overset{\displaystyle H}{|}}{C}=\overset{\overset{\displaystyle H}{|}}{C}-R_1 + R_2-\overset{\overset{\displaystyle H}{|}}{C}=\overset{\overset{\displaystyle H}{|}}{C}-R_2$$
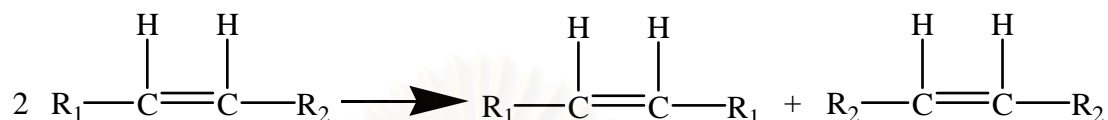
They found that olefins can be readily interconverted via a redistribution of structural configuration which, in effect, permits a controlled shuffling of molecular weights and double-bond placement. This reaction is called disproportionation.

The catalysts for the disproportionation reaction contain transition metals, preferably Mo, W or Re, and are either heterogeneous or homogeneous. Heterogeneous catalysts are generally oxides deposited on a high surface area support, e.g., silicon of aluminum oxides. Homogeneous catalysts are derived from a transition metal halide used either alone or complexed with Lewis bases and a nontransition compound.

2.1.5 Catalytic Conversion of Methanol

The synthesis of hydrocarbons from methanol using the Mobil MTG process with ZSM-5 catalyst is shown in Figure 2.6. The exact reaction pathway for olefins formation from methanol cracking is being elucidated. However, a simplified hypothesis can be assumed as follows:
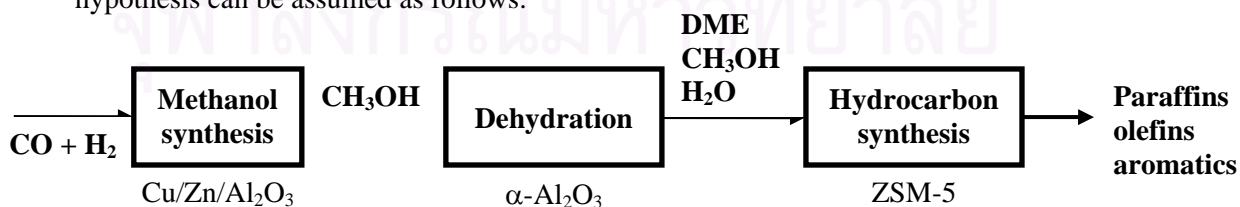
Figure 2.6 Mobil methanol to hydrocarbons technology.

Olefins are intermediates in the conversion of methanol to aromatic hydrocarbons over zeolites. In order to increase olefins production, conditions under which the final aromatization step is minimized or suppressed must be found. Various approaches to this problem have been developed. The simplest strategy is to backtrack along the reaction path by decreasing the contact time. Here, maximum olefin selectivity may be obtainable only at partial conversion, which requires separation and recycling of unreacted material. Decoupling of olefins from aromatic formation can be achieved by reducing the oxygenate partial pressure. At low partial pressure, generally below atmospheric, this methanol provides high olefin yield at complete conversion.

ZSM-5 is an effective Methanol to Olefins (MTO) catalyst and has been subject of very intensive scrutiny. Among the host of other catalysts reported in the literature to be active for MTO, the silicoaluminophosphate molecular sieves SAPO-17 and SAPO-34 seem noteworthy. The framework structures of SAPO-17 and SAPO-34 are topologically related to the zeolites erionite and chabazite, respectively. These zeolites have eight-ring pore openings, and hence their SAPO analogs should produce aliphatics to the exclusion of aromatics, SAPO-34 is apparently effective at lower temperatures then ZSM-5 for MTO.[3]

2.2 Zeolites

With the recent discoveries of molecular sieves materials containing other elements in addition to, or in lieu of, silicon and aluminum, the casual interchange of the terms "molecular sieve" and "zeolite" must be reconsidered. In 1932 McBain proposed the term "molecular sieve" to describe a class of materials that exhibited selective adsorption properties. He proposed that for a material to be a molecular sieve, it must separate components of a mixture on the basis of molecular size and shape differences. Two classes of molecular sieves were known when McBain put forth his definition: the

zeolite and certain microporous charcoal. The list now includes the silicates, the metallosilicates, the metalloaluminates, the $AlPO_4$'s and silico- and metalloaluminophosphates, as well as the zeolites.

The zeolite is microporous, crystalline aluminosilicate with a framework based on an extensive three-dimensional network of oxygen ions. Situated within the tetrahedral sites formed by the oxygen can be either a Si^{+4} or an Al^{+3} ion. The AlO_2^- tetrahedra in the structure determine the framework charge. This is balanced by cations that occupy nonframework positions. A representative empirical formula for a zeolite is written as:

$$M_{2/n}O. \ Al_2O_3. \ xSiO_2. \ yH_2O$$
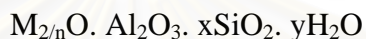
M represents the exchangeable cations, generally from the group I or II ions, although other metal, nonmetal, and organic cations may also be used to balance the framework charge, and n represents the cation valence. These cations are present either during synthesis or through post-synthesis ion exchange. The value of x is equal to or greater than 2 because Al^{+3} does not occupy adjacent tetrahedral sites. The crystalline framework structure contains voids and channels of discrete size, unlike the microporous charcoal molecular sieves, a characteristic that separates them from the amorphous carbon molecular sieves. The pore or channel openings range from 3 Å to 8 Å, depending on the structure. Water molecules present are located in these channels and cavities, as are the cations that neutralize the negative charge created by the presence of the AlO_2^- tetrahedra in the structure.

All zeolites that are significant for catalytic and adsorbent applications can be classified by the number of T atoms, where T = Si or Al, that define the pore opening. There are only three pore openings known to date in the aluminosilicate zeolite system that are of practical interest for catalytic applications; they are descriptively referred to as the 8, 10, and 12-ring openings. Zeolites containing these pore openings may also be referred to as small (8-member ring), medium (10-member ring), and large (12-member

ring) pore zeolites. In this simplified classification system, no indication is given as to the exact dimension of the pore opening or whether the zeolite contains a one-, two-, or three-dimensional pore system. The different ring sizes, based on the different member of T atoms defining the opening, are shown for three representative zeolite: erionite, ZSM-5, and type Y. Zeolites of known structure are listed in Table 2.2 classified in terms of their largest pore opening.

2.3   Aluminophosphates, $AlPO_4$'s

The aluminophosphate family of molecular sieves are microporous crystalline oxides, many of which, like the zeolites, contain pores within their framework structure that are molecular in dimension. In the aluminophosphates ($AlPO_4$'s) the framework sites are occupied by Al^{+3} or P^{+5}. The average of the ionic radii of Al^{+3} (0.39 Å) and P^{+5} (0.17 Å) is 0.28 Å, which is similar to the ionic radius of Si^{+4} (0.26 Å). The notable feature of the $AlPO_4$ composition is the invariant Al_2O_3/P_2O_5 ratio, which is in direct contrast with the variable compositions of silica/alumina found in the zeolite structures.

Unlike the zeolite molecular sieves, which contain $Al^{+3.}$ and Si^{+4} in tetrahedral positions and exhibit a net negative framework charge, The $AlPO_4$ molecular sieves may contain aluminum in coordination other than tetrahedral, and a framework charge that is neutral. Structural diversity is found in the $AlPO_4$ materials, even with such limited variation in chemical composition. The overall composition of the $AlPO_4$ molecular sieves is written as:

$$xR. \ Al_2O_3. \ 1.0(+/- \ 0.2) \ P_2O_5. \ yH_2O.$$
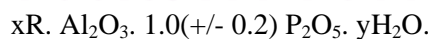
where R is an organic amine or quaternary ammonium ion. The quantities x and y represent the amount of organic or water that fills the pores of the crystal, as the $AlPO_4$ requires no counter-ions.

Table 2.2 Known zeolite structures listed by pore opening, as defined as

the number of T (or TO_4) units that shape the channel

12 RING	10 RING	8 RING
Faujasite (type X, Y)	ZSM-5 (Silicalite)	Type A, ZK-5
Mordenite	ZSM-11	Bikitaite
Cancrinite	Dachiardite	Brewsterite
Gmelinite	Epistilbite	Chabazite
Type L	Ferrierite	TMA-E (AB)
Mazzite	Laumontite	Edingtonite
Offretite	Stilbite	Erionite
Omega	ZSM-23	Gismondine
ZSM-12	Theta-1 (ZSM-22)	Heulandite
Beta	Eu-1 (ZSM-50)	Levyne
	ZSM-48 (EU-2)	Merlinoite
		Natrolite
		Philipsite
		Paulingite
		Rho
		Thomsonite
		Yugawaralite

2.3.1 Synthesis of AlPO$_4$ Molecular Sieves

The synthesis of metal-substituted silicate molecular sieves (M= B, Ga, Fe, Ge, Ti) exhibits many similarities to that of the zeolite molecular sieves. All are synthesized from reactive gels under alkaline conditions with the presence of organic additives helping to promote crystallization in some cases. On the other hand, the synthesis of the AlPO$_4$ molecular sieves, though similar in some ways to that of the zeolite materials, does have some notable differences. Like the zeolites, the AlPO$_4$ materials are synthesized hydrothermally with a preferred temperature range between 125 and 200° C. Reactive aluminophosphate gel are used. The preferred source of aluminum is boehmite, a reactive hydrated alumina, and phosphorous is added as phosphoric acid. Unlike the zeolite molecular sieves, however, the presence of organic additives appears necessary to promote crystallization in the aluminophosphate system. Also, instead of highly caustic conditions, the AlPO$_4$ gels exhibit an initial acidic pH of about 3. As in the zeolites, the numerous synthesis parameters all contribute to the crystalline phases obtained.

2.3.1.1 Effect of Temperature and Time

Temperature plays an important role in the crystallization of the molecular sieve aluminophosphates. At lower temperature (100 to 125°C) crystallization of the condensed phase aluminophosphates is observed. These include variscite, metavariscite, and the three condensed SiO$_2$-like phases, the aluminophosphate analogs of cristobalite, tridymite, and quartz. At temperatures between 150 and 200°C, zeolite-like phases are observed. Table 2.3 provides an example of the effect of temperature on the crystallization of AlPO$_4$-5. the organic crystal-directing agents (either Pr$_3$N or Pr$_4$NOH) were added as an aqueous solution to the resulting aluminophosphate gel.

Table 2.3. Effect of crystallization temperature on $AlPO_4$-5 synthesis with

gel composition 1.0R: 1.0 Al_2O_3: 1.0P_2O_5: 40H_2O

R	CRYSTALLIZATION		PRODUCTS
	TEMP., ^{o}C	TIME, HR	
Pr_3N	100	168	H3, MV, V
	125	24	5, H3, MV
	150	24	5
	200	24	T, C, 5
Pr_3NOH	55	384	B, MV
	100	168	MV, H3, V
	125	24	5, B, H3
	150	24	5
	200	24	5

B = boehmite, MV = metavariscite, V = variscite, H3 = $AlPO_4$.1.67H_2O, T = tridymite,
C = cristobalite, 5 = $AlPO_4$-5.

Time also determines the crystalline structure formed. At the
higher crystallization temperatures (200°C), other condensed nonzeolitic phases are
observed to crystallize with increasing time. The time needed to promote crystallization
of these condensed phases appears to be dependent on both the temperature and the
nature of the organic used in the reaction mixture. In the crystallization of $AlPO_4$-5 at
150°C, using tripropylamine as the organic, even after an extended crystallization period
only the $AlPO_4$-5 phase is observed. At 200°C, after only half the crystallization period
the condensed phases appear. However, changing the organic, using the
tetrapropylammonium cation instead, stabilizer the $AlPO_4$-5 phase over a longer
crystallization period. The role of time in the crystallization of $AlPO_4$-5 is shown in
Table 2.4. It also must be noted that the pH appears to rise very quickly in the
crystallization.

Table 2.4. Effect of crystallization time on AlPO$_4$-5 synthesis with gel composition 1.0Pr$_3$N: 1.0 Al$_2$O$_3$: 1.0P$_2$O$_5$: 40H$_2$O

CRYSTALLIZATION		pH		PRODUCTS
TEMP.,^{O}C	TIME, HR	INITIAL	FINAL	
150	4	3.0	8.1	5, >B
	8	3.0	8.1	5
	120	3.0	8.5	5
200	4	3.0	8.2	5
	8	3.0	8.8	5, >T
	48	3.0	8.7	T, C, >5

B = boehmite, T = tridymite, C = cristobalite, 5 = AlPO$_4$-5.

2.3.1.2 Effect of Organic Additive

The presence of the organic cationic or neutral amine strongly influences the crystallization of zeolite-like aluminophosphate phases. Without the organic, condensed phase structures crystallize. The amount of organic added contributes to the crystallization of the zeolite-like phases as well. Molar equivalent amounts of organic and Al$_2$O$_3$ (or P$_2$O$_5$) appear necessary to achieve the molecular sieve structures. This contribution by the organic to the resultant structure is shown in the AlPO$_4$-5 system in Table 2.5.

Table 2.5. Effect of organic amine concentration on the synthesis of the AlPO$_4$-5. Gel

composition xPr$_3$N: 1.0 Al$_2$O$_3$: 1.0P$_2$O$_5$: 40H$_2$O.Crystallization time = 24

hours, temperature = 150°C

X	pH		PRODUCTS
	INITIAL	FINAL	
0.0	2.0	4.7	T, Q, C
0.6	2.3	8.6	MV, 5, H3
1.0	3.0	8.3	5
1.2	3.7	8.4	5

MV = metavariscite, T = tridymite, C = cristobalite, Q = quartz, 5 = AlPO$_4$-5, H3 =

AlPO$_4$.1.67H$_2$O.

These factors-time, temperature, and concentration-individually

contribute to directing the crystallization of aluminophosphate structures. In addition,

subtle interrelationships are observed between these factors. Time and the nature of the

organic additive, temperature and time, temperature and the organic additive-these

combinations of factors will lead to a specific reaction product or set of product. As in

the synthesis of the zeolite molecular sieves, optimizing the synthesis to produce a

specific phase that is highly crystalline and of high purity may require modifications in

one parameter as well as sets of parameters to obtain the desired results. In the synthesis

of new materials with the aluminophosphate structure, some knowledge of the

contribution that each factor, as well as each combination of factors, has on the course of

the synthesis will aid in fine-tuning the search for such materials.

2.4   Silicoaluminophosphates, SAPO's

In addition to the incorporation of phosphorous into zeolite gel to produce silicoaluminophosphate molecular sieves, silica can be considered to incorporate into the $AlPO_4$ structure to form such SAPO materials. The synthesis of a large number of SAPO molecular sieves under the conditions used for preparation of the $AlPO_4$ materials appears to be fruitful in generating both zeolite-like and $AlPO_4$-like structures, as well as that are not found in either system. Three novel structures have been prepared in the SAPO system that have on structural counterpart in the other molecular sieve compositions. A list of the SAPO molecular sieves prepared is given in Table 2.6. The list identifies the analogous structure, if known, and the ring size, as well as the oxygen and water adsorption capacities.

Table 2.6. SAPO molecular sieves synthesized, their structure type, ring size,

and selected adsorption capacities

NAME	STRUCTURE TYPE	RING SIZE	ADSORPTION CAPACITIES	
			O_2	H_2O
SAPO-5	$AlPO_4$-5	12	0.23	0.31
SAPO-11	$AlPO_4$-11	10	0.13	0.18
SAPO-17	Erionite	8	0.25	0.35
SAPO-20	Sodalite	6	0	0.40
SAPO-31	$AlPO_4$-31	10	0.13	0.21
SAPO-34	Chabazite	8	0.32	0.42
SAPO-35	Levynite	8	0.26	0.48
SAPO-37	Faujasite	12	0.37	0.35
SAPO-44	Chabazite	8	0.28	0.34

2.4.1 Synthesis of SAPO Molecular Sieves

The synthesis method used in the preparation of SAPO molecular sieves is equivalent to that of the $AlPO_4$ molecular sieves discussed previously. The source of silica used in the synthesis is silica sol. The compositional range of the silicoaluminophosphates is of:

$$0\text{-}0.3R \; (Si_x \, Al_y \, P_z) \; O_2$$
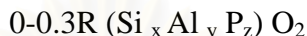
where, in the anhydrous form x, y, and z are the mole fraction of silicon, aluminum, and phosphorous in the range of 0.01 to 0.98, 0.01 to 0.6, and 0.01 to 0.52, respectively (x+y+z = 1). As in the synthesis of the zeolites and the aluminophosphates, the organic amine and ammonium cation aids are directing the structure type produced. However, the presence of the silicon in the reaction minture also contributes to directing the structure. The most notable result of the role of the silicate in the reaction mixture is the production of novel SAPO structures. Tetraethylammonium ion is a template for $AlPO_4$-5 and $AlPO_4$-18 in the aluminophosphate system, but addition of silicate to the $AlPO_4$ gel using this organic amine results in the formation of SAPO-34, which is chabazite-type structure. Structures with no $AlPO_4$ or zeolite equivalent include SAPO-40, -41, and -44 prepared from reaction mixtures containing TPA, TBA, and cyclohexylamine, respectively.

A fundamental question that arises regarding the substitution of silicon into the $AlPO_4$ structural framework is the location of this substituted ion. In the $AlPO_4$ framework, silicon theoretically can substitute for aluminum, phosphorous, or both. If the silicon substitutes for aluminum, the charge on the framework will be positive, giving rise to anionic exchange properties; substitution for phosphorous will result in an anionic framework similar to the zeolite molecular sieve; no net charge in framework will be observed if both aluminum and phosphorous are simultaneously substituted with two silicon atoms.

The ability to exchange cations as well as observed acid activity in the SAPO molecular sieves indicates that the silicon does, indeed, substitute for phosphorous although the substitution of both aluminum and phosphorous is also indicated for several structures. SAPO-34 and SAPO-37 both have mole fractions for $Si_xAl_yP_z$ with $x + z = y$, indicative of substitution of silicon for phosphorous. For SAPO-5 and SAPO-11, $x + z$ is greater than y, which is evidence for substitution of two silicon atoms for (Al + P) in addition to substitution of Si for P.

2.4.2   Substitution Mechanisms

The framework of an $AlPO_4$'s molecular sieve consists of strictly alternating (PO_4) and (AlO_4) tetrahedra and consequently has no net framework charge. Due to the restrictions on the Al and P ordering, the generation of silicon containing microporous aluminophosphate framework can be most conveniently visualized by replacing some of the Al and/or P atoms by Si atoms in an isomorphous substitution mechanisms (SM) are illustrated in Figure 2.7. Substitution of Si and Al represents the first mechanism (SM1) and Si for P substitution corresponds to the second one (SM2). The simultaneous substitution of two Si atoms for one Al and one P gives rise to a third mechanism (SM3). SM1 generates net positive framework charges which have to be neutralized by anions. When according to SM2, a PO_4 tetrahedron is replaced by SiO_4, the framework become negatively charged and cation exchange capacity is generated. The simultaneous replacement of one AlO_4 and one adjacent PO_4 tetrahedron by two SiO_4 tetrahedron (SM3) does not involve charges in the framework charge.
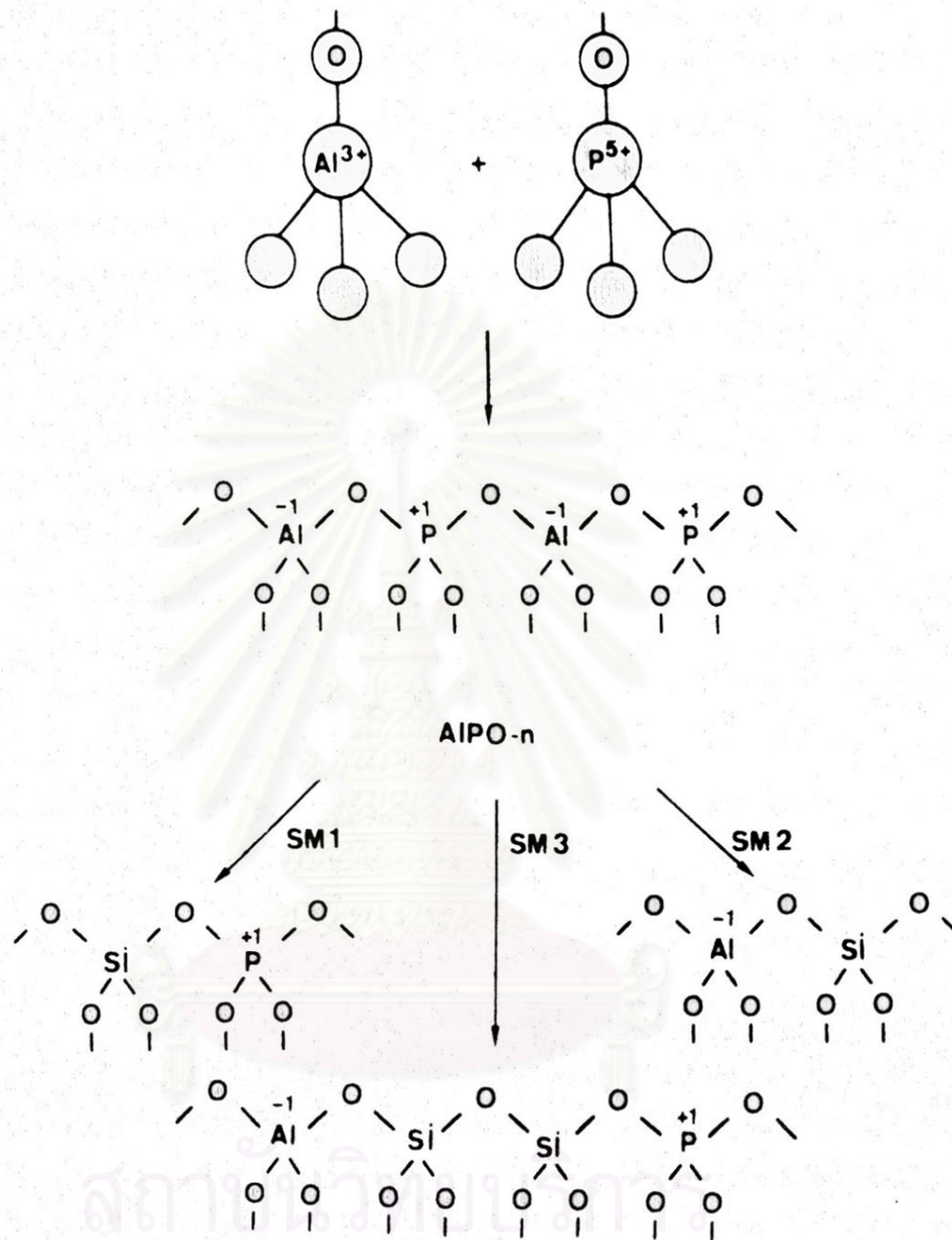
Figure 2.7 Possible isomorphous substitution mechanism of Si in AlPO$_4$ framework.

2.5   Catalysts Properties

By analogy to solution chemistry, it is postulated that the primary requirement for catalytic activity is that the solid be acidic and be capable of forming carbonuim ions by reaction with a hydrocarbon. Carbonium ions are intermediates in such reactions as cracking, polymerization, and isomerization. An acid site may be of the Brønsted type in which it donates a proton to an unsaturated hydrocarbon, or of the Lewis type in which it acts as an electron acceptor, removing a hydride ion from a hydrocarbon.

2.5.1   Acid Sites

The usual method for preparing hydrogen form zeolites is the thermal treatment of ammonium exchanged zeolites leaving hydrogen (or proton) on the zeolite framework. The hydrogen form (acid form) can be generated indirectly by replacing the sodium ions of the zeolite by ammonium ions from an aqueous solution of ammonium chloride or ammonium nitrate and heating above 300°C under vacuum. The bridged OH group across a pair of Si and Al atoms behaves as a classical Brønsted acid. Further thermal treatment at higher temperature results in a loss of water from two nearby hydroxyl groups. This process is called dehydroxylation. The dehydroxylation causes the loss of one oxygen from zeolite framework per water molecule removed, exposing a tricoordinated Al ion, which is an electron-pair acceptor, i.e. a Lewis acid site. The formation of these sites is shown in Figure 2.8
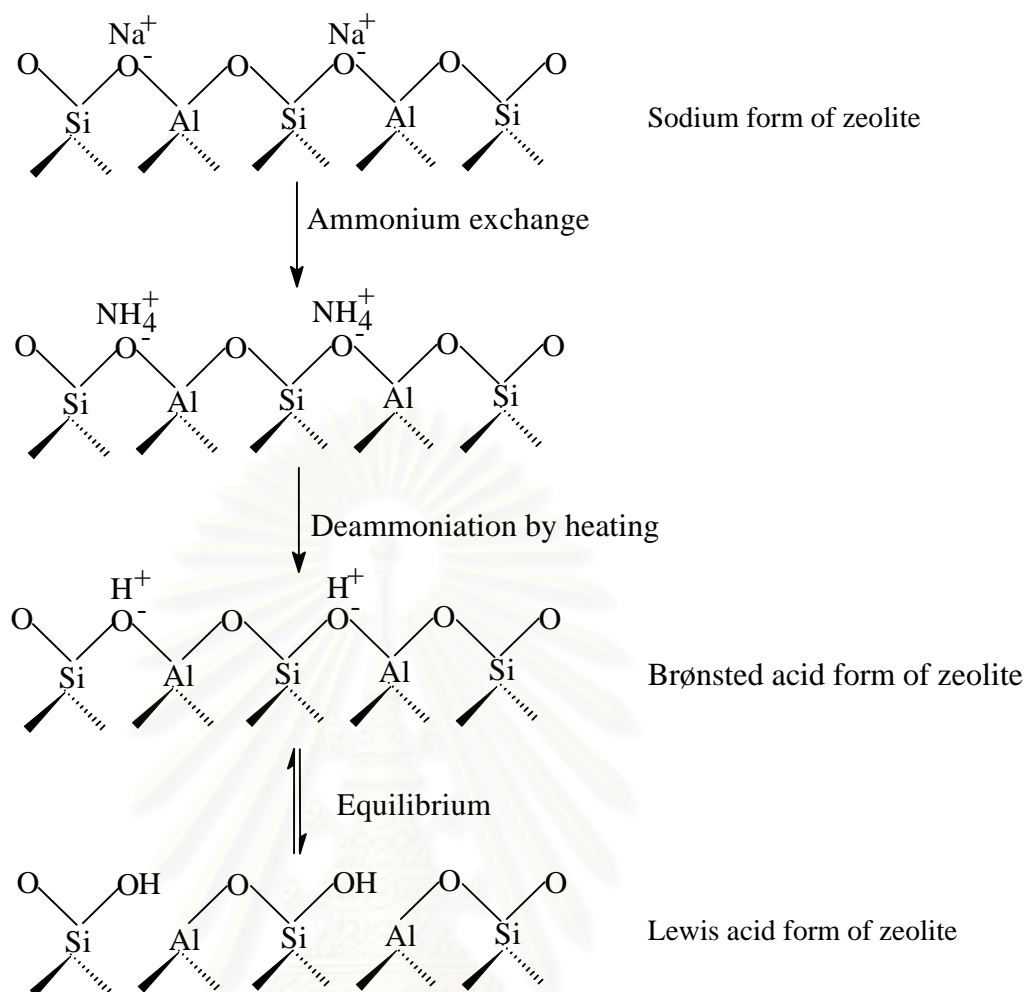
Figure 2.8 Postulated structures of silica-alumina causing Brønsted and Lewis acid sites.

2.5.2 Shape Selectivity

The pore size and shape in a zeolite may effect the selectivity of a reactoon in three ways: Reactant selectivity occurs when the aperture size of the zeolite is such that it admits only certain smaller molecules and excludes larger molecules; hence, in a mixture, effectively only the smaller molecules react. Product selectivity occurs when bulkier product molecules can not diffuse out, and if formed, they are converted to smaller molecules or to carbonaceous deposits within the pore. These eventually may cause pore blockage. Transition-state selectivity has been termed spatioselectivity. Spatioselectivity implies that monomolecular rather than bimolecular transition states are favored in small pores: thus, this steric effect and/or diffusional

effects may operate to produce shape selectivity. These types of selectivity are depicted in Figure 2.9.

For shape selectivity to occur, essentially all the active catalytic sites must be in the interior of the pores. The exterior area of zeolite crystals is only about one percent of the total, but if diffusion limitations are significant, it may become necessary to poison or inactivate exterior site so they do not contribute excessively to reaction. Some zeolites having suitable aperture size are not stable under reaction conditions. With some metal-loaded zeolites, metal may migrate out of the pores with time, thus destroying this type of catalyst selectivity.
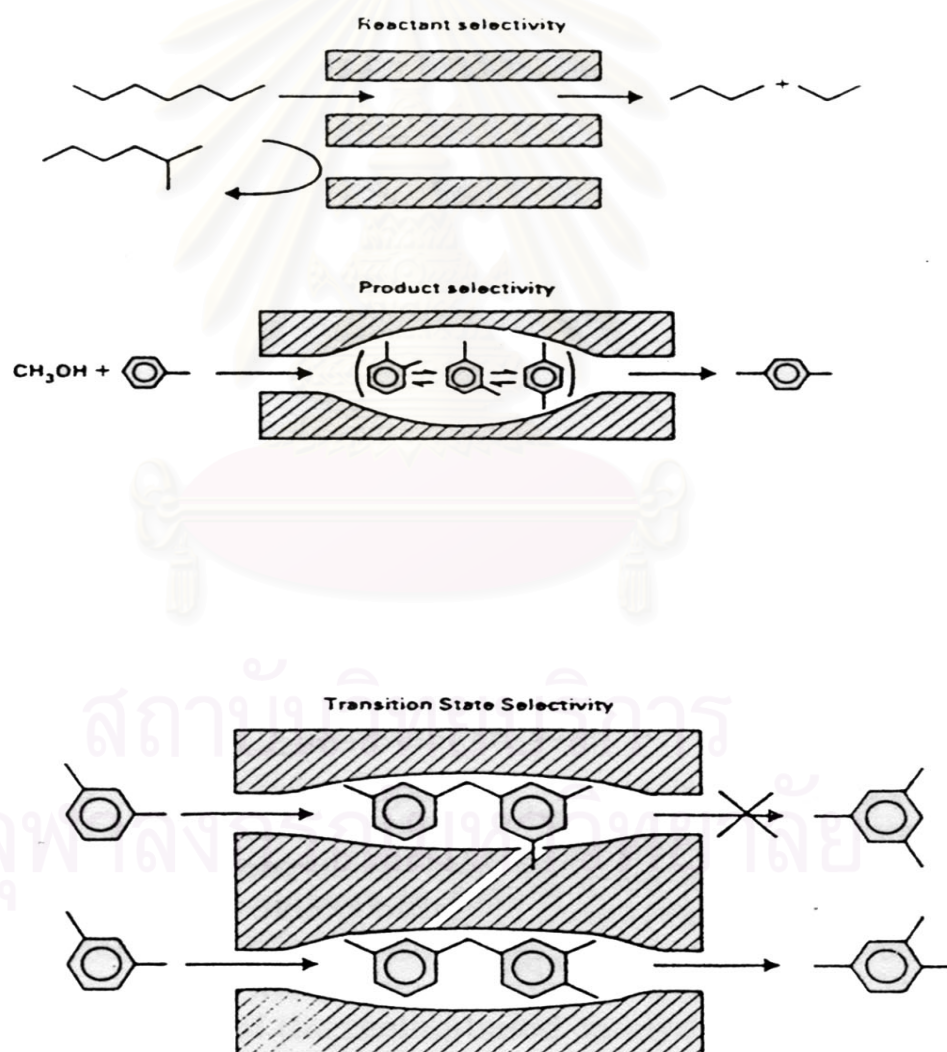
Figure 2.9 Diagram depicting the three types of selectivity: reactant, product, and transition-state shape selectivity.

2.6   Reaction Mechanisms for MTO Process

The methanol is initially converted to an equilibrium mixture of methanol, dimethyl ether and water, which can be processed catalytically to either gasoline (methanol-to-gasoline, MTG) or olefins (methanol-to-olefin, MTO), depending on the catalyst and/or the process operation conditions. The main reaction steps of methanol conversion to olefins can be summarized as follows:

$$2\ MeOH \underset{+H_2O}{\overset{-H_2O}{\rightleftharpoons}} CH_3OCH_3 \xrightarrow{-H_2O} Light\ Olefins \longrightarrow \begin{array}{l} Paraffins \\ Higher\ olefins \\ Aromatics \\ Naphthenes \end{array} \quad (2.1)$$
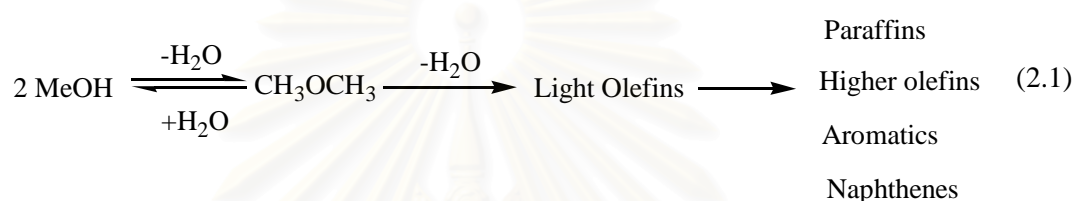
There is general consensus that the intermediate in the dehydration of methanol to dimethyl ether (DME) [step 1 in Eq.(2.1)] over solid acid catalysts is a protonated surface methoxyl, which is subject to a nucleophilic attack by methanol. The subsequent conversion of light olefins to paraffins, aromatics, naphthens and higher olefins [step 3 in Eq.(2.1)] proceeds via classical carbenium ion mechanisms with concurrent hydrogen transfer, which is well known in hydrocarbon chemistry. The MTO process consists of three steps of reactions: (1) the formation of dimethyl ether, (2) the initial C-C bond formation resulting in light olefins, and (3) the subsequent conversion of the primary products (light olefins) into higher olefins. Brønsted acidity is known to be the main source of catalyst activity for the MTO products, while the conjugate Lewis basic site would be responsible for the initial C-C bond formation.

2.6.1 Formation of Dimethyl Ether

Park *et al.*[16] studied a reaction for the formation of dimethyl ether which is shown in Scheme 2.1. The magic-angle-spinning (MAS) NMR data showed that the methanol was reversibly adsorbed through hydrogen to the bridged hydroxyl on Br∅nsted acid sites. The protonation took place very fast on strong acidic sites and reached equilibrium finally. The protonated methanol transformed via dehydration to a surface methoxy species, which was covalently bonded to the lattice oxygen of ZSM-5 and reacted in turn with methanol to form a dimethyloxonium ion (DMO$^+$). Deprotonation of the latter yielded dimethyl ether and H$^+$.
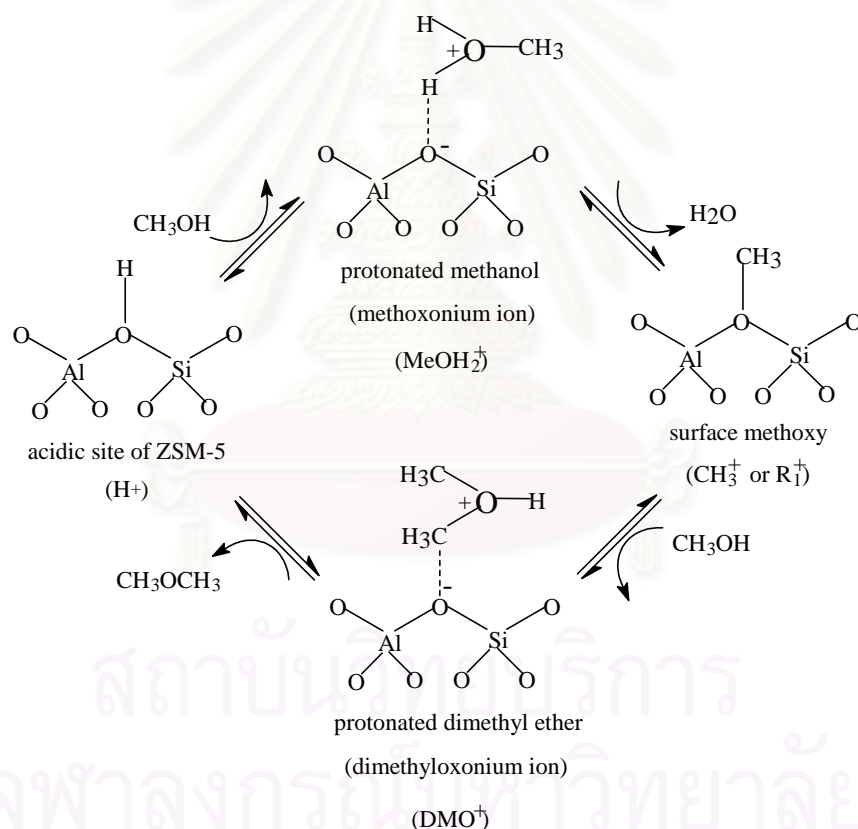
Scheme 2.1 Formation of dimethyl ether during the course of MTO process.

2.6.2 Formation of Primary Hydrocarbon Products

The mechanism of initial C-C bond formation has been proposed to account for the conversion of methanol to olefins. There are several patterns of this kind of mechanism. Although, there is little experimental evidence, the C-C formation is presently the most promising mechanism to express the formation of light olefins from the equilibrium system of methanol, dimethyl ether and water.

a. Oxonium ylide mechanism

Van den Berg *et al.*[60] postulated that dimethyl ether interacted with a Brønsted acid site on the solid catalyst to form a dimethyl oxonium ion, which reacted further with another dimethyl ether to form a trimethyl oxonium ion. This trimethyl oxonium ion was subsequently deprotonated by a basic site to form a surface associated dimethyl oxonium methyl ylide species. The next step was either an intramolecular Stevens rearrangement, leading to the formation of methylethyl ether, or an intermolecular methylation, leading to the formation of the ethyldimethyl oxonium ion. In both cases ethylene was formed via β-elimination as shown in Scheme 2.2. Bimolecular methylation of the dimethyl oxonium ylide resulted in the ethyldimethyl oxonium ion, rather than an intramolecular Stevens rearrangement. In addition, a number of other investigators favor this mechanism as a result of the linear dependence of hydrocarbon formation and zeolite Brønsted acidity.

$$CH_3OCH_3 \xrightarrow{\ CH_3OH_2^{\oplus}\ }$$
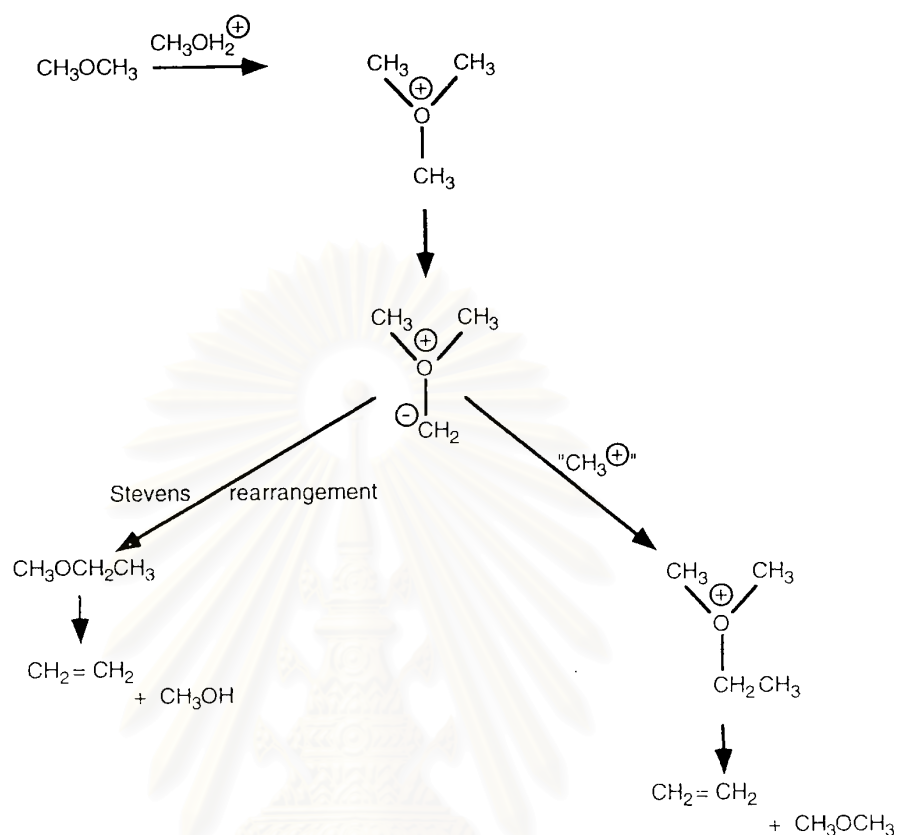
Scheme 2.2 A proposed oxonium ylide mechanism in the MTO process.

In summary, the oxonium ylide mechanism involves the formation of a surface-bound intermediate as the initial reaction step. The zeolite surface OH-group is methylated to form the methyloxonium intermediate, which gives rise to a surface-bound methylene-oxonium ylide due to deprotonation. The surface-bound methylene oxonium ylide is isoelectronic with a surface-associated carbene, as outlined in Scheme 2.3

$$Z\text{-}OH \ + \ CH_3OH \longrightarrow Z\text{-}O\text{-}CH_3 \ + \ H_2O$$

$$Z\text{-}O\text{-}CH_3 \longrightarrow Z\text{-}O\text{-}CH_2 \qquad \text{surface-incorporated ylide}$$

$$Z\text{-}O: \ :CH_2 \qquad \text{surface-associated carbene}$$
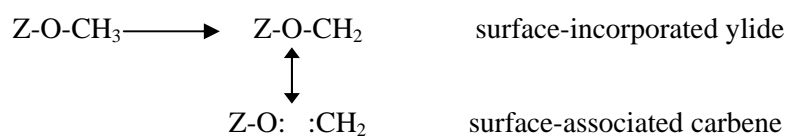
Scheme 2.3 A proposed oxonium ylide mechanism applied to the zeolite surface.

Hutchings *et al.*[68] proposed a mechanism for the formation of the nucleophilic carbon atom in the form of a surface ylide species. An adsorbed methanol molecule was dehydrated to form a surface-bound methoxy species of which a proton was then transferred to a neighboring bridged oxygen to form a charged surface ylide nearby a Brønsted acide site. The formation of the surface methoxy in which the surface oxygen, methyl carbon and the leaving OH group were roughly colinear follows a classic S_N2 mechanism (Eq. 2.2 in Scheme 2.4). The initial C-C bond should then be formed in a more facile reaction between a methanol (or dimethyl ether) and the surface ylide (Eq. 2.3 in Scheme 2.4) which would lead to the formation of a surface ethoxy group. Ethylene was able to be formed by β-elimination along with reforming the Brønsted acid site. Alternatively, the surface ethoxy species could react with further methanol molecules to form a surface iso-propoxy group and subsequently a tertiary butoxy group. These surface species undergoing β-elimination would lead to the formation of propylene and iso-butylene, respectively.
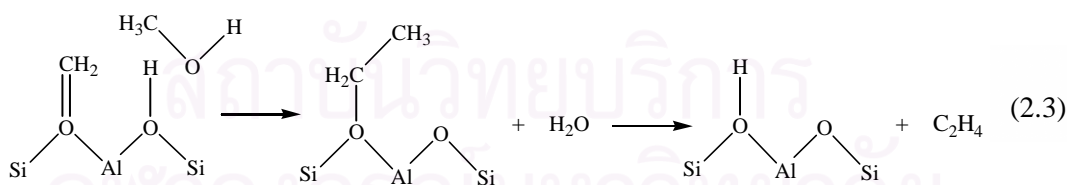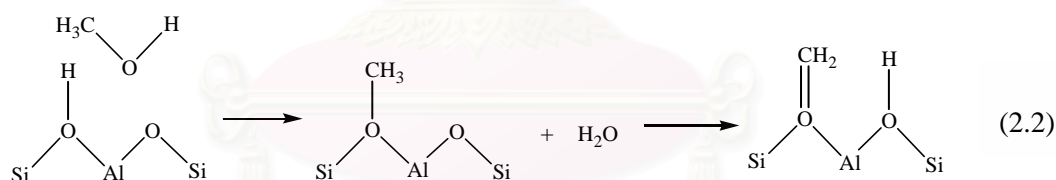
Scheme 2.4 A proposed mechanism for the formation of surface ylide species.

Sánchez del Campo *et al.*[75] supported the oxonium ylide mechanism for methanol transformation into olefins on SAPO-34. The oxonium ions were successively methylized by propagation reaction in solid phase resulting in the formation of ethyloxonium and propyloxonium. The oxonium ions formed were decomposed to give ethylene and propylene, as shown in Scheme 2.5.
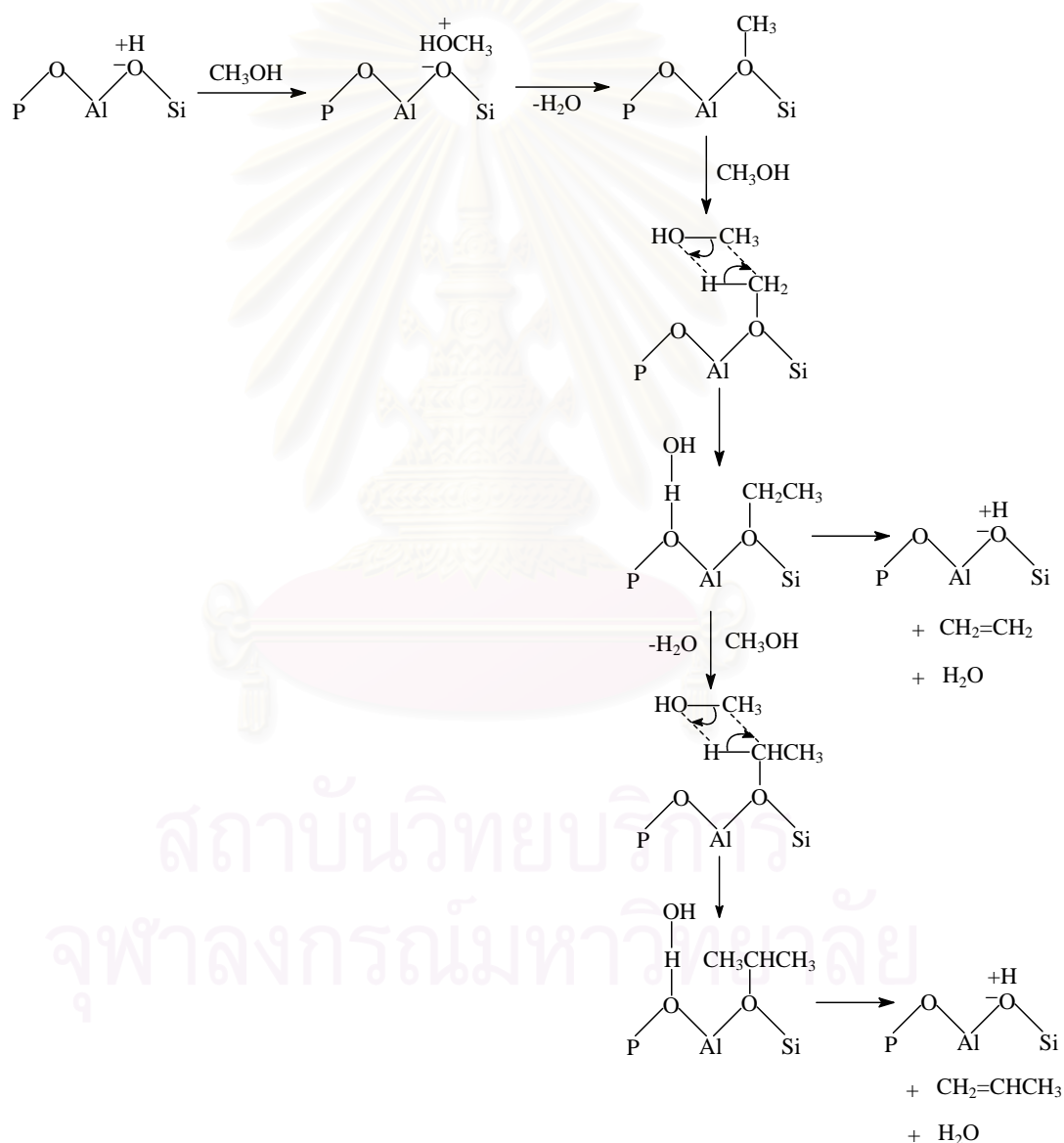
Scheme 2.5   Another proposed mechanism of surface oxonium ions.

b. Carbene mechanism

The carbene mechanism[60,67] involved the α-elimination of water from methanol followed by either polymerization of the resultant cerbene to olefins or by concurrent sp^3 insertion of carbene into methanol or dimethyl ether. The formation of the carbene by the cooperative action of acid and basic sites in mordenite, was suggested by Swabb and Gates and can be summarized in Scheme 2.6
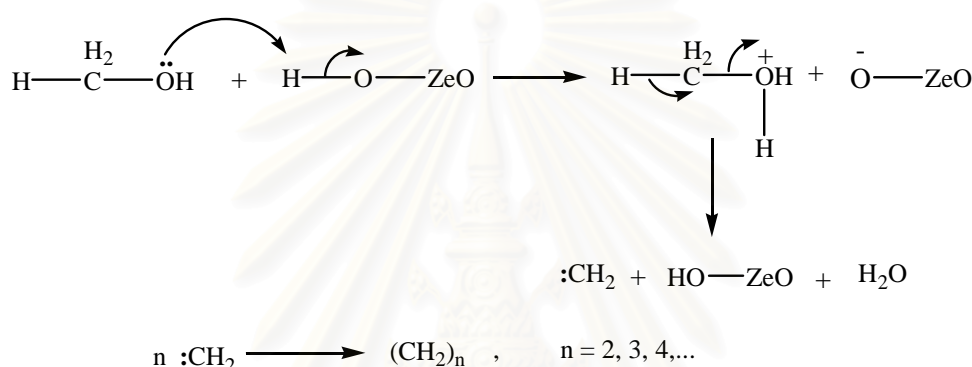
Scheme 2.6   The carbene formation from methanol adsorbed on the zeolite surface

Whereas the oxonium ylide mechanism essentially involves the formation of a surface-bound intermediate as the initial reaction step, the carbene mechanism involves only surface associated intermediates. As previous mentioned the surfaced-associated carbene is isoelectronic with the surface-bound methylene oxonium ylide species.

c. Carbenium ion intermediates.

While C_3-C_7 olefins apparently result from the direct transformation of dimethyl ether (or methanol), this is not the case for ethylene, even during the initial stages. At high temperatures (400-450 $^\circ$C) and low methanol pressure (10^{-2} bar) the reaction does not favor the secondary transformation of olefin (repeated methylation, oligomerization and cracking of higher olefins) and the size of melucules seems to be over the average pore-size of the zeolite.

Fougerit et $al.$[58] investigated at a contact time which allows a quasicomplete conversion (90%) of the dimethyl ether-water mixture into hydrocarbons. It should be emphasized that C_6-C_7 olefin are mainly transformed by cracking with the formation of the products expected from an acid mechanism (with carbenium ion intermediates), i.e. propylene from hexenes and, to a smaller extent, butylenes/ethylene mixture, and essentially propylene and butylenes from n-heptenes. Propylene, butylenes and pentenes are mainly transformed through successive oligomerization and cracking steps as shown in Scheme 2.7.

$$2\,C_3^= \rightleftharpoons C_6^= \underset{-\,C_3^=}{\overset{+\,C_3^=}{\rightleftharpoons}} C_9^=$$

$$C_2^= + C_4^= \qquad C_4^= + C_5^=$$
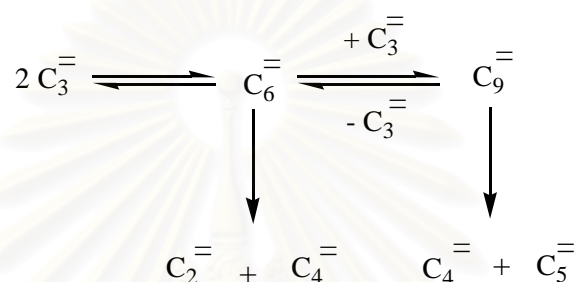
Scheme 2.7 Possible of products from the transformation of C_6 olefin.

All the reactions allowing the formation of ethylene require very unstable carbenium ions as intermediates, e.g. the cracking of iso-hexenes resulting from 1-hexene isomerization as shown in Scheme 2.8. This is why the formation of other products that involve more stable intermediates is much more favored.

$$C-C=C-C-C \xrightarrow{H^+} C-\overset{+}{C}-C-C-C \longrightarrow C-C=C + \overset{+}{C}-C$$
$$\hspace{0.8cm}|\hspace{3.0cm}|\hspace{5.0cm}|$$
$$\hspace{0.8cm}C\hspace{3.0cm}C\hspace{5.0cm}C$$

$$C-C-C=C-C \xrightarrow{H^+} C-C-C-\overset{+}{C}-C \longrightarrow C-\overset{+}{C}-C + C=C-C$$
$$\hspace{0.8cm}|\hspace{3.3cm}|$$
$$\hspace{0.8cm}C\hspace{3.3cm}C$$
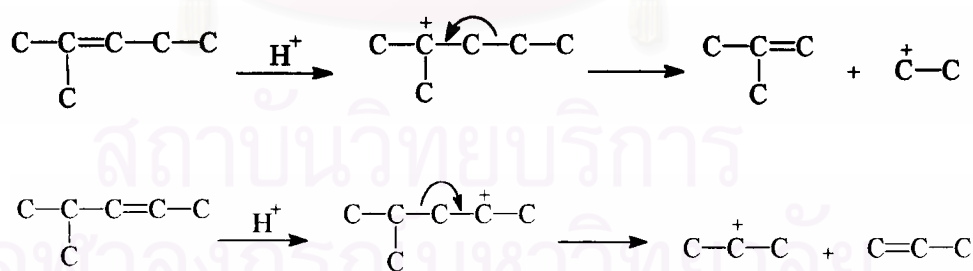
Scheme 2.8 Cracking of isohexenes to ethylene and other products via carbenium ion

intermediates

It was proposed that the formation of the ethyldimethyloxonium ion, the Stevens rearrangement and the formation of an isopropyl carbenium ion were much faster than the formation of the very unstable ethyl carbenium ion (see Scheme 2.9).
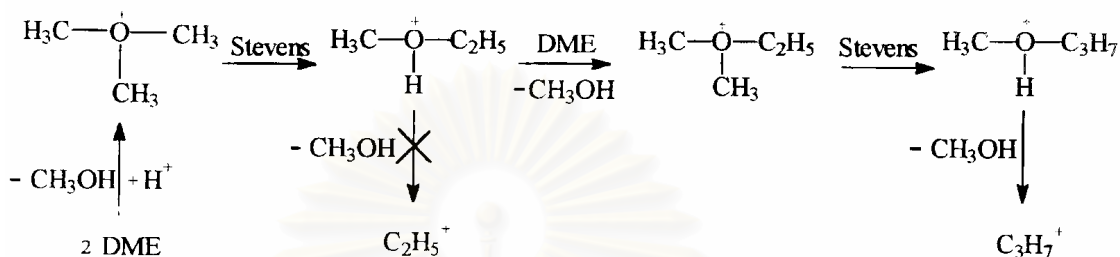
Scheme 2.9   The formation of the isopropyl carbenium ion via carbenium ion and Stevens rearrangement.

It should, however, be emphasized that the Stevens rearrangement occurs through ylide intermediates. In the rearrangement of the ethyldimethyloxonium ion, the ylide intermediate $(\overset{-}{CH_2})O(CH_3)\overset{+}{CH_2}CH_3$ which leads to an unstable propyl carbenium ion, should be favored in comparison to $(CH_3)O(CH_3)\overset{+}{CH}\overset{-}{CH_3}.$
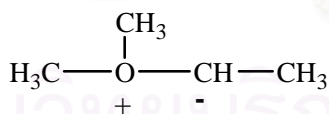
which leads to the isopropyl-carbenium ion, because of the higher acidity of the hydrogens of the methyl group.

d. Hydrocarbon Chain

The consecutive type mechanism with one carbon from methanol adding during each step, addition of methanol and cracking of olefin intermediates may take place as illustrated in Scheme 2.10.

$$2C_1 \longrightarrow C_2H_4 + H_2O$$

$$C_2H_4 + C_1 \longrightarrow C_3H_6$$

$$C_3H_6 + C_1 \longrightarrow C_4H_8 \ldots$$
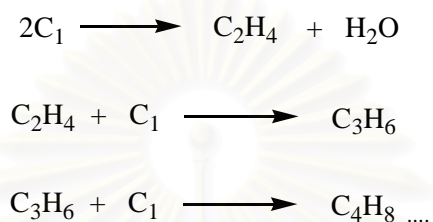
Scheme 2.10 The consecutive-type mechanism of the hydrocarbon chain reactions.

A parallel type mechanism, known as "hydrocarbon pool mechanism" was suggested by Dahl *et al.*[59,62,63], who studied the methanol conversion to hydrocarbon using SAPO-34 as catalyst, ^{13}C-labeled methanol as feed and ^{12}C-ethylene made in situ from ethanol (Scheme 2.11).
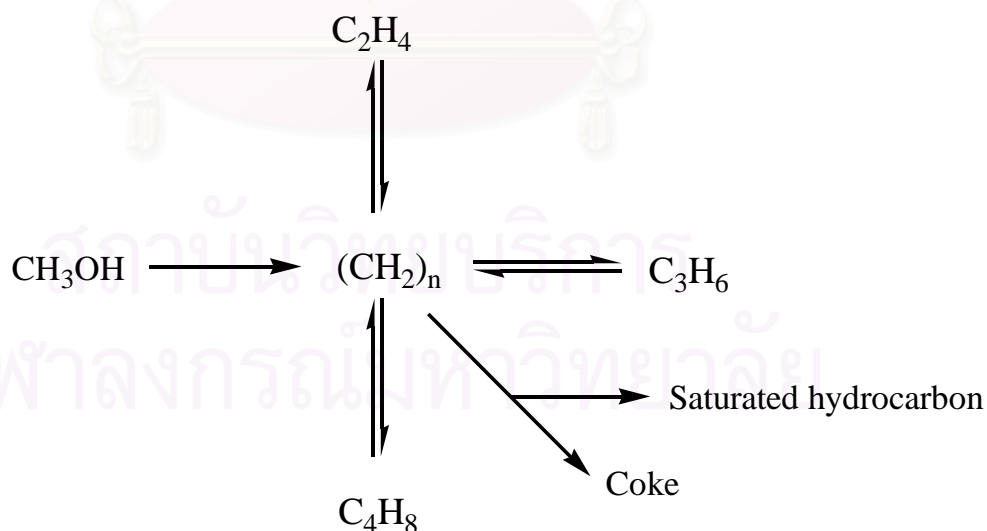
Scheme 2.11 The parallel-type mechanism of hydrocarbon chain reaction.

The 'hydrocarbon-pool' = $(CH_2)_n$ represents an adsorbate which may characteristics in common with ordinary coke, and which might easily contain less hydrogen than indicated. It would perhaps be better represented by $(CH_x)_n$ with $0 < x < 2$. Using SAPO-34 in the methanol conversion reaction, the product pattern is thus simpler than the case using ZSM-5, where a much wider range of products was found. Therefore, it might be easier to obtain a picture of the reaction pathway using SAPO-34, and the authors showed that the consecutive mechanism, as far as propylene formation was concerned, did not turn out to be valid. Only a minor part of the propylene molecules might have been formed by addition of methanol to ethylene since this would imply a $^{12}C/^{13}C$ ratio larger than one. In fact, the ratio seemed to be lower, thus the majority of the propylene molecules should be formed directly from methanol.

CHAPTER III

EXPERIMENTS

3.1   Instruments and Apparatus

Ovens and Furnaces

During the synthesis course of catalysts, the starting mixture was heated at a required temperature using a Memmert UM-500 oven. Heating of any solid sample at 100°C was carried out using the same oven. Calcination of the solid catalysts at elevated temperature was achieved in a Carbolite RHF 1600 muffle furnace with programmable heating rate.

XRD

Synthesized mesoporous materials were identified for the structure using a Rigaku D/MAX-22000 X-ray diffractometer (XRD) at The Petroleum and Petrochemical College, Chulalongkorn University with nickel filtered Cu Kα radiation (30 kV, 30mA) at an angle of 2θ range from 5 to 50°. The scan speed was 2°/min and the scan step was 0.02°. The three slits (scattering, divergent and receiving slits) are fixed at 0.5°, 0.5° and 0.3 mm, respectively.

XRF spectrometer

Silicon, phosphorus and aluminum contents in the catalysts were determined using a SISONS Instrument ARL 8410 X-ray fluorescence spectrometer at Department of Scientific Service, Ministry of Science and Technology.

ICP-AES spectrometer

Nickel contents in the catalysts were analyzed using a Perkin Elmer Plasma-1000 inductively coupled plasma-atomic emission spectrometer (ICP-AES) at the Scientific and Technological Research Equipment Center of Chulalongkorn University.

SEM

Crystal and aggregate morphology of the catalysts were determined using a JEOL JSM-5800LV scanning electron microscope (SEM) at Scientific and Technological Research Equipment Center of Chulalongkorn University.

Nitrogen Adsorptometer

BET specific surface area of the catalysts was carried out using a Quantachrome Autosorb-1 nitrogen adsorptometer at National Metal and Materials Technology Center (MTEC), National Science and Technology Development Agency.

NH_3-TPD Machine

Acid strength of catalysts were determined using a Micromeritics AutoChem 2910 at Petroleum Authority of Thailand.

Gas Chromatograph

Hydrocarbon gases were analyzed using a Shimadzu GC-9A gas chromatograph equipped with a 30-m long and 0.53-mm outer diameter Alumina-PLOT column. Methanol vapor were analyzed using a Shimadzu GC-14A gas chromatograph equipped with a 30-m long and 0.25-mm outer diameter Carbowax (0.25 μm film thickness) column. All GC detectors are flame ionization detectors (FID). The GC heating programs for 10-μl gas and 15-μl methanol vapor analysis are shown in Scheme 3.1 and 3.2, respectively.
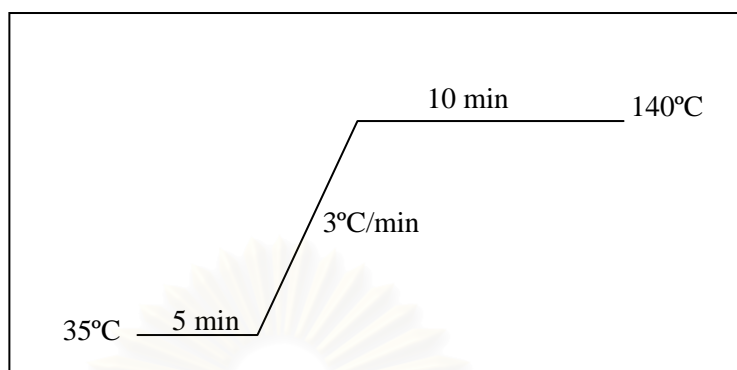
Scheme 3.1   The GC heating program for gas analysis.
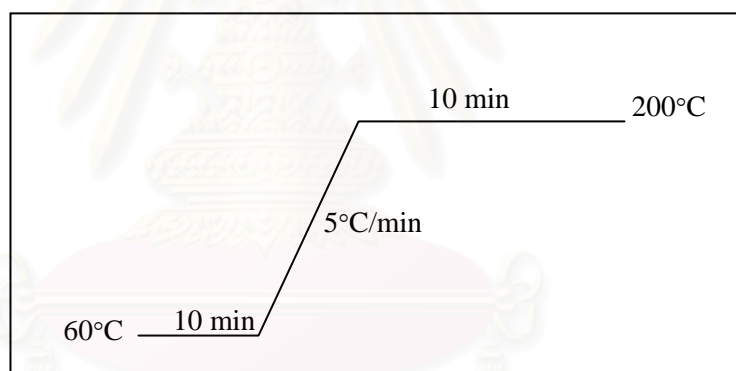
Scheme 3.2   The GC heating program for methanol vapor.

The Apparatus for MTO Catalysis

A catalytic apparatus for methanol conversion to olefin (MTO) assembled in our laboratory comprises of a borosilicate tube reactor of a 0.54-cm internal diameter our own made split tube furnace, a K-type thermocouple connected with temperature programming assembly, a gas manifold, a gas-liquid saturator and a nitrogen gas cylinder. The catalytic apparatus is shown in Scheme 3.3.
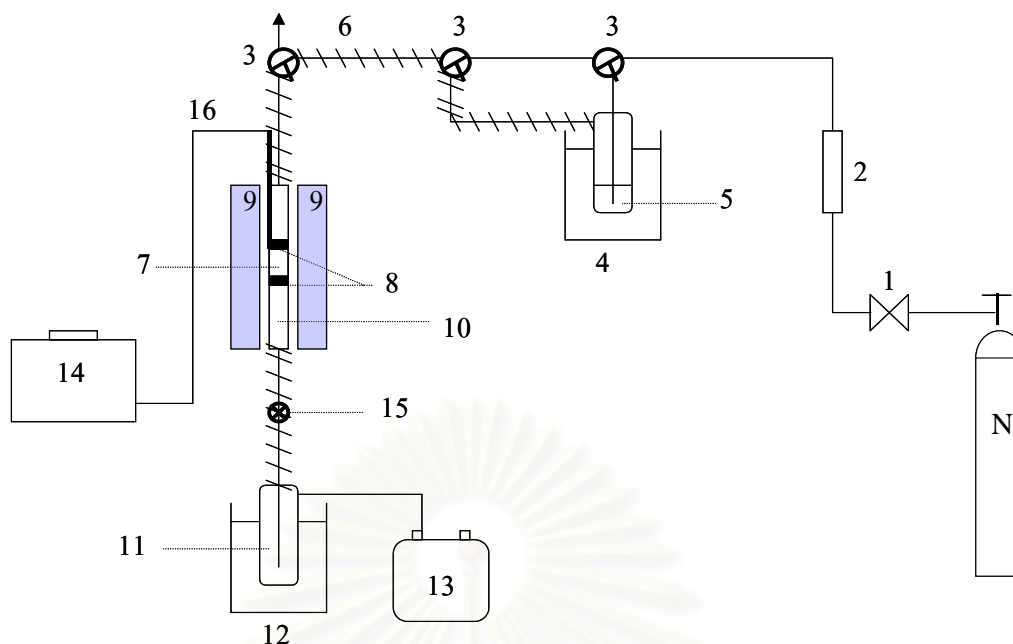
Scheme 3.3 Schematic diagram of the reaction apparatus for the methanol conversion.

1. needle valve	2. flow controller	3. three-way valve
4. water bath	5. methanol	6. heating tape
7. catalyst	8. quartz wool	9. electric furnace
10. tubular reactor	11. cold trap	12. dry ice/acetone bath
13. Tedlar bag	14. temperature controller	
15. outlet sampling point	16. thermocoulple	

3.2   Chemicals and Gases

To remove a trace amount of moisture nitrogen, highly pure grade was purchased from Thai Industrial Gases (TIG) was passed through a 40 cm x 2.5 cm tube of the molecular sieve 4A. Colloidal silica (Ludox AS-40, 40% SiO_2), tetraethylammonium hydroxide (TEAOH 20% in water), and cyclohexylamine were purchased from Aldrich. Aluminum isopropoxide was supplied from Merck. Phosphoric acid (85%) was purchased from Baker. Absolute methanol and nickel nitrate hexahydrate were supplied from Carlo Erba. A standard nickel solution with the concentration of 1,000 ppm for AAS was purchased from Fluka. Standard gas mixture and liquid mixture for GC analysis was

kindly obtained from Thai Olefins. Other chemicals were from Merck, otherwise specifically identified.

3.3   Synthesis of Ni-SAPO-34

3.3.1   Effect of TEAOH/P_2O_5 Ratio on Formation of Ni-SAPO-34 Phase

This synthesis method was attempted for Ni-SAPO-34 with some modification of the method reported by Inui *et al.*[11] Apparatus for preparation of the gel mixture is shown in Figure 3.1. The schematic diagram of this procedure is shown in Scheme 3.4. Into a 250-cm^3 round bottom flask with 4 necks cooled in an ice/water bath the gel mixture with composition of 1.0 or 2.0 TEAOH : 0.6 SiO_2 : 2.0 AIP : 2.0 H_3PO_4 : 0.015 NiO : 72 H_2O or equivalent to 1.0 or 2.0 TEAOH : 0.6 SiO_2 : 1.0 Al_2O_3 : 1.0 P_2O_5 : 0.015 NiO : 72 H_2O. were prepared under nitrogen atmosphere by in sequence gradually adding 10.21 g aluminum isopropoxide (AIP), 18.41 or 36.82 g TEAOH, 2.25 g colloidal silica, 5.76 g phosphoric acid, 0.11 g nickel nitrate hexahydrate, and 1.00 g distilled water. After adding each substance, the mixture was vigorously stirred for 30 min. The resulted gel was further stirred at room temperature for 7 h and transferred into a Teflon lined stainless steel bomb and tightly capped. The bomb was placed in an oven at room temperature. The crystallization of Ni-SAPO-34 was carried out at the temperature of 200ºC for 4 h by increasing the temperature from room temperature to 160ºC, subsequently 200ºC and held for 4 h using the heating program shown in Scheme 3.5. The solid sample was separated by centrifugation (4000 rpm, 30 min), washed several times with deionized water until pH of 7, and dried in an oven at the temperature of 100ºC for 10 h. The so-call as-synthesized product was white solid and obtained at a yield of 1.48 g. It was analyzed for Ni-SAPO-34 phase using XRD. To remove template from the catalyst pore system, the as-synthesized sample was calcined at the temperature of 540ºC for 24 h. The heating program for removal of template from the catalyst pore system is shown in Scheme 3.6.

4-NECKED FLASK

ICE BATH

Aluminum isopropoxide

Tetraethylammonium hydroxide

Colloidal silica

Phosphoric acid

Nickel nitrate

Water

GEL MIXTURE

Crystallization

Washing

Drying

Calcination

As-synthesized Ni-SAPO-34
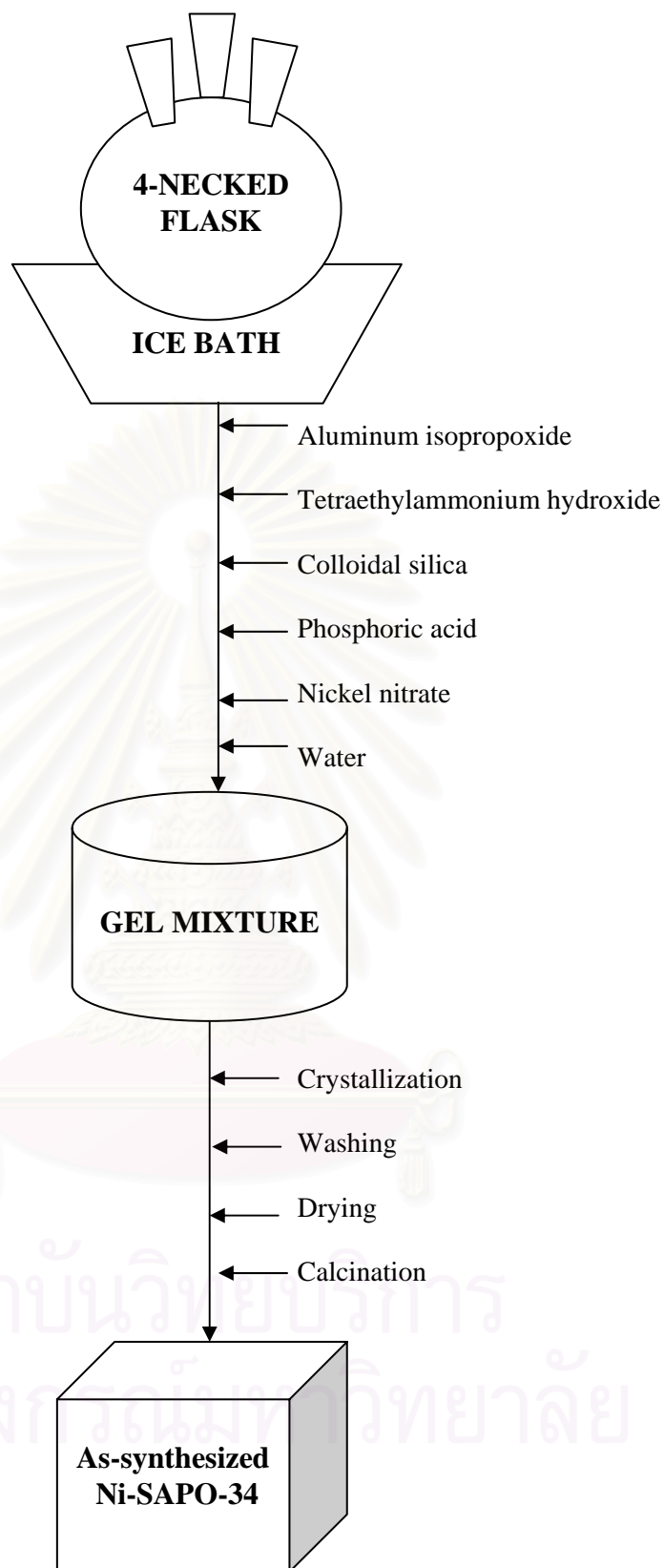
Scheme 3.4 Schematic diagram for the synthesis of Ni-SAPO-34.
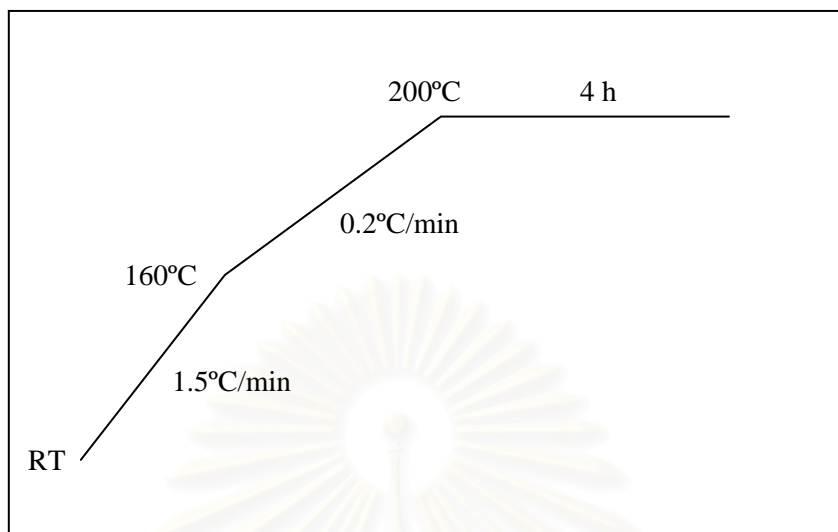
Scheme 3.5   The heating diagram for crystallization of Ni-SAPO-34.
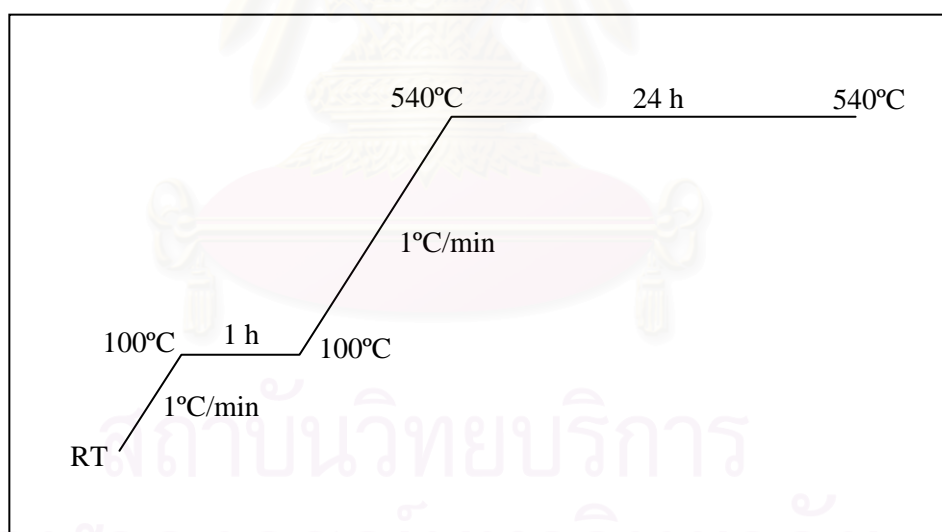
Scheme 3.6   The heating diagram for removal of template from the pore system of

Ni-SAPO-34 and Ni-SAPO-44 catalysts.

3.3.2   Synthesis of Ni-SAPO-34 with Two Different Si/Ni Ratios

The gel mixture for Ni-SAPO-34 with the Si/Ni of 40 and 80 were prepared using the ratio in gel of 2.0 TEAOH : 0.6 SiO_2 : 2.0 AIP : 2.0 H_3PO_4 : 0.015 or 0.0075 NiO : 72 H_2O or equivalent to 2.0 TEAOH : 0.6 SiO_2 : 1.0 Al_2O_3 : 1.0 P_2O_5 : 0.015 or 0.0075 NiO : 72 H_2O. The preparation methods followed the recipe in Section 3.3.1 except that two different amounts of 0.11 g or 0.05 g nickel nitrate hexahydrate were used. The white solid of each product was obtained at a yield of 1.50 g. It was analyzed for Ni-SAPO-34 phase using XRD. To remove template from the catalyst pore system, the as-synthesized sample was calcined at the temperature of 540ºC for 24 h using the heating program shown in Scheme 3.6. The calcined Ni-SAPO-34 samples with different Si/Ni ratios were analyzed for chemical composition using ICP-AES, and XRF, crystal and aggregate morphology using SEM. Due to not enough samples, the used catalysts were regenerated by calcination at 540ºC for 12 h and analyzed for BET specific surface area using nitrogen adsorption, and acid strength using NH_3-TPD.

3.4   Synthesis of Ni-SAPO-44

3.4.1   Effect of Cyclohexylamine/P_2O_5 Ratio on Formation of Ni-SAPO-44 Phase

This synthesis method was attempted for Ni-SAPO-34 with some modification of the method reported by Inui *et al.*[51] Ni-SAPO-44 was synthesized using the same apparatus for synthesizing Ni-SAPO-34 and the schematic diagram for this synthesis is shown in Scheme 3.7. Into a 250-cm^3 round bottom flask with 4 necks cooled in an ice/water bath the gel mixture with composition of 1.7 or 2.0 cyclohexylamine : 0.6 SiO_2 : 1.8 AIP :   1.8 H_3PO_4 : 0.015 NiO : 50 H_2O or equivalent to 1.7   or 2.0 cyclohexylamine : 0.6 SiO_2 : 0.9 Al_2O_3 : 0.9 P_2O_5 : 0.015 NiO : 50 H_2O were prepared under nitrogen atmosphere by in sequence gradually adding 9.19 g aluminum isopropoxide (AIP) , 5.19 g phosphoric acid, , 2.25 g colloidal silica, 0.11 g nickel nitrate

hexahydrate 4.28 or 5.01 g cyhexylamine, and 20.35 g distilled water. After adding each substance, the mixture was vigorously stirred for 30 min. The resulted gel was further stirred at room temperature for 7 h and transferred into a Teflon lined stainless steel bomb and tightly capped. The bomb was placed in an oven at room temperature. The oven was then heated up to 200ºC and the temperature was kept constant for 10 days as shown in Scheme 3.8. The solid sample was separated by centrifugation (4000 rpm, 30 min), washed several times with deionized water until pH of 7, and dried in an oven at the temperature of 100ºC for 10 h. The schematic diagram of this procedure is shown in Scheme 3.7. The white solid product was obtained at a yield of 4.98 g. It was analyzed for Ni-SAPO-44 phase using XRD.

3.4.2   Synthesis of Ni-SAPO-44 with Two Different Si/Ni Ratios

The gel mixture for Ni-SAPO-34 with the Si/Ni of 40 and 80 were prepared using the ratio in gel of 1.7 cyclohexylamine : 0.6 SiO_2 : 1.8 AIP : 1.8 H_3PO_4 : 0.015 or 0.0075 NiO : 50 H_2O or equivalent to 1.7 cyclohexylamine : 0.6 SiO_2 : 0.9 Al_2O_3 : 0.9 P_2O_5 : 0.015 or 0.0075 NiO : 50 H_2O The preparation methods was followed the recipe in Section 3.4.1 except that two different amounts of 0.11 g or 0.05 g nickel nitrate hexahydrate were used. The so-called as-synthesized Ni-SAPO-44 product was white solid and was obtained at a yield of 5.00 g. It was analyzed for Ni-SAPO-44 phase using XRD. To remove template from the catalyst pore system, the as-synthesized sample was calcined at the temperature of 540ºC for 24 h using the same heating program shown in Scheme 3.5. The calcined Ni-SAPO-44 samples with different Si/Ni ratios were analyzed for chemical composition using ICP-AES, and XRF, crystal and aggregate morphology using SEM. Due to not enough samples, the used catalysts were regenerated by calcination at 540ºC for 12 h and analyzed for BET specific surface area using nitrogen adsorption, and acid strength using NH_3-TPD.
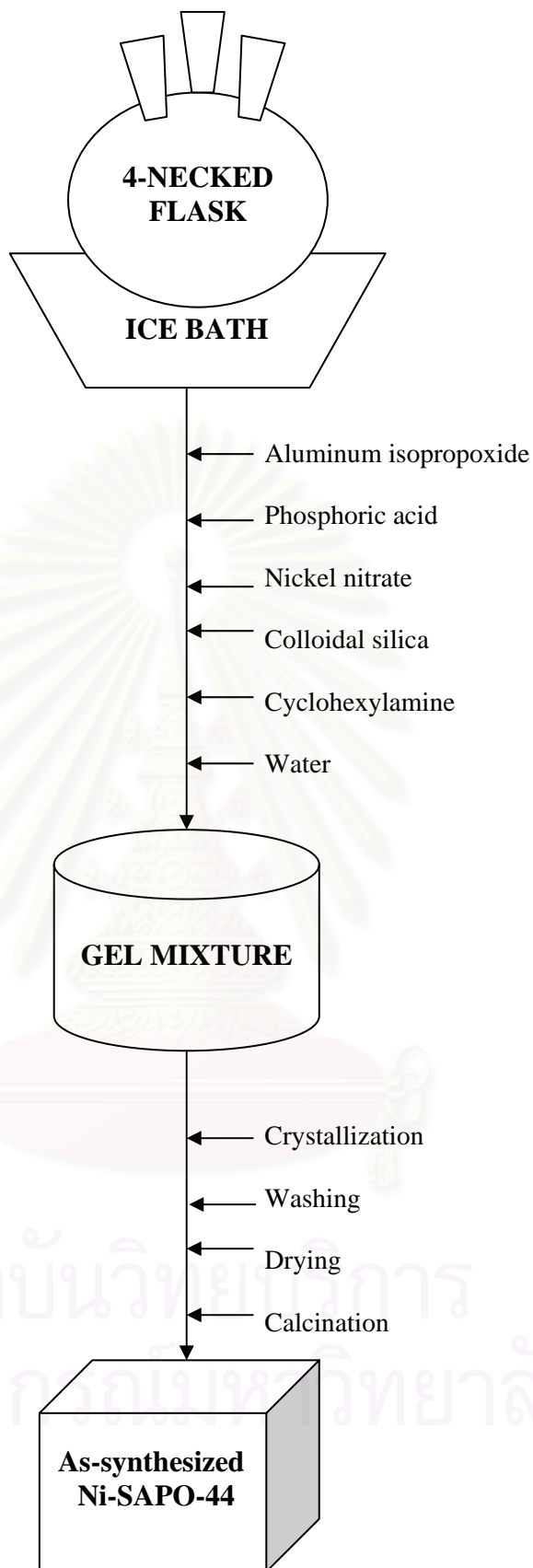
Scheme 3.7   Schematic diagram for the preparation of Ni-SAPO-44.
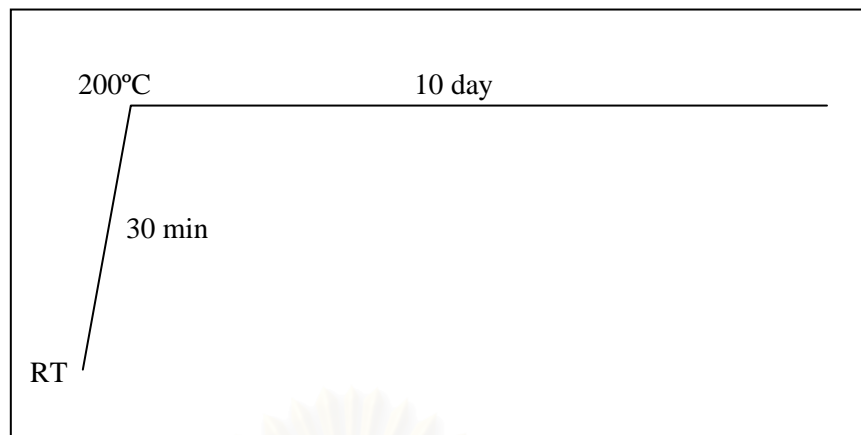
Scheme 3.8   The heating diagram for crystallization of Ni-SAPO-44.

3.5   Preparation of ICP-AES Samples

In a 100-cm^3 Teflon beaker, 0.0300 g of a calcined catalyst was soaked with 10 cm^3 of 6 M HCl and subsequently with 10 cm^3 of 48 % hydrofluoric acid to get rid of silica in the form of volatile SiF$_4$ species. The solid was heated but not boiled until dryness on a hot plate. The fluoride treatment were repeated twice more. An amount of 10 cm^3 of a mixture of 6 M HCl and 6M HNO$_3$ at a ratio 1 : 3 was added and further heated until nearly dryness. An amount of 5 cm^3 of 6 M HCl was added to the beaker and warmed for 5 min. An amount of 10-cm^3 deionized water was added to the beaker and warmed for 5 min to complete dissolution. The solution was transferred to a 100-cm^3 PP volumetric flask and made to the volume by adding deionized water. The flask was capped and shaken thoroughly. If the sample is not analyzed for titanium content immediately, the solution was then transferred into a plastic bottle with a treaded cap lined under with a polyethylene seal. The standard solutions of nickel ions of 0, 1, 2, 3, 4, and 5 ppm were used to establish a calibration curve.
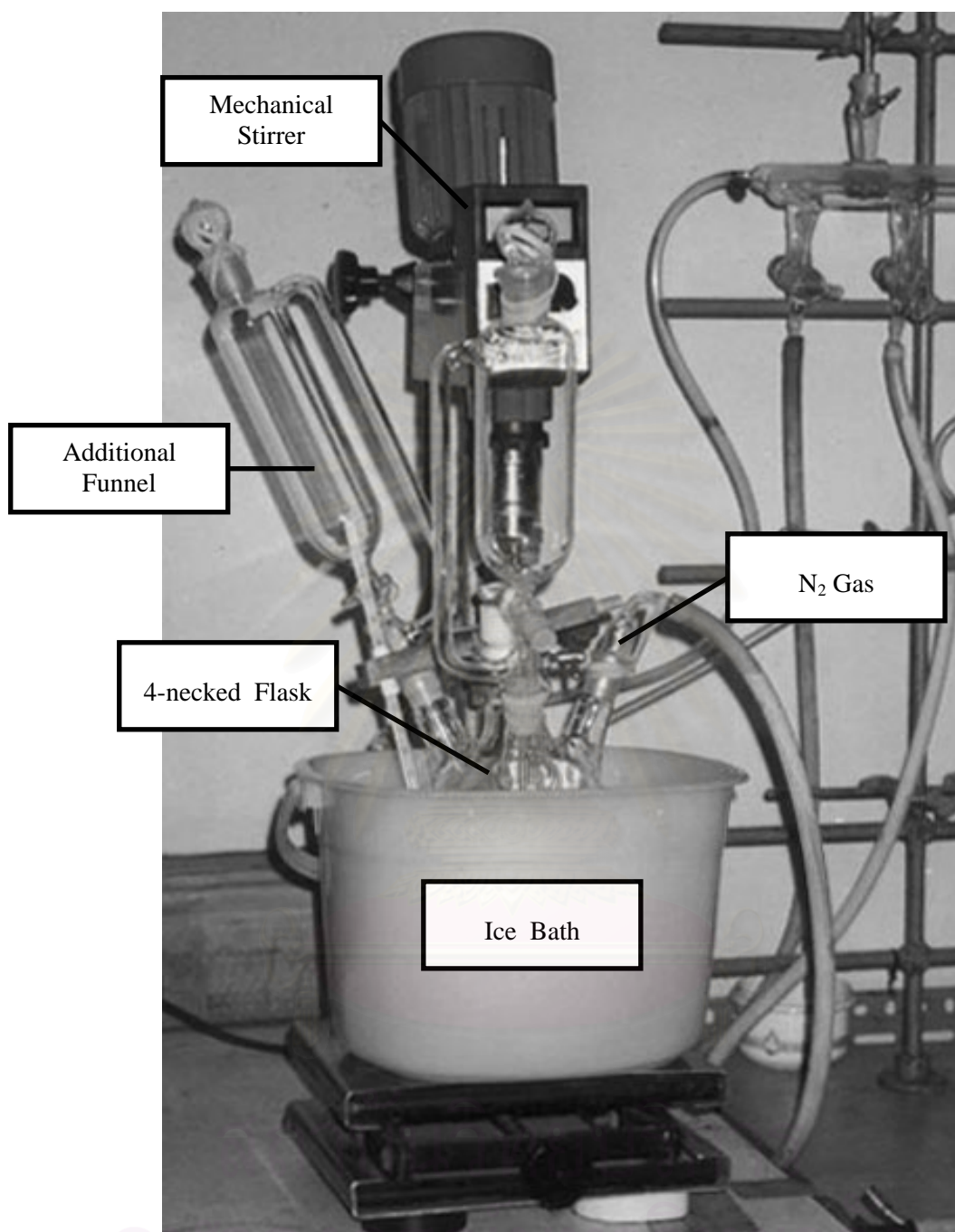
Figure 3.1   Apparatus for preparation of the gel mixture in synthesis of Ni-SAPO34

and Ni-SAPO-44.

3.6   Catalytic Activities of Ni-SAPO-34 and Ni-SAPO-44 in MTO Catalysis

Four catalysts under the examination on the methanol conversion to olefins are Ni-SAPO-34 with Si/Al ratios in gel of 40 and 80 and Ni-SAPO-44 with Si/Al ratios in gel of 40 and 80. The catalysis was carried out using apparatus shown in Figure 3.1. The feed of 22 % methanol in nitrogen was introduced to the tubular reactor at the constant gas-hourly space velocity (GSHV) of 2000 h^{-1} that is correspondent to a gas flow of 8.48 cm^3/min for 0.20 g of catalyst.

The partial vapor pressure was determined using the Antoin equation as shown in Equation 3.1.

$$\log p \quad = \quad A - B/(t + C) \quad \ldots\ldots\ldots\ldots\ldots\ldots\ldots\ldots (3.1)$$

where p is vapor pressure of methanol, mmHg; t is temperature, ºC; A, B, and C are constants for methanol at the temperature ranged from –14 to 65ºC (A = 7.89750, B = 1474.08, and C = 229.13).

3.6.1   Preparation of Tiny Pellet Catalysts

An amount of 0.10 g of each ground catalyst was pressed to a 0.7-mm thick self-supporting wafer using a stainless steel die of a 13-mm inner diameter, in the similar manner to making KBr samples for IR measurement. The pressing force of 3 tons was held on the catalyst wafer for 5 min. In an agate mortar, the catalyst wafer was crushed into tiny pellets of a size 2.0 x 2.0 x 0.7 mm^3, approximately.

3.6.2 Effect of Time on Stream on Methanol Conversion

An amount of 0.20 g of the tiny pellet Ni-SAPO-34 catalyst with the Si/Al ratio in gel of 40 was loaded into a middle part of a borosilicate tube reactor, 5.4-mm inner diameter and hold in place by a plug of quartz wool. The catalyst portion was also covered with small amount of quartz wool. The height of the catalyst portion was 13 mm resulted in the catalyst volume of 0.30 cm^3. For activation of the catalyst, the catalyst in the tube reactor was then heated at 500°C for 1 h, at the pure nitrogen flow of 8.48 cm^3/min. The feed of 22 % methanol in nitrogen was passed from the top through the catalyst at GHSV of 2000 h^{-1} or 8.48 cm^3/min at the tube outlet while the catalyst was still heated at 500°C. The gas products were collected into a Tedlar bag for 20 or 40 min before switching off the bag. They were analyzed for hydrocarbon components using GC equipped with the Alumina-PLOT column.

3.6.3 Effect of Temperature on Methanol Conversion Over Ni-SAPO-34

The Ni-SAPO-34 catalysts with Si/Ni ratio in gel of 40 and 80 were activated at 500°C under the nitrogen flow for 1 h. Then, the feed of methanol in nitrogen was introduced through the catalyst at the GHSV of 2000 h^{-1}. The catalytic reactions were performed at different temperatures: 300, 350, 400, 450, and 500°C. After 40 min of time on stream, gas products were collected and analyzed using GC.

3.6.4 Effect of Temperature on Methanol Conversion Over Ni-SAPO-44

In similar to manner to the activity test of Ni-SAPO-34, a the Ni-SAPO-44 catalysts with Si/Ni ratio in gel of 40 and 80 were activated at 500°C under the nitrogen flow for 1 hr. Then, the feed of methanol in nitrogen was introduced through the catalyst with GHSV of 2000 h^{-1} . After 40 min of time on stream, gas products were collected and analyzed using GC.

3.7   Coke Formation

After the experiment in Section 3.6.3 and 3.6.4, the used catalysts were dried in an oven at the temperature of 200ºC for 2 h. To determine the amount of coke deposited in the catalysts, the dried catalysts were calcined in a muffle furnace at 600ºC for 8 h. The coke amounts were determined using Equation 3.2.

$$\%\text{wt coke} = \frac{(W_{un-cal} - W_{cal}) \times 100}{W_{un-cal}} \quad\quad\text{.......................... (3.2)}$$

where W_{un-cal} is weight of the used catalyst before calcination at 600ºC and W is weight of the used catalyst after calcination at 600ºC.
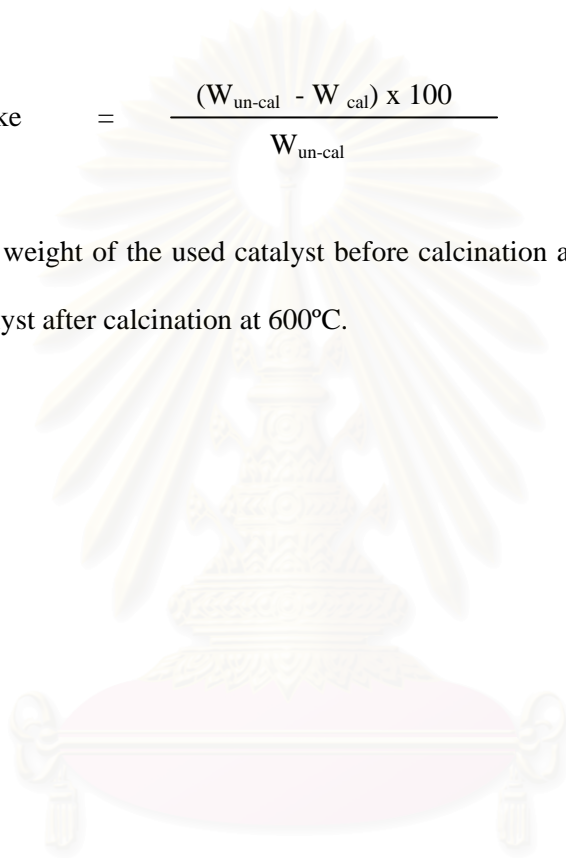
CHAPTER IV

RESULTS AND DISCUSSION

4.1 The Optimal Condition for Ni-SAPO-34 Synthesis

4.1.1 Effect of TEAOH /P_2O_5 Ratio on Formation of Ni-SAPO-34

The Ni-SAPO-34 catalyst with the Si/Ni ratio of 40 was synthesized by modifying the rapid crystallization method described in the literature.[11] In this study, a gel with the composition of 1.0-2.0 TEAOH : 0.6 SiO_2: 1.0 Al_2O_3: 1.0 P_2O_5: 0.015 NiO: 72 H_2O was used. The gel mixture was heated from room temperature to 160ºC and then up to 200ºC with heating rates of 1.5 and 0.2°C/min, respectively, and kept at 200ºC for 4 h.

The X-ray diffraction patterns of the product obtained by varying TEAOH/P_2O_5 in this work are shown in Figure 4.1 (a and b) while those of Ni-SAPO-34,[32] SAPO-34[32] and SAPO-5[23] from literature are also demonstrated in comparison in Figure 4.1 (c, d, and e). It was claimed that[32] SAPO-34 was obtained with some impurity of nickel oxide with the reflection peaks at $2\theta = 18.8$ and 40.6º in XRD pattern illustrated in Figure 4.1 (c). In this work as shown in Figure 4.1 (a), it was found that the Ni-SAPO-34 product prepared at the TEAOH/P_2O_5 ratio of 1.0 exhibits the characteristic peaks of both SAPO-34 and SAPO-5 structures, where the latter was formed as a major product. The baseline of the XRD patterns is flat, therefore, amorphous phase such as condense gel is not present in the product. Considering Figure 4.1 (b), the Ni-SAPO-34 product prepared at the TEAOH/P_2O_5 ratio of 2.0 contains the neat phase of SAPO-34 without any impurity of SAPO-5 or any other phase. The effect of the TEAOH/P_2O_5 ratio on formation of Ni-SAPO-34 along with SAPO-5 is agreed with what observed for SAPO-34 by Liang *et al.*[12] When the ratio of

TEAOH/P_2O_5 was equal to 1.0, The formation of SAPO-5 was favored. The pure phase of SAPO-34 was only obtainable when the ratio of TEAOH/P_2O_5 was in the range of 2.0-3.0.

In fact, after the first cycle of washing, the product obtained in this study was found to contain two solid portions obviously in the centrifuge tube, the green gelatinous portion on top and the white one at bottom. However, the dry green portion shows no reflection peak in XRD pattern, therefore it must be amorphous nickel species and the dry white portion reflects the X-ray at the 2θ of 18.8 and 40.6º at the low intensity compared to the characteristic peaks of Ni-SAPO-34. Upon washing several times with deionized water (more than 20 cycles of 30-min stirring in water and 30-min centrifugation), the green portion can be removed completely from the white product and the amount of impurity in the white portion was also decreased as followed up by XRD measurements. In addition, SAPO-34 was prepared in similar means without addition of the nickel source. It is found that its XRD pattern presents the impurity phase similar to Figure 4.1 (c). Thus the impurity phase is impossible to be assigned to nickel oxide as claimed in the literature.[32] Similar to that found for Ni-SAPO-34, the impurity can be completely removed from SAPO-34 by washing with deionized water several times.

By matching with the data of JCPDS,[57] it is indicated that the two extra peak at 2θ of 18.8 and 40.6º belong to aluminum hydroxide. The results suggest the existence of aluminum hydroxide in the crystalline form of alumina trihydrate, $Al_2O_3.3H_2O$.

From the results discussed above, the optimal condition for preparing the pure phase of Ni-SAPO-34 catalyst with high crystallinity was using the gel with composition of 2.0 TEAOH : 0.6 SiO_2: 1.0 Al_2O_3: 1.0 P_2O_5: x NiO: 72 H_2O and crystallization was carried out at the temperature of 200ºC for 4 h with two stage heating rates from room temperature to 160ºC at 1.5ºC /min and then to 200ºC at 2ºC /min.
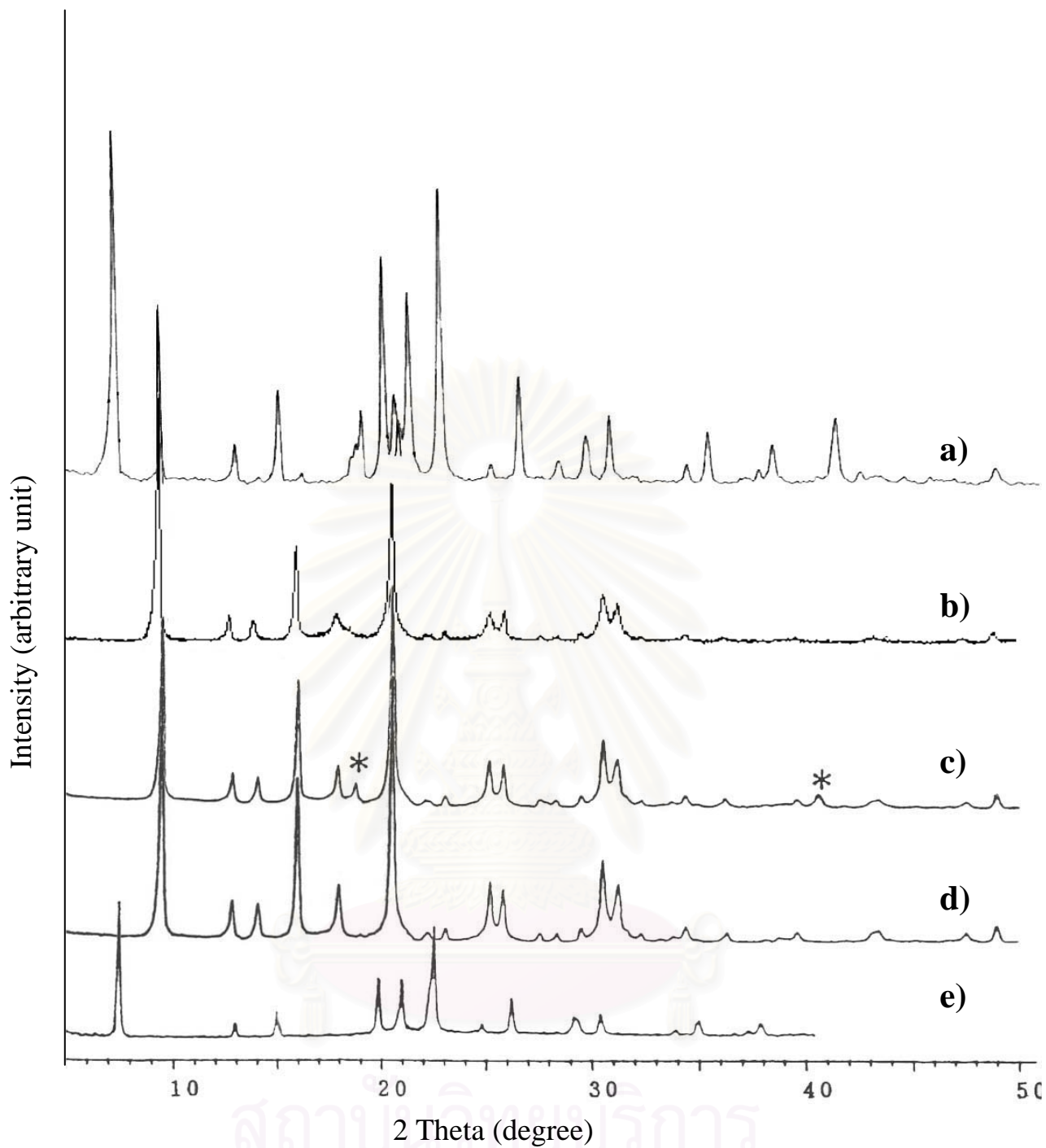
Figure 4.1 XRD patterns of (a) Ni-SAPO-34 (Si/Ni in gel = 40) synthesized using

TEAOH/ P_2O_5 of 1.0, (b) Ni-SAPO-34 (Si/Ni in gel = 40) synthesized using

TEAOH/P_2O_5 of 2.0, (c) Ni-SAPO-34,[32] (d) SAPO-34[32] and (e) SAPO-5.[23]

(a and b are from this work while c, d and e are from literature)

4.1.2   Ni-SAPO-34 Catalysts with Two Different Si/Ni Ratios

XRD patterns of Ni-SAPO-34 with Si/Ni ratios in gel of 40 and 80 are presented in Figure 4.2. The crystallinity of both catalysts is not different. The structure of Ni-SAPO-34 is not affected by the nickel content in gel.

The chemical compositions in gel and in product of the Ni-SAPO-34 catalysts are shown in Tables 4.1 and 4.2, respectively. The quantities of all oxides except silicon oxide are in the vicinity of those in gel. Silicon contents in product are less than one half of those in gel. It seems that not only the Ni-SAPO-34 was formed but the Ni-AlPO$_4$-34 was as well. This is beyond the capability of XRD to identify the phase difference due to both have the same structure as the chabazite-type zeolite.

From SEM photograph of Ni-SAPO-34 with different Si/Ni ratio in Figure 4.3, the morphology of Ni-SAPO-34 seems roughly to be cubic as mistaken by several authors, but in fact, with closely inspected, it belongs to the triclinic structure where $a \neq b \neq c$ as reported by Chakrabarty et al.[9] The increase in Si/Ni ratio or decrease of nickel content in the catalyst results in the increase in crystal size by 5 times. The crystal sizes of Ni-SAPO-34 samples were found to fall over a wide range.

The values of BET specific surface area of Ni-SAPO-34 samples are presented in Table 4.3. The values of 410 and 470 m^2/g are in the range of zeolite with small pores. The Ni-SAPO-34 sample with the higher nickel content exhibits in relative lower surface area. This implies that nickel has some interaction with the framework atoms, Al, P or Si and its occupancy at the pore wall results in the decrease of space in the pore volume and BET specific surface area.
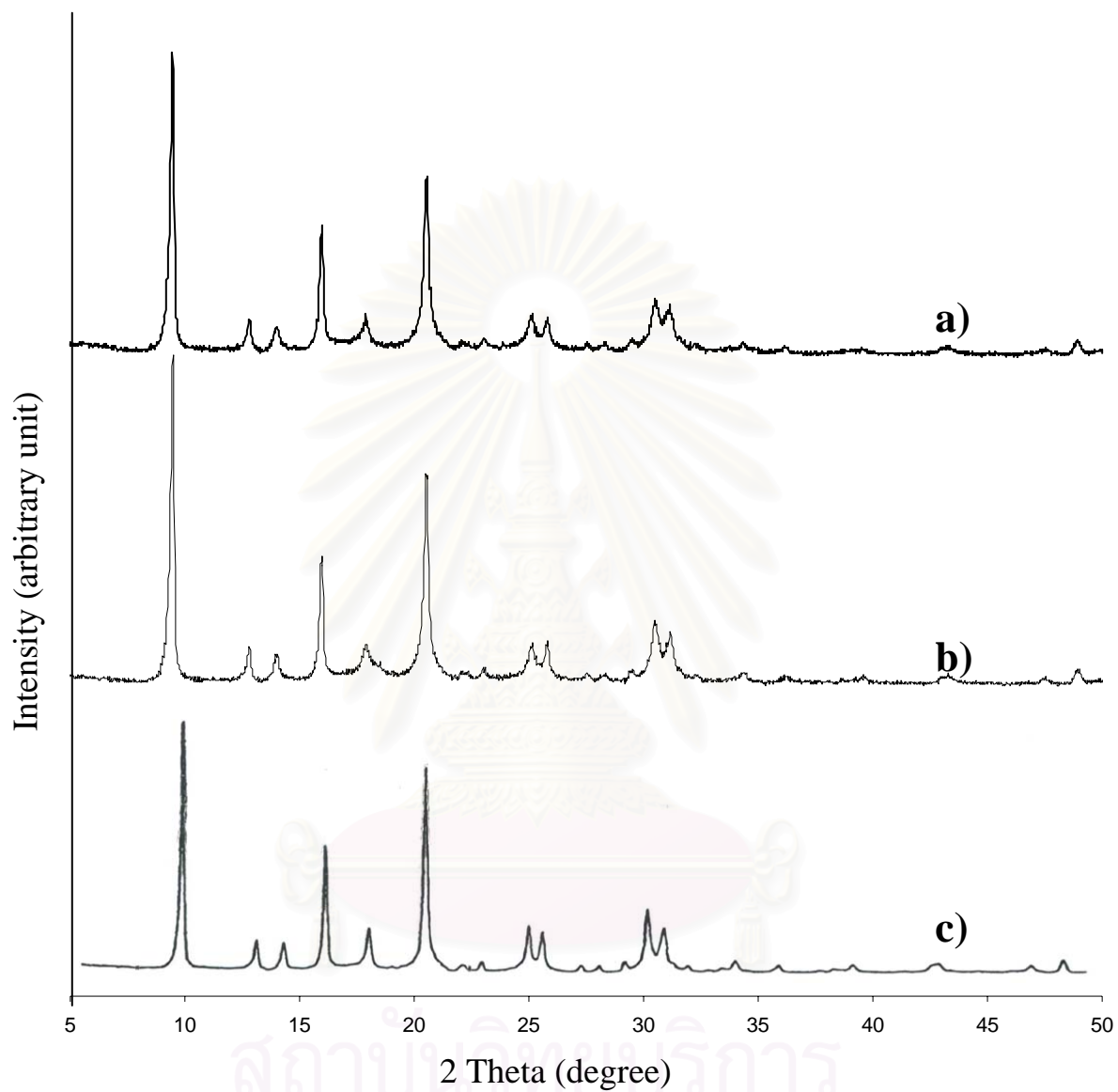
Figure 4.2 XRD patterns of (a) Ni-SAPO-34 (Si/Ni in gel = 40), (b) Ni-SAPO-34 (Si/Ni in gel = 80) and (c) SAPO-34.[32] (a and b are from this work while c is from literature)

Table 4.1 Chemical composition of Ni-SAPO-34 estimated by calculation

Catalyst	Chemical composition (%wt)				Si/Ni	Ni/Al (10^{-3})
	Al_2O_3	P_2O_5	SiO_2	NiO		
Ni-SAPO-34 (Si/Ni = 40)	36.3	50.5	12.8	0.4	40	7.5
Ni-SAPO-34 (Si/Ni = 80)	36.3	50.6	12.8	0.2	80	3.8

Table 4.2 Chemical analysis of Ni-SAPO-34 determined by XRF and ICP-AES

Catalyst	Chemical composition (%wt)				Si/Ni	Ni/Al (10^{-3})
	Al_2O_3 [a,]	P_2O_5 [a,]	SiO_2 [a,]	NiO [b]		
Ni-SAPO-34 (Si/Ni = 40)	37.3	56.4	5.4	0.36	18.6	6.4
Ni-SAPO-34 (Si/Ni = 80)	37.7	55.8	5.0	0.23	27.0	4.1

[a] analyzed by XRF
[b] analyzed by ICP-AES

Table 4.3 BET surface area of Ni-SAPO-34

Catalysts	BET surface areas (m^2/g of catalyst)
Ni-SAPO-34 (Si/Ni = 40)	410
Ni-SAPO-34 (Si/Ni = 80)	470
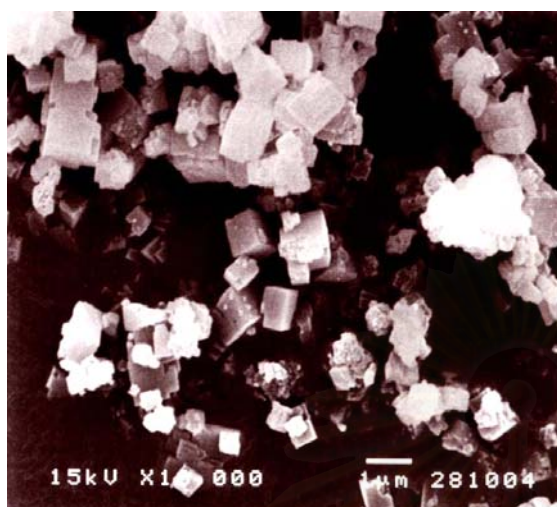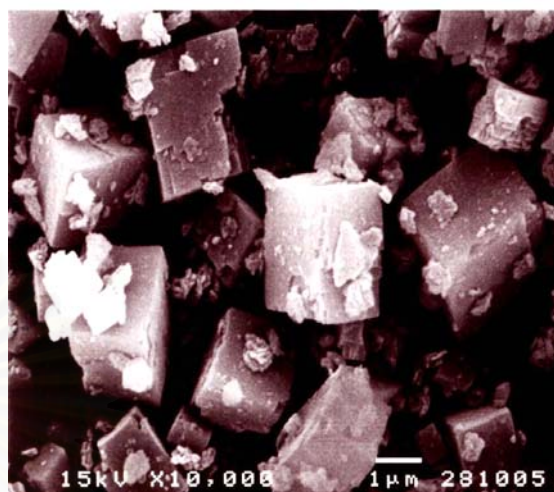
Si/Ni of 40 (X 10000)   **Si/Ni of 80 (X 10000)**
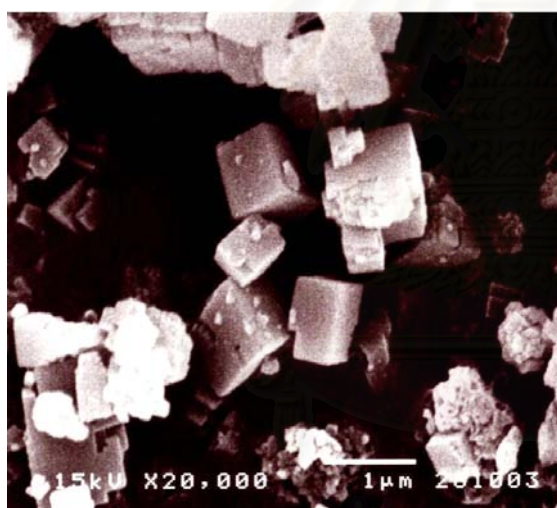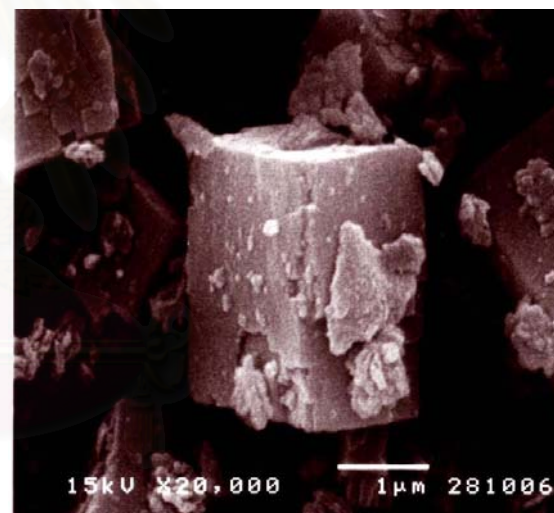
Si/Ni of 40 (X 20000)   **Si/Ni of 80 (X 20000)**

Figure 4.3   SEM photographs of Ni-SAPO-34 with different Si/Ni ratios of 40 and 80.

4.2 The Optimal Condition for Ni-SAPO-44 Synthesis

4.2.1 Effect of Cyclohexylamine/P_2O_5 Ratio on Formation of Ni-SAPO-44

The nickel-containing SAPO-44 catalyst with the Si/Ni ratio of 40 was synthesized hydrothermally following the procedures described in the patented literature[51] except metal species. The composition of the final reaction mixture can be expressed in molar ratio as 1.7 or 2.0 cyclohexylamine: 0.6 SiO_2: 0.9 Al_2O_3: 0.9 P_2O_5: 0.015 NiO: 50 H_2O. The samples were obtained by crystallization in an oven at the temperature of 200ºC for 10 days. XRD patterns of the so-called Ni-SAPO-44 are compared with those of SAPO-44[9] and SAPO-5[23] from literature in Figure 4.5. At the ratio of cyclohexylamine/P_2O_5 of 2.2, some peaks of SAPO-5 were found at low crystallinity. When the ratio of cyclohexylamine/P_2O_5 was decreased to 1.9, the monophasic Ni-SAPO-44 with high crystallinity is achieved. This is in agreement with the results reported by Chen *et al.*[48] It was reported that the Si: Al: P ratio was fixed at 0.3: 1: 1, if cyclohexylamine/Al was less than 0.85, SAPO-5 appeared in the product. If the ratio of cyclohexylamine/Al greater than 1.0 was used, an unidentified phase was obtained (a similar phenomenon was also observed in the synthesis of SAPO-34). Therefore, the optimal condition for synthesis of Ni-SAPO-44 is using the gel composition of 1.7 cyclohexylamine : 0.6 SiO_2: 0.9 Al_2O_3: 0.9 P_2O_5: x NiO: 50 H_2O and crystallization was carried out at the temperature of 200ºC for 10 days.

4.2.2 Ni-SAPO-44 Catalysts with Two Different Si/Ni Ratios

XRD patterns of Ni-SAPO-44 with different Si/Ni ratios of 40 and 80 are presented in Figure 4.6. Both patterns are similar in intensities and similar to the reference pattern of the SAPO-44 structure. There is no other phase found in the samples. This result indicates that both samples have high crystallinity.
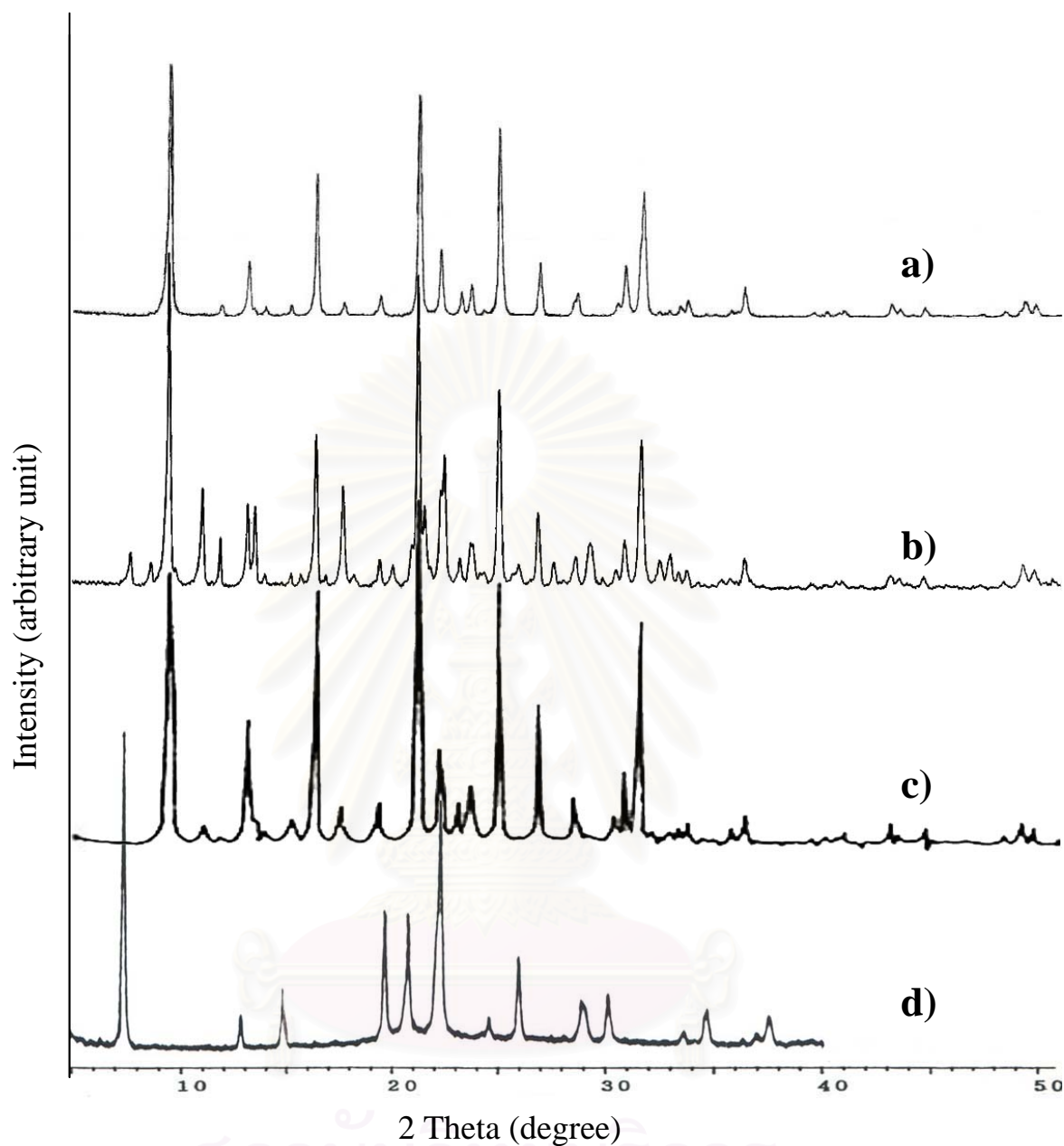
Figure 4.4 XRD patterns of (a) Ni-SAPO-44 (Si/Ni in gel = 40) synthesized using Cyclohexylamine/P_2O_5 of 1.9, (b) Ni-SAPO-44 (Si/Ni in gel = 40) synthesized using Cyclohexylamine/P_2O_5 of 2.2, (c) SAPO-44[9] and (d) SAPO-5.[23] (a and b are from this work while c and d are from literature)
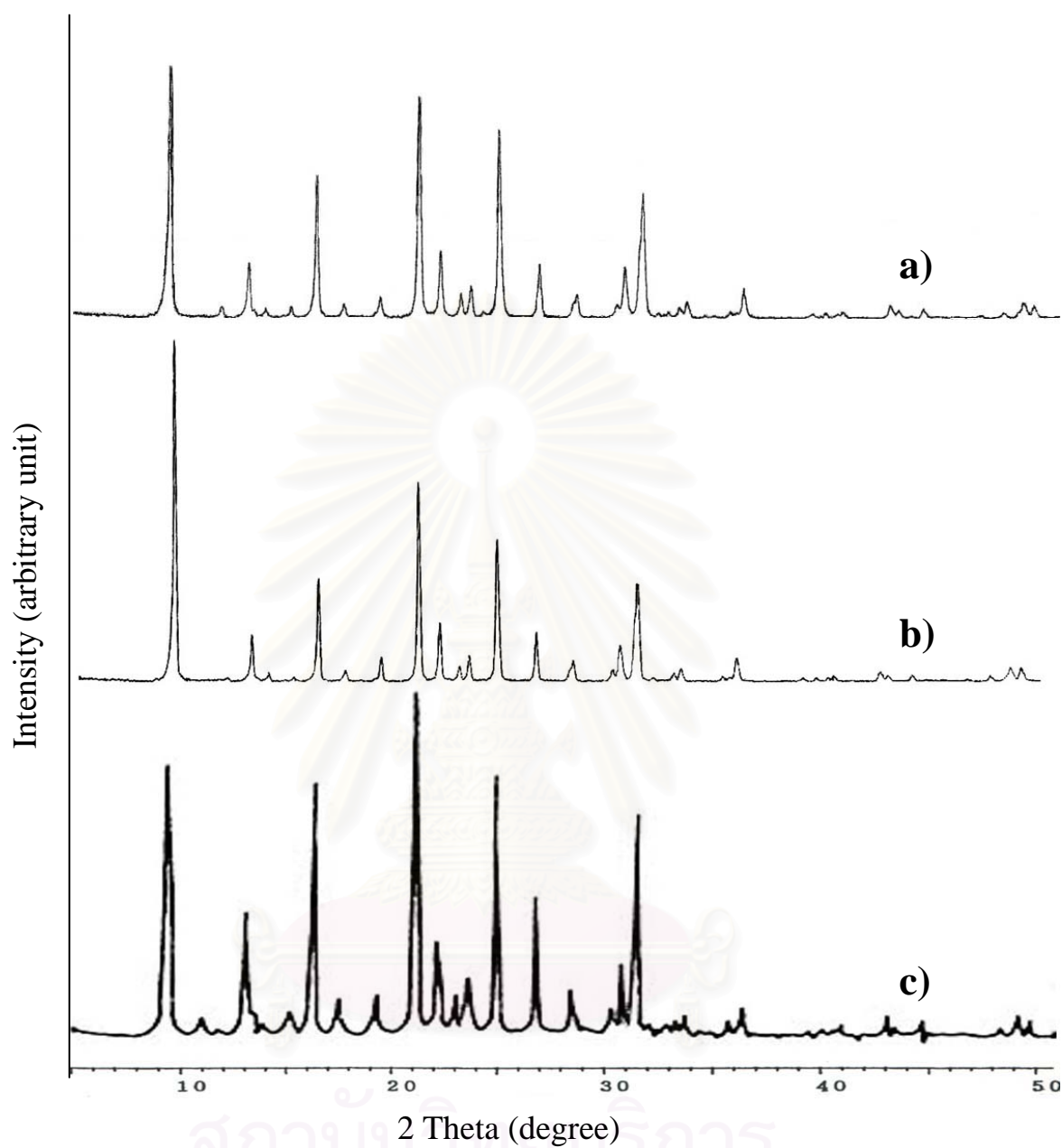
Figure 4.5   XRD patterns of (a) Ni-SAPO-44 (Si/Ni in gel = 40), (b) Ni-SAPO-44

(Si/Ni in gel = 80) and (c) SAPO-44.[9] (a and b are from this work while c is

from literature)

The chemical compositions in gel and in product of the Ni-SAPO-44 catalysts are shown in Table 4.4 and 4.5, respectively. For low nickel loading, the quantities of all oxides are close to those in gel. At high nickel loading the chemical composition especially the nickel oxide content seems to be far from what added in the gel. The silicon is incorporated in the structure of SAPO-44 more facile than in SAPO-34. Prolongation of crystallization time may encourage or assist the condensation of those soluble species from solution to form the crystals. This effect also causes the crystal size of Ni-SAPO-44 far larger than Ni-SAPO-34.

From SEM photograph of Ni-SAPO-44 with different Si/Ni ratio in Figure 4.7, the morphology of Ni-SAPO-44 is quite different from that of Ni-SAPO-34 catalysts. Ni-SAPO-34 (Figure 4.3) was formed as discrete crystal while Ni-SAPO-44 was formed as polycrystals.   Similar to Ni-SAPO-34, the crystal and aggregate sizes of Ni-SAPO-44 samples were found to fall over a wide range.

The values of BET specific surface area of the regenerated Ni-SAPO-44 samples are presented in Table 4.6. The values of 56 and 93 m^2/g are very small due to the structure collapsed after the regeneration of the catalysts at elevated temperature. These values may be applied to only the external surface area. It is neglected to discuss about due to the limitation of the BET method to obtain the right value of specific surface area. These values may be the fake ones.

Table 4.4 Chemical composition of Ni-SAPO-44 estimated by calculation

Catalyst	Chemical composition (%wt)				Si/Ni	Ni/Al (10^{-3})
	Al_2O_3	P_2O_5	SiO_2	NiO		
Ni-SAPO-44 (Si/Ni = 40)	35.8	49.7	14.0	0.4	40	8.2
Ni-SAPO-44 (Si/Ni = 80)	35.8	49.7	14.0	0.2	80	4.1

Table 4.5 Chemical analysis of Ni-SAPO-44 determined by XRF and ICP-AES

Catalyst	Chemical composition (%wt)				Si/Ni	Ni/Al (10^{-3})
	Al_2O_3 [a]	P_2O_5 [a]	SiO_2 [a]	NiO [b]		
Ni-SAPO-44 (Si/Ni = 40)	33.1	55.1	10.0	0.23	54.0	4.8
Ni-SAPO-44 (Si/Ni = 80)	41.1	43.1	15.4	0.19	100.7	3.2

[a] analyzed by XRF
[b] analyzed by ICP-AES

Table 4.6 BET surface area of Ni-SAPO-44

| Catalysts	BET surface areas $(m^2/g$ of catalyst)
Ni-SAPO-44 (Si/Ni = 40)	56
Ni-SAPO-44 (Si/Ni = 80)	93
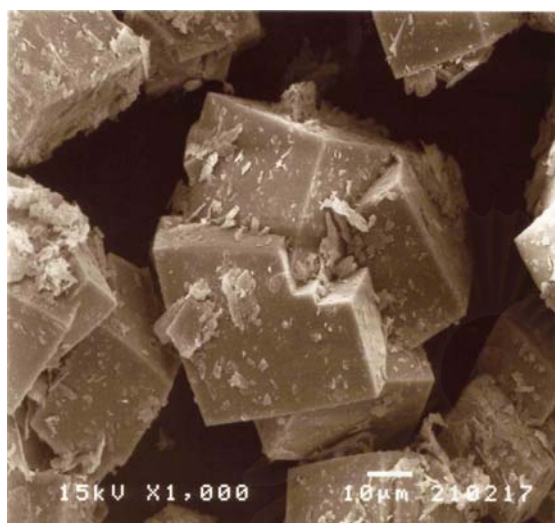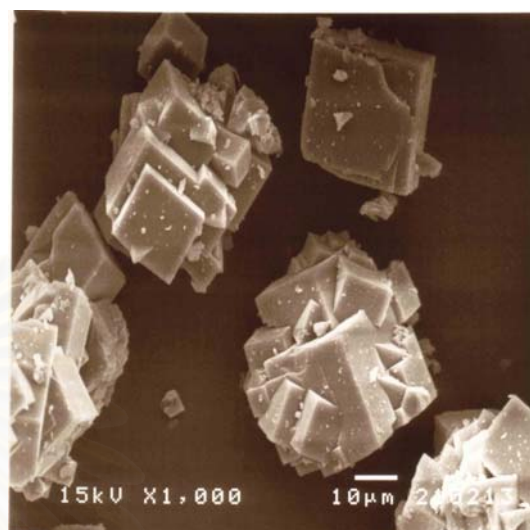
Si/Ni of 40 (X 1000)   Si/Ni of 80 (X 1000)
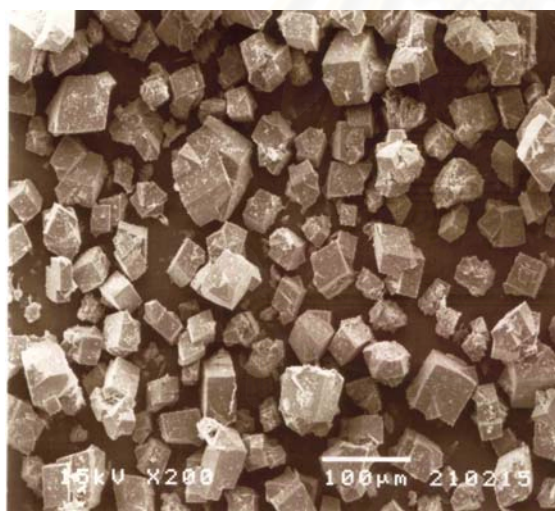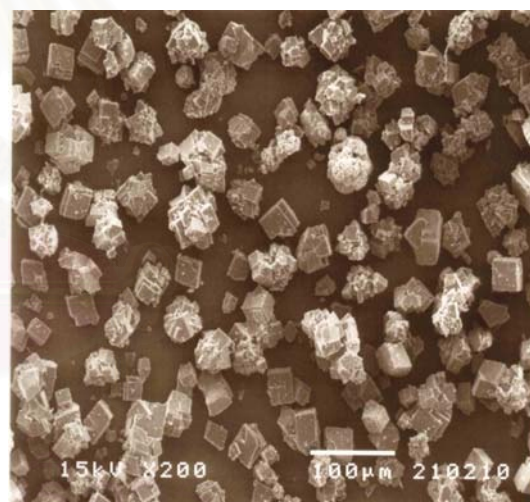
Si/Ni of 40 (X 200)   Si/Ni of 80 (X 200)

Figure 4.6   SEM photographs of Ni-SAPO-44 with different Si/Ni ratios of 40 and 80.

The profiles from ammonia temperature programmed desorption (NH$_3$-TPD) of the calcined used Ni-SAPO-34 and calcined used Ni-SAPO-44 catalysts with Si/Ni ratio of 40 and 80 are depicted in Figure 4.7. The NH$_3$-TPD profiles for those Ni-SAPO-34 catalysts present the profiles with three maxima at the temperatures of 150, 350, and 600ºC. The first two peaks for ammonia desorption are assigned to the weak and strong acid sites. The temperatures for ammonia desorption are lower than those found in acidic zeolites, 200 and 400ºC.[72] This is evident that Ni-SAPO-34 catalysts are weaker acid than zeolite H-ZSM-5. Therefore, as required, they should promote the MTO rather MTG process. The peak at 600ºC was due to the release of residual coke remained from the incomplete coke removal from very small pores.

The profiles from NH$_3$-TPD of the Ni-SAPO-44 catalysts with the Si/Ni ratios of 40 and 80 present similar feature of the profiles with two maxima at the temperatures of 150ºC and above 600ºC. The peak intensity at the temperature for ammonia desorption of 150ºC is very low compared to those of Ni-SAPO-34 samples. This is evident that Ni-SAPO-44 samples prepared in this work almost contain neither weak nor strong acid sites. Therefore, their potential catalytic activities are in doubt. The absence of acid sites in Ni-SAPO-44 catalysts may be due to the loss of porous structure upon regeneration at elevated temperature.

In particular, in the case of SAPO, the incorporation of silicon into the framework displayed acid sites. Therefore, the amount of acid sites depends on the Si content. Incorporation of silicon into the AlPO$_4$ framework can be conveniently discussed in terms of the proposed mechanism of substitution of a silicon atom for a phosphorus atom (SM2) or of two silicon atom for a (Al-P) pair of atoms (SM3) from the framework.[56] SM2 is well-known and this generates a negatively charged framework that is countered by protons making the acidic. SM3 will not generate any framework charge. Such substitution does not take place due to the instability of the Si-O-P bond. However, the Si-O-P bond can be

avoided in a number of silicon atoms are linked to each other via oxygen where silicon occupies both Al and P sites forming a heterogeneous region known as silicon island.[74, 76] The silicon content in the Ni-SAPO-44 product is higher than the Ni-SAPO-34 as can be seen from the chemical analysis results. It can imply that the silicon incorporated to Ni-SAPO-44 via SM3 from silicon island, which effect to low amount of acidity in NH_3-TPD of Ni-SAPO-44 catalysts.
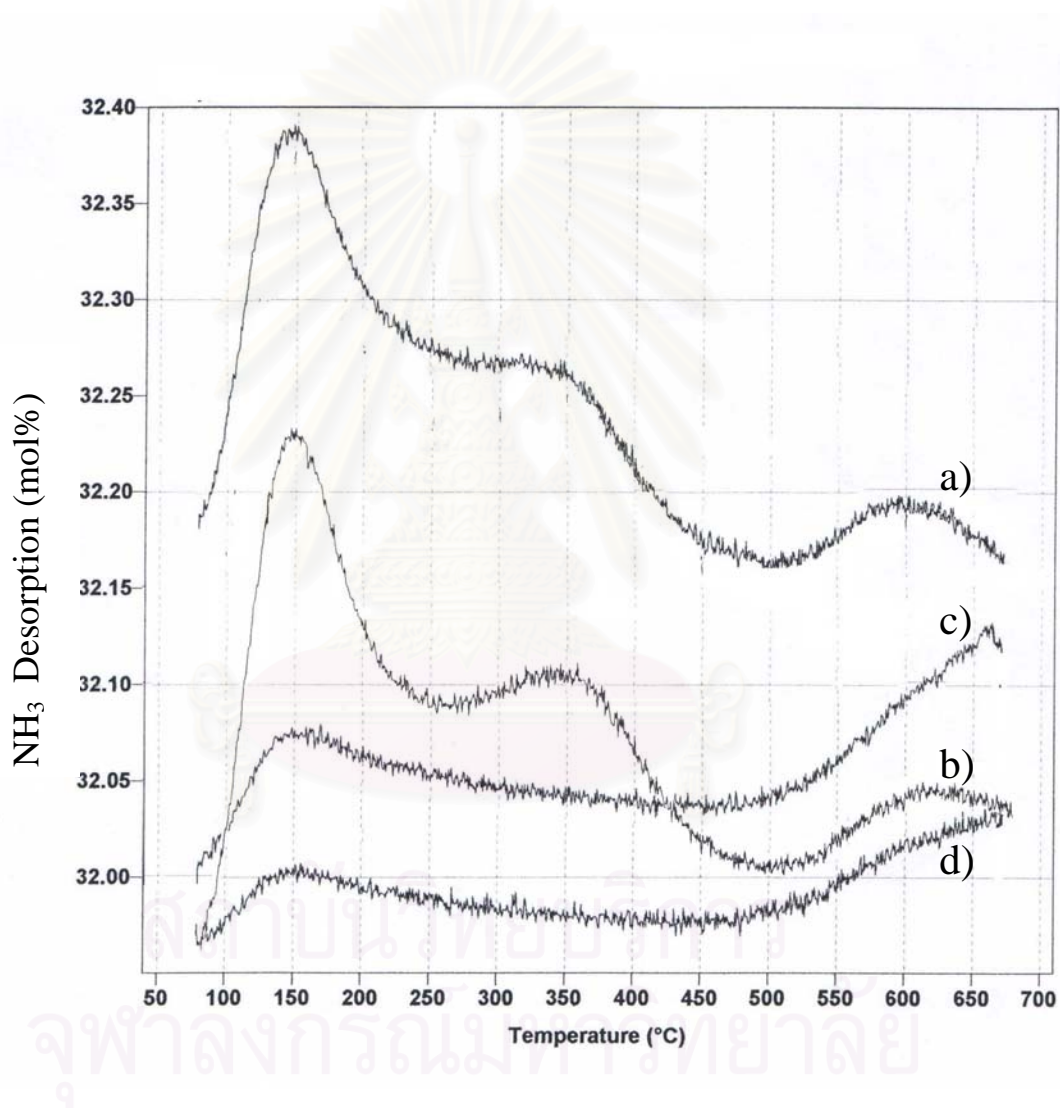
Figure 4.7 NH_3-TPD profiles of (a) Ni-SAPO-34 (Si/Ni =80), (b) Ni-SAPO-34 (Si/Ni =40), (c) Ni-SAPO-44 (Si/Ni =40) and (d) Ni-SAPO-44 (Si/Ni =80).

4.3 Catalytic Activities of the SAPO's Catalysts

4.3.1   Effect of Time on Stream on Methanol Conversion

Methanol conversion and gas product distribution over the Ni-SAPO-34 catalyst with the Si/Ni ratio in gel of 40 at different time on stream (TOS) of 20 and 40 min are shown in Table 4.7. Longer time on stream results in the increase of conversion of methanol from 93% to 100%. With increasing TOS, yield of liquid fraction is decreased while yield of gaseous products is increased. The change of TOS from 20 to 40 min does significantly change the product distribution in gaseous phase. The major product in gaseous phase is ethylene (47 to 54% yield) with constant amount of propylene (32% yield). The coke was found at about 3% for both cases.

4.3.2   Effect of Temperature on Methanol Conversion over Ni-SAPO-34

4.3.2.1   Ni-SAPO-34 with the Si/Ni Ratio in Gel of 40

The values of %conversion and product yield obtained from the methanol conversion to olefins using Ni-SAPO-34 with the Si/Ni ratio in gel of 40 at various temperatures of 300, 350, 400, 450, and 500ºC are compared in Table 4.8. It is found that the activity of Ni-SAPO-34 catalyst in MTO is very high except at low temperature as 300ºC. In the present study, conversions of methanol are almost 100% at temperature ranged from 400 to 500ºC. At all temperatures, the products are mainly in liquid phase which decreases in amount at higher temperatures. In contrast, the yield of products in gaseous phase is the least at the temperature of 300ºC and increases with increasing temperature. Formation of coke is hardly found in all cases and falls in the range of 3.28 to 5.47%. Coke tends to decrease from 5 to 3% with increasing temperature from 300 to 450ºC and increases to 4% again at the temperature above 450ºC.

4.3.2.2   Ni-SAPO-34 with the Si/Ni Ratio in Gel of 80

The values of %conversion and product yield obtained from the methanol conversion to olefins using Ni-SAPO-34 with the Si/Ni ratio in gel of 80 at various temperatures of 300, 350, 400, 450, and 500ºC are compared in Table 4.9. It is found that the activity of Ni-SAPO-34 catalyst in MTO increases to the maximum of 98% at the temperature of 400 and 450ºC. The value of %conversion decreases if the temperature was decreased or increases from this range. It is found that the maximum amount of gaseous products (40% yield) is obtained at the minimum amount of liquid fraction (55% yield) at the temperature of 450ºC. Methane was maximized to 16% yield at the temperature of 300ºC. With increasing the temperature, the methane was formed much less at minimum of 2% yield at the temperature of 400ºC. Light olefins (86% yield), especially ethylene (54% yield) is obtained at maximum at the temperatures of 450ºC. Formation of coke falls in the range of 2.3 to 4%. Coke tends to be unaffected by temperature above 350ºC with the constant amount of about 2% even at 500ºC.

At maximum %conversion, as well as the maximum composition of ethylene and light olefins, and the minimum composition of methane, the optimal temperature is 450ºC for using the Ni-SAPO-34 catalyst with the Si/Ni ratio of 80.

Table 4.7 Methanol conversion and gas product distribution using Ni-SAPO-34 (Si/Ni = 40) as the catalyst at various time on stream (Conditions: W_{cat} = 0.2 g, T_{MeOH} = 30ºC, $T_{catalyst}$ = 450ºC, GHSV = 2000 h^{-1})

	Time on stream (min)	
	20	40
% Conversion	93.8	100
Yield of Product Distribution (%)		
- methane	3.94	4.29
- ethane	0.63	0.64
- ethylene	46.52	53.59
- propane	4.00	2.85
- propylene	32.51	32.69
- *n*-butane	0.41	0.31
- *trans-2-* butylene	2.92	2.32
- *1*-butylene	1.63	1.58
- *iso*-butylene	0.12	0.19
- *cis-2*-butylene	1.57	1.53
- *methyl acetylene*	0.01	0.01
Yield of C_2+C_3 olefins (%)	79.03	86.28
Yield of Alkanes (C_1-C_4) (%)	8.98	8.09
Yield of gas product (wt. %.)	5.86	26.92
Yield of liquid product (wt. %.)	83.06	66.39
Coke (% wt. of catalyst)	3.50	3.28

Table 4.8 Methanol conversion and gas product distribution using Ni-SAPO-34 (Si/Ni = 40) as the catalyst at various temperatures of the catalyst (Conditions: W_{cat} = 0.2g, GHSV = 2000 h^{-1}, T_{MeOH} = 30ºC, TOS = 40 min)

	Temperatures (ºC)				
	300	350	400	450	500
% Conversion	68.8	93.1	99.5	100	95.7
Yield of Product Distribution (%)					
- methane	14.01	4.07	3.16	4.29	14.65
- ethane	0	0.37	0.83	0.64	1.29
- ethylene	24.53	35.13	44.00	53.59	52.76
- propane	4.48	8.15	8.59	2.85	1.34
- propylene	22.66	35.79	34.79	32.69	21.83
- *n*-butane	0.63	1.50	1.04	0.31	0.13
- *trans-2-* butylene	1.42	3.83	3.03	2.32	1.51
- *1*-butylene	0.54	1.90	1.91	1.58	1.04
- *iso*-butylene	0	0.18	0.25	0.19	0.04
- *cis-2*-butylene	0.54	2.18	1.89	1.53	1.07
- *Methyl acetylene*	0	0	0	0.01	0.04
Yield of C_2+C_3 olefins (%)	47.19	70.92	78.79	86.28	74.59
Yield of C_1-C_4 alkanes (%)	19.12	14.09	13.62	8.09	18.41
Yield of gas product (wt. %.)	6.39	6.91	16.83	26.92	27.31
Yield of liquid product (wt. %.)	84.94	83.63	77.42	66.39	64.67
Coke (% wt. of catalyst)	4.76	5.47	3.16	3.28	4.17

Table 4.9 Methanol conversion and gas product distribution using Ni-SAPO-34 (Si/Ni = 80) as the catalyst at various temperatures of the catalyst (Conditions: W_{cat} = 0.2 g, GHSV = 2000 h^{-1}, T_{MeOH} = 30ºC, TOS = 40 min)

	Temperatures (ºC)				
	300	350	400	450	500
% Conversion	75.5	70.5	97.9	97.8	88.6
Yield of Product Distribution (%)					
- methane	15.77	2.85	2.41	3.13	4.54
- ethane	0.08	0.36	0.70	0.63	0.59
- ethylene	28.41	27.38	43.79	53.89	52.49
- propane	6.04	5.49	7.02	2.63	1.50
- propylene	21.68	27.43	35.70	31.92	25.15
- *n*-butane	0.80	1.02	0.82	0.24	0.12
- *trans-2*- butylene	1.53	3.01	3.26	2.31	1.68
- *1*-butylene	0.63	1.35	1.95	1.56	1.22
- *iso*-butylene	0	0.08	0.23	0.17	0.12
- *cis-2*-butylene	0.57	1.52	2.01	1.52	1.16
- *Methyl aceylene*	0	0	0.01	0.02	0.03
Yield of C_2+C_3 olefins (%)	50.09	54.81	79.49	85.81	77.64
Yield of C_1-C_4 alkanes (%)	22.69	9.72	10.95	6.63	6.75
Yield of gas product (wt. %.)	8.14	17.87	37.10	40.47	25.62
Yield of liquid product (wt. %.)	80.51	74.28	58.09	54.88	69.93
Coke (% wt. of catalyst)	0.94	4.31	2.59	2.53	2.36

Coke and methane formation are highly essential features, with respect to the reaction mechanism and the contribution of diffusion constrains in the narrow pore structure. There is no doubt that the formation of methoxy group is an important first step of the methanol interaction with the acid sites. Further interaction of these methoxy groups with other methanol molecules adsorbed around the acid sites may cause not only a C-C bond formation but also transformations leading to adsorptions of methane in the gaseous phase and a coke formation on the surface.

From NMR[66, 68] and isotopic labeling[62, 63] studies, a simple mechanism of coke formation has been proposed:

$$CH_3OH \longrightarrow (CH_2)_n$$

with branches to C_2H_4, C_3H_6, C_4H_8, Saturated hydrocarbon, and Coke.
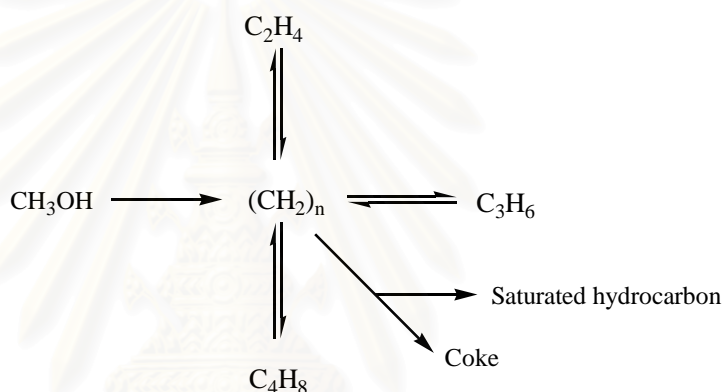
where the oxygenates include methanol and dimethylether, and all hydrocarbons are lumped together based on the observation that the olefins are formed from the oxygenates in parallel. The intermediates are considered to be a mixture of carbenium ions with different carbon numbers inside the pore. This simple mechanism for coke formation is similar to the hydrocarbon pool mechanism.[62, 63]

From the results observed, it can be stated that there is an optimal temperature for the Ni-SAPO-34 with the Si/Ni of 40 can present the best conversion of methanol to olefins. If the temperature is too low, the catalyst is not so active and the gas product as methane is favored. If the temperature is too high, the activity is slightly decreased. Product distribution is significantly changed upon increasing temperature. At high temperature of 500ºC, cracking of hydrocarbon is a competitive reaction. This is common for catalysis over acidic catalysts.

4.3.3   Effect of Temperature on Methanol Conversion over Ni-SAPO-44

4.3.3.1   Ni-SAPO-44 with the Si/Ni Ratio in Gel of 40

The values of %conversion and product yield obtained from the methanol conversion to olefins using Ni-SAPO-44 with the Si/Ni ratio in gel of 40 at various temperatures of 300, 350, 400, 450, and 500ºC are compared in Table 4.10. It is found that the activity of Ni-SAPO-44 catalyst in MTO is relatively lower than Ni-SAPO-34 at all temperatures especially at low temperature. For example, %conversion is only 76% over Ni-SAPO-34 while only 20% was obtained over Ni-SAPO-44 at the temperature of 300ºC. The highest activity of Ni-SAPO-44 at 83% conversion was obtained at the temperature of 500ºC. At all temperatures, the products are mainly in liquid phase. However, in gaseous products ethylene was obtained at the highest yield of 48% at the temperature of 500ºC. Surprisingly, formation of coke is hardly found in all cases only 1-2%. It can be concluded that the Ni-SAPO-44 with the Si/Ni ratio in gel of 40 exhibits the highest activity at 500ºC with liquid fraction as a major product but among the gaseous products it provides the high selectivity to ethylene and less to propylene.

The activity of Ni-SAPO-44 is lower than that of Ni-SAPO-34 at the same temperature. Larger particle size results in lower surface area and lower activity of Ni-SAPO-44. Furthermore, the acid sites on Ni-SAPO-44 are very few, therefore, its activity for MTO reaction is not expected. However, to obtain the highest activity of Ni-SAPO-44 with the Si/Ni of 40, the optimal temperature is 500ºC. At this temperature, the selectivity to light olefins as well as ethylene is relatively high.

4.3.2.2   Ni-SAPO-44 with the Si/Ni Ratio in Gel of 80

The values of %conversion and product yield obtained from the methanol conversion to olefins using Ni-SAPO-44 with the Si/Ni ratio in gel of 80 at various temperatures of 300, 350, 400, 450, and 500ºC are compared in Table 4.11. It is found that the activity of Ni-SAPO-44 catalyst in MTO increases to the maximum of 75% at the temperature of 450ºC. The value of %conversion decreases if the temperature was either

decreased or increases from this point. It is found that the maximum amount of gaseous products (34% yield) is obtained at the minimum amount of liquid fraction (65% yield) at the temperature of 450ºC. Methane was maximized to 11% yield at the temperature of 300ºC. With increasing temperature to 450ºC, the selectivity to methane was reduced to only 4%. The highest selectivity to light olefins (64%), especially ethylene (40%), is obtained at the temperature of 450ºC. Coke tends to be unaffected by temperature with the average amount of about 1% or even less. Similar to Ni-SAPO-34, the optimal condition for MTO over Ni-SAPO-44 is at the temperature of 450ºC.

The trends in effect of temperature on activity of Ni-SAPO-44 with Si/Ni ratios of 80 and 40 are different. Considering the activity along with selectivity to light olefins and methane, the optimal temperature for using the Ni-SAPO-44 catalyst with the Si/Ni ratio of 80 is 450ºC.

For comparison of activities of all catalysts at $450^{o}C$ after 40 min of reaction time as shown in Table 4.8-4.11, the methanol conversions for Ni-SAPO-34 catalysts are about 100% and 70-75% for Ni-SAPO-44 catalysts. The product distributions are different depending on the types of catalysts, but not the Si/Ni ratios in catalyst. The ethylene yield for Ni-SAPO-34 is 54%, and then the order in ethylene yield was followed as next; Ni-SAPO-34 (Si/Ni = 40) ~ Ni-SAPO-34 (Si/Ni = 80) > Ni-SAPO-44 (Si/Ni = 40) ~ Ni-SAPO-44 (Si/Ni = 80). The result is related that a small particle size and amount of acid site in catalysts enhanced the activity and ethylene yield on methanol conversion. Considering the catalysis results for Ni-SAPO-44 catalysts in Table 4.10 and 4.11, the %yield of ethylene reach the maximum at the temperature of $450^{o}C$, where methane is formed at the relative low yields. However, Ni-SAPO-44 catalysts have lower activity than Ni-SPO-34. There is not enough information to explain at this moment. The specific surface area and nitrogen adsorption studies of the fresh Ni-SAPO-44 catalysts need to be characterized.

Table 4.10 Methanol conversion and gas product distribution using Ni-SAPO-44 (Si/Ni = 40) as the catalyst at various temperatures of the catalyst (Conditions: W_{cat} = 0.2 g, GHSV = 2000 h^{-1}, T_{MeOH} = 30ºC, TOS = 40 min)

	Temperatures (ºC)				
	300	350	400	450	500
% Conversion	19.9	57.2	71.6	69.6	83.1
Yield of <u>Product Distribution (%)</u>					
- methane	5.76	6.13	3.14	3.33	7.01
- ethane	0	0.74	1.37	0.85	0.80
- ethylene	7.13	22.82	31.97	37.06	48.32
- propane	1.13	4.46	4.79	2.22	1.31
- propylene	4.95	17.21	24.44	21.65	21.63
- *n*-butane	0.17	1.02	0.63	0.23	0.12
- *trans-2-* butylene	0.50	2.57	2.69	1.93	1.74
- *1*-butylene	0.11	0.89	1.21	1.08	1.08
- *iso*-butylene	0.13	1.22	0.04	0.03	0.003
- *cis-2*-butylene	0.02	0.14	1.30	1.16	1.07
- *Methyl aceylene*	0	0	0.01	0.03	0.07
Yield of C_2+C_3 olefins (%)	12.08	40.02	56.41	58.71	69.95
Yield of C_1-C_4 alkanes (%)	7.06	12.35	9.94	6.63	9.23
Yield of gas product (wt. %.)	11.83	24.99	35.08	24.69	28.21
Yield of liquid product (wt. %.)	84.81	71.17	61.85	73.18	69.14
Coke (% wt. of catalyst)	1.64	2.02	1.59	1.04	1.23

Table 4.11 Methanol conversion and gas product distribution using Ni-SAPO-44 (Si/Ni = 80) as the catalyst at various temperatures of the catalyst (Conditions: W_{cat} = 0.2 g, GHSV = 2000 h^{-1}, T_{MeOH} = 30ºC, TOS = 40 min)

	Temperatures (ºC)				
	300*	350	400	450	500
% Conversion	34.4	47.5	72.2	75.5	61.8
Yield of Product Distribution (%)					
- methane	11.09	5.23	3.57	4.00	6.61
- ethane	0	0.39	1.47	0.79	0.88
- ethylene	12.28	19.24	32.17	39.80	35.48
- propane	1.57	4.50	4.87	2.15	1.29
- propylene	7.91	13.18	24.43	23.96	14.73
- *n*-butane	0.18	0.91	0.61	0.23	0.10
- *trans-2-* butylene	1.02	2.22	2.67	2.27	1.17
- *1*-butylene	0.19	0.77	1.20	1.13	0.72
- *iso*-butylene	0	0	0	0	0
- *cis-2*-butylene	0.16	1.06	1.29	1.09	0.77
- *Methyl aceylene*	0	0	0.01	0.04	0.03
Yield of C_2+C_3 olefins (%)	20.19	32.42	56.60	63.75	50.21
Yield of C_1-C_4 alkanes (%)	12.84	11.03	10.40	7.17	8.88
Yield of gas product (wt. %)	15.40	12.84	17.09	33.54	15.66
Yield of liquid product (wt. %)	83.68	84.80	80.77	65.22	82.70
Coke (% wt. of catalyst)	0.42	1.16	1.04	0.65	0.92

* using the regenerated catalyst as sample.

CHAPTER V

CONCLUSION

Ni-SAPO-34 and Ni-SAPO-44 with different Si/Ni ratios in gel (Si/Ni = 40 and 80) were sucessfully synthesized by hydrothermal crystallization. The optimal condition for preparing the pure phase of Ni-SAPO-34 catalyst with high crystallinity was using the gel with composition of 2.0 TEAOH : 0.6 SiO_2: 1.0 Al_2O_3: 1.0 P_2O_5: x NiO: 72 H_2O and crystallization was carried out at the temperature of 200ºC for 4 h with two stage heating rates from room temperature to 160ºC at 1.5ºC /min and then to 200ºC at 2ºC /min. In case of Ni-SAPO-44 synthesis, the optimal condition for synthesis of Ni-SAPO-44 is using the gel composition of 1.7 cyclohexylamine : 0.6 SiO_2: 0.9 Al_2O_3: 0.9 P_2O_5: x NiO: 50 H_2O and crystallization was carried out at the temperature of 200ºC for 10 days. According to XRD and SEM results, the crystallinity and the particle size decreased with increasing the Ni content. However, not all nickel in the gel was incorporated in the framework, as can be seen from the chemical analysis results. The catalytic performance on methanol conversion of these catalysts has been studied. In particular, the Ni-SAPO-34 with Si/Ni ratio as 40 exhibited the best yield to light olefins ($C_2+C_3 \approx 86\%$) and complete methanol conversion were attained under mild condition at the temperature of 450°C and a GHSV of 2000 h^{-1} with time on stream of 40 min using the 22% methanol feed balanced with nitrogen gas.

Suggestions:

1. Synthesis of Ni-SAPO-44 applying the rapid crystallization and its catalytic reaction on MTO should be studied.

2. The extension of study using other chabazite-like structure SAPO materials, such as SAPO-47 on MTO should be attempted. SAPO-47 seems to be active for MTO but selectivity to light olefins is not high. Improvement of its performance is vary challenging.

REFERENCES

1. Astle, M. J.: <u>The Chemistry of Petrochemicals</u>: Reinhold, New York, **1958**.

2. Meketta, J. J.: <u>Chemical Processing Handbook</u>: Marcel Dekker, New York, **1993**.

3. Cheng, W.; Kung, H. H.: <u>Methanol Production and Use</u>: Marcel Dekker, New York, **1994**.

4. Djieugoue, M.; Prakash, A. M.; Kevan, L. "Catalytic study of methanol-to-olefins conversion in four small-pore silicoaluminophosphate molecular sieves: influence of the structural type, nickel incorporation, nickel location, and nickel concentration" *J. Phys. Chem. B,* **2000**. *104*, 6452-6461.

5. Wendelbo, R.; Akporiaye, D.; Andersen, A.; Dahl, I. M.; Mostad, H. B. "Synthesis, characterization and catalytic testing of SAPO-18, MgAPO-18, and ZnAPO-18 in the MTO reaction" *Appl. Catal. A.* **1996**, *142*, L197-L207.

6. Campelo, J. M.; Lafont, F.; Marinas, J. M.; Ojeda, M. "Studies of catalyst deactivation in methanol conversion with high, medium and small pore silicoaluminophosphates" *Appl. Catal. A.* **2000**, *192*, 85-96.

7. Ashtekar, S.; Chilukuri, S. V. V.; Prakash, A. M.; Chakrabarty, D. K. "Small pore aluminum phosphate molecular sieves with chabazite structure: incorporation of manganese in the structure -34 and -44" *J. Phys. Chem.* **1996**, *100*, 3665-3670.

8. Ashtekar, S.; Chilukuri, S. V. V.; Prakash, A. M.; Harendranath, C. S.; Chakrabarty, D. K. "Small pore aluminum phosphate molecular sieves with chabazite structure: incorporation of cobalt in the structure -34 and -44" *J. Phys. Chem.* **1995**, *99*, 6937-6943.

9. Ashtekar, S.; Chilukuri, S. V. V.; Chakrabarty, D. K. "Small pore molecular sieves SAPO-34 and SAPO-44 with chabazite structure: a study of silicon incorporation" *J. Phys. Chem.* **1994**, *98*, 4878-4883.

10. Hočevar, S.; Batista, J.; Kaučič, V. "Acidity and catalytic activity of MeAPSO-44 (Me = Co, Mn, Cr, Zn, Mg), SAPO-44, AlPO$_4$-5 and AlPO$_4$-14 molecular sieves in methanol dehydration" *J. Catal.* **1993**, *139*, 351-361.

11. Inui, T.; Phatanasri, S.; Dhupatemiya, P.; Inoue, M. "Synthesis course of the Ni-SAPO-34 catalyst for methanol-to-olefin conversion" *Microporous Mesoporous Mater.* **1999**, *28*, 19-24.

12. Ling, J.; Li, H.; Zhao, S.; Guo, W.; Wang, R.; Ying, M. "Characteristics and performance of SAPO-34 catalyst for methanol-to-olefin conversion" *Appl. Catal.* **1990**, *64*, 31-40.

13. Dahl, I. M.; Mostad, H.; Akporiaye, D.; Wendelbo, R. "Structural and chemical influences on the MTO reaction: a comparison of chabazite and SAPO-34 as MTO catalysts" *Microporous Mesoporous Mater.* **1999**, *29*, 185-190.

14. Möller, K. P.; Böhringer, W.; Schnitzler, A. E.; van Steen, E.; O'Connor, C. T. "The use of a jet loop reactor to study the effect of crystal size and the co-feeding of olefins and water on the conversion of methanol over HZSM-5" *Microporous Mesoporous Mater.* **1999**, *29*, 127-144.

15. Schulz, H.; Wei, M. "Deactivation and thermal regeneration of zeolite HZSM-5 for methanol conversion at low temperature (260-290°C)" *Microporous Mesoporous Mater.* **1999**, *29*, 205-218.

16. Park, T.; Froment, G. F. "Kinetic modeling of the methanol to olefins process: 1. model formation" *Ind. Eng. Chem. Res.* **2001**, *40*, 4172-4186.

17. Abdillahi, M. M.; El-Nafaty, U. A.; Al-Jarallah, A. M. "Barium modification of a high-silica zeolite for methanol conversion to light alkenes" *Appl. Catal. A.* **1992**, *91*, 1-12.

18. Lücke, B.; Martin, A.; Günschel, H.; Nowak, S. "CMHC: coupled methanol hydrocarbon cracking formation of lower olefins from methanol and hydrocarbons over modified zeolites" *Microporous Mesoporous Mater.* **1999**, *29*, 145-157.

19. Dehertog, W. J. H.; Froment, G. F. "Production of light alkenes from methanol on ZSM-5 catalysts" *Appl. Catal.* **1991**, *71*, 153-165.

20. Tsoncheva, T.; Dimitrova, R. "Methanol conversion to hydrocarbons on porous aluminosilicates" *Appl. Catal. A.* **2002**, *225*, 101-107.

21. Marchi, A. J.; Froment, G. F. "Catalytic conversion of methanol into light alkenes on mordenite-like zeolite" *Appl. Catal. A.* **1993**, *94*, 91-106.

22. Mikkelsen, Ø.; Kolboe, S. "The conversion of methanol to hydrocarbon over zeolite H-beta" *Microporous Mesoporous Mater.* **1999**, *29*, 173-184.

23. Young, D.; Davis, M. E. "Studies on SAPO-5: synthesis with higher silicon contents" *Zeolites.* **1991**, *11*, 277-281.

24. Marchi, A. J.; Froment, G. F. "Catalytic conversion of methanol to light alkenes on SAPO molecular sieves" *Appl. Catal.* **1991**, *71*, 139-152.

25. Inui, T.; Matsuda, H.; Okaniwa, H.; Miyamato, A. "Preparation of silico-alumino-phosphates by the rapid crystallization method and their catalytic performance in the conversion of methanol to light olefins" *Appl. Catal.* **1990**, *58*, 155-163.

26. Barger, P.; Wilson, S. "The characteristics of SAPO-34 which influence the conversion of methanol to light olefins" *Microporous Mesoporous Mater.* **1999**, *29*, 117-126.

27. Kang, M. "Methanol conversion on metal-incorporated SAPO-34s (MeAPSO-34s)" *J. Mol. Catal. A.* **2000**, *160*, 437-444.

28. Popova, M.; Minchev, Ch.; Kanazirev, V. "Methanol converion to light alkenes over SAPO-34 molecular sieves synthesized using various sources of silicon and aluminum" *Appl. Catal. A.* **1998**, *169*, 227-235.

29. Flanigen, E. M.; Lok, B. M.; Messina, C. A.; Patton, R. L.; Gajek, R. T.; Cannon, T. R. "Crystalline silicoaluminophosphates" *US Pat. 4,440,87,.* **1984.**

30. Inui, T.; Kang, M. "Reliable procedure for the synthesis of Ni-SAPO-34 as a highly selective catalyst for methanol to ethylene conversion" *Appl. Catal. A.* **1997**, *164*, 211-223.

31. Hočevar, S.; Levec, J. "Acidity and catalytic activity of MeAPSO-34 (Me = Co, Mn, Cr), SAPO-34 and ZSM-5 molecular sieves in methanol dehydration" *J. Catal.* **1992**, *135*, 518-532.

32. Kang, M.; Inui, T. "Synthesis of NiAPSO-34 catalysts containing a larger concentration of Ni and effect of its sulfidation on methanol conversion" *J. Mol. Catal. A.* **1999**, *144*, 329-335.

33. Kang, M.; Lee, C. "Synthesis of Ga-incorporated SAPO-34s (GaAPSO-34) and their catalytic performance on methanol conversion" *J. Mol. Catal. A.* **1999**, *150*, 213-222.

34. van Niekerk, M. J.; Fletcher, J. C. Q.; O'Connor, C. T. "Effect of catalyst modification on the conversion of methanol to light olefins over SAPO-34" *Appl. Catal. A.* **1996**, *138*, 135-145.

35. Dumitriu, E.; Azzouz, A.; Hulea, V.; Lutic, D.; Kessler, H. "Synthesis, characterization and catalytic activity of SAPO-34 obtained with piperidine as templating agent" *Microporous Mater.* **1997**, *10*, 1-12.

36. Marchese, L.; Frache, A.; Gianotti, E.; Martra, G.; Causà, M.; Coluccia, S. "ALPO-34 and SAPO-34 synthesized by using morpholine as templating agent. FTIR and FT-Raman studies of the host-guest and guest-guest interaction within the zeolitic framework" *Microporous Mesoporous Mater.* **1999**, *30*, 145-153.

37. Inui, T.; Phatanasri, S.; Matsuda, H. "Highly selective synthesis of ethene from methanol on a novel nickel-silicoaluminophosphate catalyst" *J. Chem. Soc. Chem. Commun.* **1990,** 205-206.

38. Thomas, J. M.; Xu, Y.; Catlow, C. R. A.; Couves, J. W. "Synthesis and characterization of a catalytically active nickel-silicoaluminophosphate catalyst for the conversion of methanol to ethene" *Chem. Mater.* **1991**, *3*, 667-672.

39. Kang, M.; Um, M.; Park, J. "Synthesis and catalytic performance on methanol conversion of NiAPSO-34 crystals (I): effect of preparation factors on the gel formation" *J. Mol. Catal. A*. **1999**, *150*, 195-203.

40. Zhu, Z.; Hartmann, M.; Kevan, L. "Catalytic conversion of methanol to olefins on SAPO-n (n = 11, 34, and 35), CrAPSO-n, and Cr-SAPO-n molecular sieves" *Chem. Mater.* **2000,** *12*, 2781-2787.

41. Kang, M. "Synthesis and catalytic performance on methanol conversion of NiAPSO-34 crystals (II): catalytic performance under various reaction conditions" *J. Mol. Catal. A*. **1999**, *150*, 205-212.

42. Chen, D.; Moljord, K.; fuglerud, T.; Holmen, A. "The effect of crystal size of SAPO-34 on the selectivity and deactivation of the MTO reaction" *Microporous Mesoporous Mater.* **1999**, *29*, 191-203.

43. Kang, M.; Inui, T. "Effects of decrease in number of acid sites located on the external surface of Ni-SAPO-34 crystalline catalyst by the mechanochemincal method" *Catal. Lett.* **1998**, *53*, 171-176.

44. Briend, M.; Vomscheid, R.; Peltre, M. J.; Man, P. P.; Barthomeuf, D. "Influence of the choice of the template on the short- and long-term stability of SAPO-34 zeolite" *J. Phys. Chem.* **1995**, *99*, 8270-8276.

45. Liu, Z.; Yang, L.; Xu, L.; Sun, C.; Xiong, Y. "Method for making a metal containing small pore molecular sieve catalyst" *US. Pat. 6,448,19,* **2002**.

46. Sun, H.; Vaughn, S. N. "Use of transition metal containing small pore molecular sieve catalysts in oxygenate conversion" *US. Pat. 5,962,76,* **1999**.

47. Prakash, A. M.; Hartmann, M.; Zhu, Z.; Kevan, L. "Incorporation of transition metal ions into MeAPO/MeAPSO molecular sieves" *J. Phys. Chem. B.* **2000**, *104*, 1610-1616.

48. Chen, J.; Thomas, J. M. "Synthesis of SAPO-41 and SAPO-44 and their performance as acidic catalysts in the conversion of methanol to hydrocarbons" *Catal. Lett.* **1991**, *11*, 199-208.

49. Prakash, A. M.; Unnikrishanan, S.; Rao, K. V. "Synthesis and characterization of silicon-rich SAPO-44 molecular sieves" *Appl. Catal. A.* **1994**, *110*, 1-10.

50. Liu, Z.; Guo, X.; Cai, G. "Synthesis of SAPO-44" *US Pat 6,319,487 B1*, **2001.**

51. Flanigen, E. M.; Lok, B. M.; Marcus, B. K. "Cobalt-aluminum-phosphorus-silicon-oxide molecular sieves" *EP Pat. 0,161,489,* **1985.**

52. Kang, M.; Inui, T. "Dynamic reaction characteristics affected by water molecules during the methanol to olefin conversion on NiAPSO-34 catalysts" *J. Mol. Catal. A.* **1999**, *140*, 55-63.

53. Szostak, R.: Molecular Sieves: Principle of Synthesis and Identification: Van Nostrand Reinhold, New York, **1989**.

54. Satterfield, C. N.: Heterogeneous Catalysis in Practice: McGraw-Hill, New York, **1980.**

55. Breck, D. W.: Zeolite Molecular Sieves: Structure Chemistry and Use: John Wiley & Sons, New York, **1974**.

56. Mertens, M.: Synthesis and Characterization of Crystalline Microporous Silicoaluminophosphate: Doctoral Dissertation, Katholieke Universiteit te Leuven, **1990**.

57. 1980 Powder Diffraction File 'Inorganic Phases' JCPDS. International Center for Diffraction Data, U.S.A.

58. Fougerit, J.M.; Guep, N.S.; Guisnet, M. "Selective transformation of methanol into light olefins over a mordenite catalyst: reaction scheme and mechanism" *Microporous Mesoporous Mater.* **1999**, *29*, 79-89.

59. Ivar, M.D. "On the reaction mechanism for propene formation in the MTO reaction over SAPO-34" *Catal. Lett.* **1993**, *20*, 329-336.

60. Stöcker, M. "Review: methanol-to-hydrocarbon: catalytic materials and their behavior" *Microporous Mesoporous Mater.* **1999**, *29*, 3-48.

61. Dumitriu, E.; Lutic, D.; Hulea, V.; Dorohoi, D.; Azzouz, A.; Colnay, E.; Kappenstein, C. "Synthesis optimization of chabazite-like SAPO-47 in the presence of sec-butylamines" *Microporous Mesoporous Mater.* **1999**, *31*, 187-193.

62. Dahl, I. M.; Kolboe, S. "On the reaction mechanism for hydrocarbon formation from methanol over SAPO-34: 2. Isotopic labeling studies of the co-reaction of propene and methanol" *J. Catal.* **1996**, *161*, 304-309.

63. Dahl, I. M.; Kolboe, S. "On the reaction mechanism for hydrocarbon formation from methanol over SAPO-34: 1. Isotopic labeling studies of the co-reaction of ethene and methanol" *J. Catal.* **1994**, *149*, 458-464.

64. Chen, D.; Rebo, H. P.; Grønvold, A.; Moljord, K.; Holmen, A. "Methanol conversion to light olefins over SAPO-34: kinetic modeling of coke formation" *Microporous Mesoporous Mater.* **2000**, *35-36*, 121-135.

65. Dewaele, O.; Geers, V. L.; froment, G. F.; Marin, G. B. " The conversion of methanol to olefins: a transient kenetic study" *Chem. Eng. Sci.* **1999**, *54*, 4385-4395.

66. Gale, J. D.; Shah, R.; Payne, M. C.; Stich, I.; Terakura, K. "Methanol in microporous materials from first principles" *Catal. Today.* **1999**, *50*, 525-532.

67. Sinclair, P. E.; Catlow, C. R. a. "Generation of carbenes during methanol conversion over Brønsted acidic aluminosilicates. A computational Study" *J. Phys. Chem. B.* **1997**, *101*, 295-298.

68. Hutchings, G. J.; Watson, G. W.; Willock, D. j. "Methanol conversion to hydrocarbons over zeolite catalysts: comments on the reaction mechanism for the formation of the first carbon-carbon bond" *Microporous Mesoporous Mater.* **1999**, *29*, 67-77.

69. Keil, F. J. "Methanol-to-hydrocarbons: process technology" *Microporous Mesoporous Mater.* **1999**, *29*, 49-66.

70. Arstad, B.; Kolboe, S. "The Reactivity of molecules trapped within the SAPO-34 cavities in the methanol-to-hydrocarbons reaction" *J. Am. Chem. Soc.* **2001**, *123*, 8137-8138.

71. Dahl, I. M.; Wendelbo, R.; Andersen, A.; Akporiaye, D.; Mostad, H.; Fuglerud, T. "The effect of crystallite size on the activity and selectivity of the reaction of ethanol and 2-propanol over SAPO-34" *Microporous Mesoporous Mater.* **1999**, *29*, 159-171.

72. Wu, X.; Anthony, R. G. "Effect of feed composition on methanol conversion to light olefins over SAPO-34" *Appl. Catal. A.* **2001**, *218*, 241-250.

73. Campbell, S. M.; Jiang, X.; Howe, R. F. "Methanol to hydrocarbons: spectroscopic studies and the significance of extra-framework aluminum" *Microporous Mesoporous Mater.* **1999**, *29*, 91-108.

74. Sastre, G.; Lewis, D. W.; Catlow, C. R. A. "Structure and stability of silica species in SAPO molecular sieves" *J. Phys. Chem.* **1996**, *100*, 6722-6730.

75. Sánchez del Campo, A. E.; Gayubo, A. G.; Aguayo, A. T.; Tarrio, A.; Bilbao, J. "Acidity, surface species, and mechanism of methanol transformation into olefins on a SAPO-34" *Ind. Eng. Chem. Res.* **1998**, *37*, 2336-2340.

76. Tan, J.; Liu, Z.; Bao, X.; Liu, X.; Han, X.; He, C.; Zhai, R. "Crystallization and Si incorporation mechanism of SAPO-34" *Microporous Mesoporous Mater.* **2002**, *53*, 97-108.

77. Jeanvoine, Y.; Ángyán, J. G. "Brønsted acid sites in HSAPO-34 and chabazite: an ab initio structural study" *J. Phys. Chem. B.* **1998**, *102*, 5573-5580.

78. Djieugoue, M.; Prakash, A. M.; Kevan, L. "Electron spin resonance and electron spin-echo modulation studies of synthesized NiAPSO-34 molecular sieve and comparison with ion-exchanged NiH-SAPO-34 molecular sieve" *J. Phys. Chem. B.* **1999**, *103*, 804-811.

APPENDICES

APPENDICES

A-1 Calculation for Vapor Pressure of Methanol

Antoine's equation

$$\text{In } (P \times (Vp/P_c)) = (1-X)^{-1}[(VpA)X + (VpB)X^{1.5} + (VpC)X^3 + (VpD)X^6] \qquad \text{(A-1)}$$

Where P = Total pressure

Vp = Vapor pressure

P_c = Critical pressure

$X = 1 - (T/T_c)$; T_c = critical temperature, T = trial temperature (K)

VpA, VpB, VpC, VpD = constant

Example: Determination of vapor pressure of methanol at 30°C

For methanol; $T_c = 512.6$ K, $P_c = 80.9$ atm $P = 1$ atm

$VpA = -8.54796$, $VpB = 0.76982$, $VpC = -3.10850$,

$VpD = 1.54481$, $T = 30°C = 303.15$ K

$X = 1 - (303.15/512.6) = 0.4089$

$\text{In } (1 \times (Vp/80.9)) = (1-0.4089)^{-1}[(-8.54796)(0.4089) + (0.76982)(0.4089)^{1.5}$

$+ (-3.10850)(0.4089)^3 + (1.54481)(0.4089)^6]$

$\text{In } (Vp/80.9) = -5.9199$

$Vp/80.9 = \exp(-5.9199) = 2.6854 \times 10^{-3}$

$Vp = 0.2172$ atm

A-2 Calculation for Feed Flow Rate

The used catalyst = 0.2 g

Packed catalyst into borosilicate reactor (inside diameter = 0.54 cm)

Determine the average height of catalyst bed = 1.0 cm, so that,

$$\text{Volume of bed} = \pi r^2 h = (22/7) \times (0.27)^2 \times 1.0$$

$$= 0.2291 \text{ cm}^3\text{-cat.}$$

Use Gas Hourly Space Velocity (GHSV) = 2000 h^{-1}

$$\text{GHSV} = \frac{\text{Volumetric flow rate}}{\text{Volume of bed}} \quad \text{at STP condition}$$

$$\text{Volumetric flow rate} = 2000 \times 0.2291 = 458.20 \text{ cm}^3/h$$

$$= 458.20/60 \quad = 7.64 \text{ cm}^3/\text{min}$$

At room temperature

$$\text{Volumetric flow rate} = 7.64 \times \frac{(273.15 + T)}{273.15},$$

Where   T = measured temperature of methanol saturator (°C)

A-3 Calculation for Conversion of Methanol in MTO reaction

Methanol conversion activity was evaluated in term of conversion of methanol into other hydrocarbons.

$$\text{Methanol conversion (\%)} = \frac{(A_{in} - A_{out})}{A_{in}} \times 100 \qquad (A\text{-}2)$$

Where   A = GC peak area of methanol

If $A_{in} = 18610$; $A_{out} = 0$

$$\text{Methanol conversion (\%)} = \frac{(18610 - 0)}{18610} \times 100$$

$$= 100\%$$

A-4 Calculation of GC Peak Area to Concentration

$$C_x \quad = \quad \frac{A_x \times C_{std} \times V_{std}}{A_{std} \times V_x} \qquad\qquad (A\text{-}3)$$

$$\% \text{ selectivity} \quad = \quad \frac{C_x \times 100}{C_{total}} \qquad\qquad (A\text{-}4)$$

When C_{std} = Concentration of the component of interest in the standard mixture, % mol

C_x = Concentration of the component in the sample, % mol.

C_{total} = Concentration of the total component in the sample, % mol.

A_{std} = Peak area of the component in standard mixture, au.

A_x = Peak area of the component in the sample, au.

V_{std} = injected volume of the standard mixture, µl.

V_x = injected volume of the sample, µl.

If data of ethylene, $A_{ethylene}$ = 162382; A_{std} = 77574; C_{std} = 24.88 % molar;

V_{std} = 1.5 µl; $V_{ethylene}$ = 10 µl, C_{total} = 14.57 % molar

$$C_{ethylene} = \frac{162382 \times 24.88 \times 1.5}{77574 \times 10}$$

$$= \quad 7.81 \text{ % molar}$$

$$\% \text{ selectivity to propylene} \quad = \quad \frac{7.81 \times 100}{14.57}$$

$$= \quad 53.59$$

A-5 Calculation for Initial Weight of Feed Methanol

$$P V \quad = \quad n RT \qquad\qquad (A-5)$$

When P = partial pressure of methanol, atm

    V = volumn of gas, L

    n = mole of methanol, mol

    R = constant = 0.082 atm $\bullet$ L $\bullet$ mol^{-1} $\bullet$ K^{-1}

    T = temperature of methanol, K

If P = 0.2172 atm, V = 0.3391 L, T = 30°C = 303.15 K

$$n \quad = \quad \frac{P V}{R T}$$

$$= \quad \frac{0.2172 \times 0.3391}{0.082 \times 303.15}$$

$$= \quad 0.002962 \text{ mol} \quad = \quad 0.0949 \text{ g}$$

A-6 Calculation for Yield of Gas Product and Liquid Product

$$\% \text{ Yield of liquid product} = \frac{\text{wt. liquid product} \times 100}{\text{wt. MeOH}} \qquad \text{(A-6)}$$

$$\% \text{ Yield of gas product} = \frac{\text{wt. gas product} \times 100}{\text{wt. MeOH}} \qquad \text{(A-7)}$$
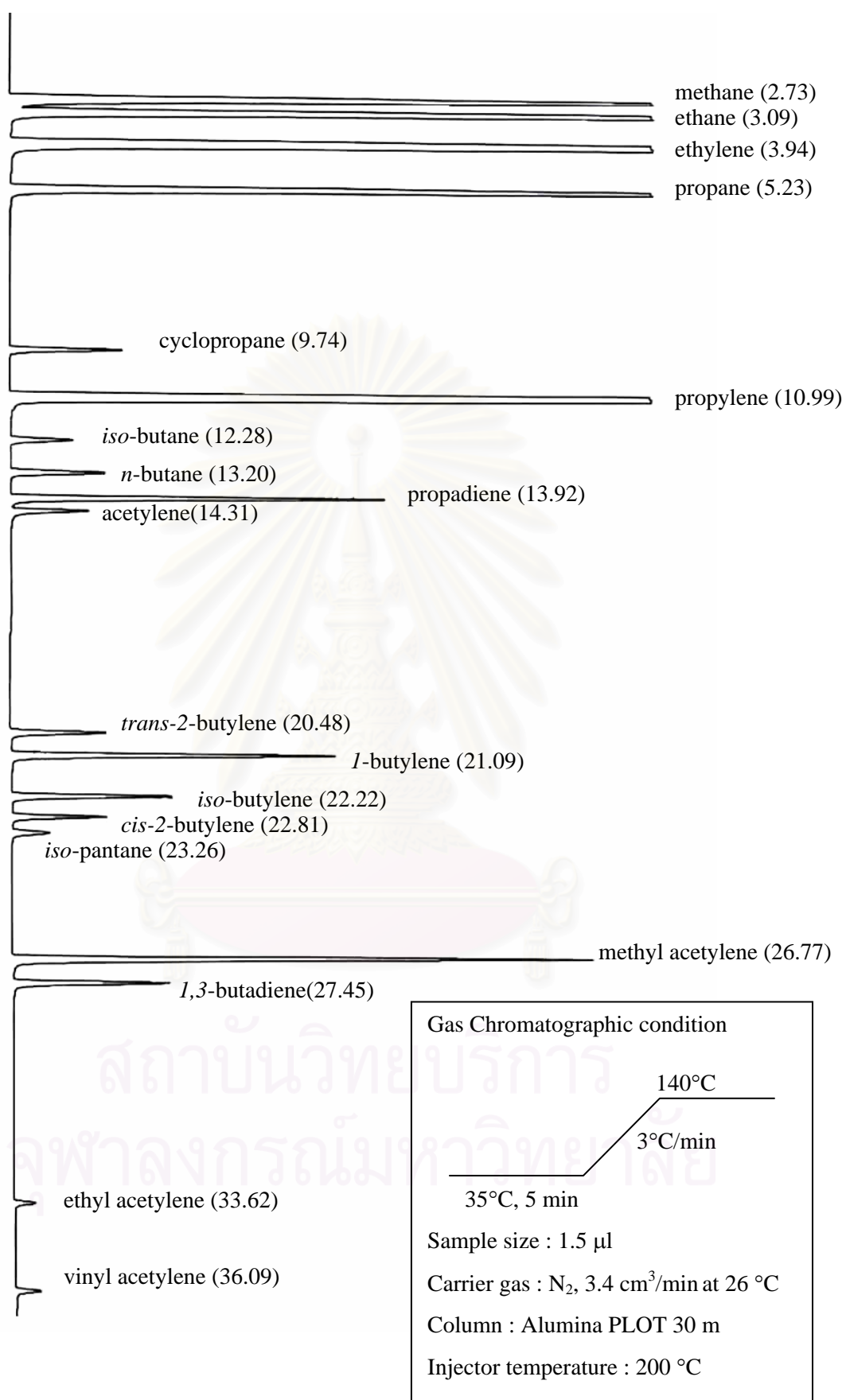
When wt. gas product = wt.MeOH – wt. liquid product – wt. coke

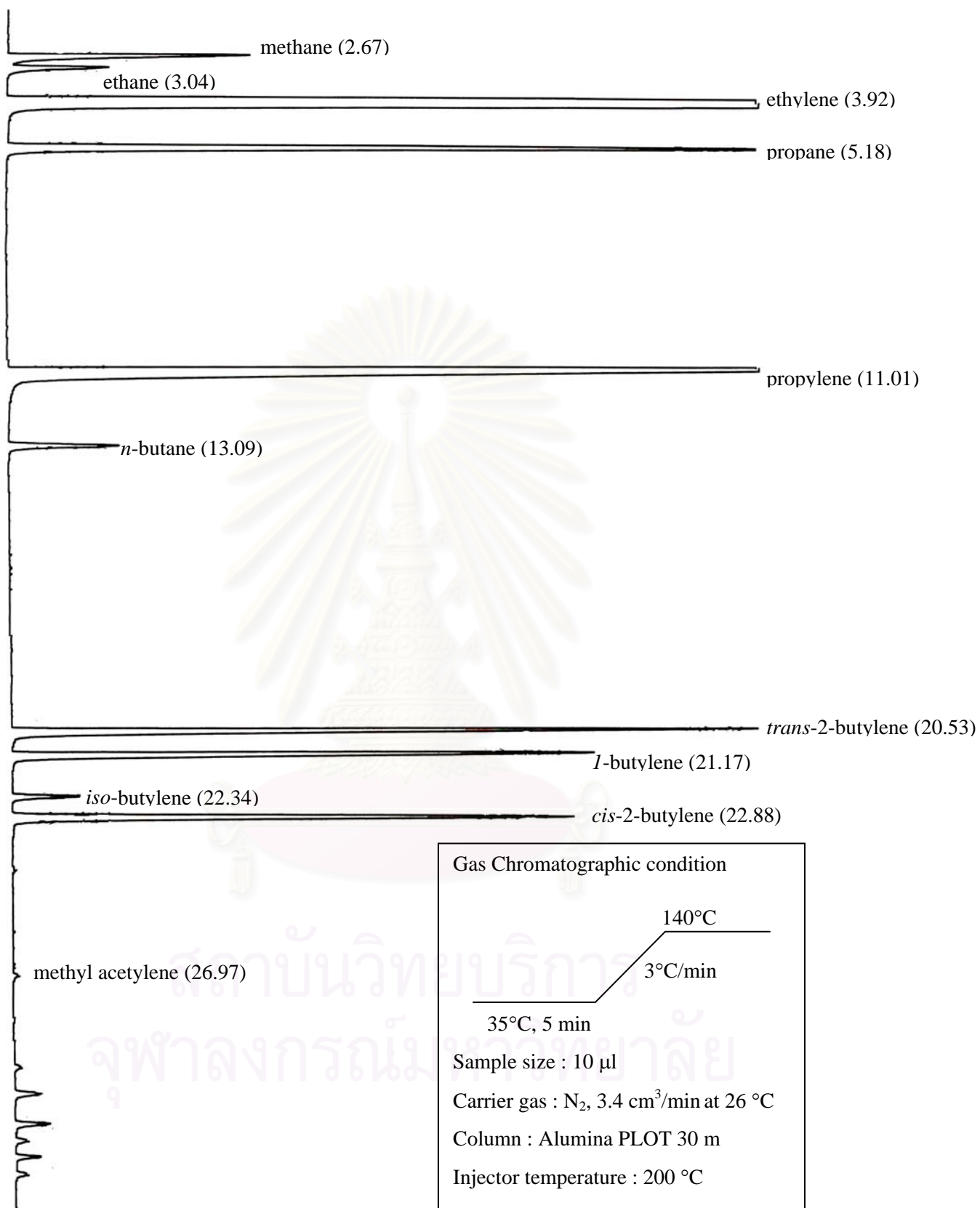If wt. MeOH = 0.0949 g, wt. liquid product = 0.0625 g, wt. coke = 0.0063 g

$$\% \text{ Yield of liquid product} = \frac{0.0625 \times 100}{0.0949}$$

$$= 68.85$$

$$\% \text{ Yield of gas product} = \frac{0.0949 - 0.0625 - 0.0063 \times 100}{0.0949}$$

$$= 27.50$$

methane (2.73)
ethane (3.09)
ethylene (3.94)
propane (5.23)
cyclopropane (9.74)
propylene (10.99)
iso-butane (12.28)
n-butane (13.20)
propadiene (13.92)
acetylene(14.31)
trans-2-butylene (20.48)
1-butylene (21.09)
iso-butylene (22.22)
cis-2-butylene (22.81)
iso-pantane (23.26)
methyl acetylene (26.77)
1,3-butadiene(27.45)

Gas Chromatographic condition

140°C

3°C/min

35°C, 5 min

ethyl acetylene (33.62)

vinyl acetylene (36.09)

Sample size : 1.5 μl

Carrier gas : N_2, 3.4 cm^3/min at 26 °C

Column : Alumina PLOT 30 m

Injector temperature : 200 °C

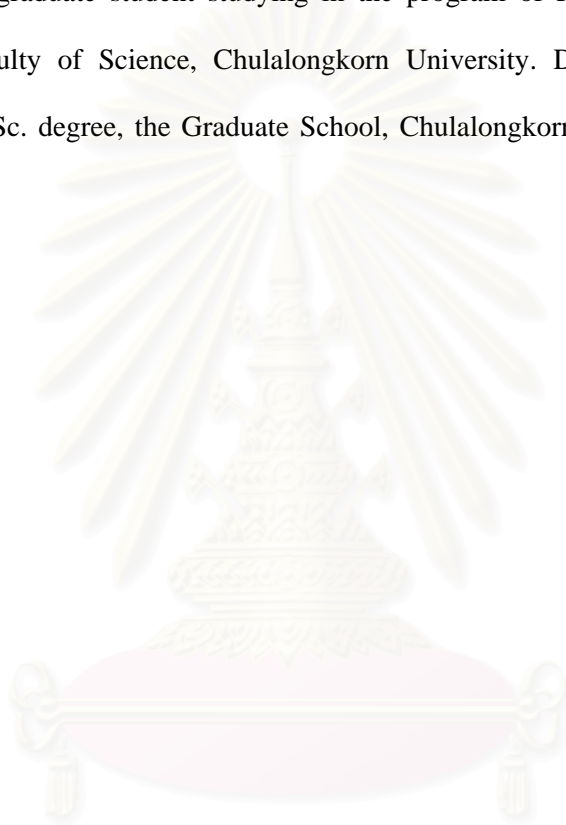**Figure A-1**   Gas chromatogram of standard mixture C_4 gas.

Figure A-2 Gas chromatogram of gas product from methanol conversion reaction on

Ni-SAPO-34 (Si/Ni ratio = 40) at 450°C (Condition: 0.2 g of catalyst, feed at

GHSV of 2000 h^{-1}, T_{MeOH} = 30°C, time on stream 40 min.).

VITAE

Mister Thanit Veriyaprom was born on December 21, 1977 in Nakorn si thammarat. He received the B.Sc. Degree in Chemistry at Chulalongkorn University in 1999. Since then, he has been a graduate student studying in the program of Petrochemistry and Polymer Science at Faculty of Science, Chulalongkorn University. During his graduate studies towards his M.Sc. degree, the Graduate School, Chulalongkorn University awarded him a research grant.